BLEJSKE DELAVNICE IZ FIZIKE LETNIK 10, ŠT. 1
BLED WORKSHOPS IN PHYSICS VOL. 10, NO. 1

ISSN 1580-4992

Proceedings of the Mini-Workshop

Problems in Multi-Quark States

Bled, Slovenia, June 29 – July 6, 2009

Edited by

Bojan Golli
Mitja Rosina
Simon Širca

University of Ljubljana and Jožef Stefan Institute

DMFA – ZALOŽNIŠTVO
LJUBLJANA, NOVEMBER 2009

The Mini-Workshop *Problems in Multi-Quark States*

was organized by

Jožef Stefan Institute, Ljubljana
Department of Physics, Faculty of Mathematics and Physics, University of Ljubljana

and sponsored by

Slovenian Research Agency
Department of Physics, Faculty of Mathematics and Physics, University of Ljubljana
Society of Mathematicians, Physicists and Astronomers of Slovenia

Organizing Committee

Mitja Rosina, Bojan Golli, Simon Širca

List of participants

Boris Arbuzov, Moscow, arbuzov@theory.sinp.msu.ru
Enrique Ruiz Arriola, Granada, earriola@ugr.es
Elmar Biernat, Graz, elmar.biernat@uni-graz.at
Alex Blin, Coimbra, alex@fis.uc.pt
Wojtek Broniowski, Krakow, b4bronio@cyf-kr.edu.pl
Ki-Seok Choi, Graz, ki.choi@uni-graz.at
Veljko Dmitrašinović, Belgrade, dmitrasin@yahoo.com
Bojan Golli, Ljubljana, bojan.golli@ijs.si
Brigitte Hiller, Coimbra, brigitte@fis.uc.pt
Sasha Osipov, Coimbra, alexguest@malaposta.fis.uc.pt
Willi Plessas, Graz, willibald.plessas@uni-graz.at
Milan Potokar, Ljubljana, Milan.Potokar@ijs.si
Saša Prelovšek, Ljubljana, Sasa.Prelovsek@ijs.si
Dan-Olof Riska, Helsinki, riska@mappi.helsinki.fi
Mitja Rosina, Ljubljana, mitja.rosina@ijs.si
Ica Stancu, Liege, fstancu@ulg.ac.be
Simon Širca, Ljubljana, simon.sirca@fmf.uni-lj.si
Masashi Wakamatsu, Osaka, wakamatu@kern.phys.sci.osaka-u.ac.jp
Tomi Živko, Ljubljana, tomi.zivko@ijs.si

Electronic edition

http://www-f1.ijs.si/BledPub/

Contents

Preface

Repetitio est mater studiorum, said the ancient Romans. It is now time to repeat the lessons, ideas and criticisms encountered at Bled 2009. We would like to thank you for the neat presentations summarized in these Proceedings which try to represent some flesh and spirit of our coming-together.

One of the red threads was the Nambu–Jona-Lasinio model. To what extent can it be derived from QCD? The Bogolyubov compensation method does provide a link. Work was done on pion polarizabilities and inclusion of four-body forces, which not only stabilizes the vacuum but also influences the behaviour in certain phase transitions. The simpified NJL gives some insights into the large-N_c limit and in the deduction of pion scattering lengths.

Low-lying baryon resonances are experiencing steady progress. The peculiar shape of the electro-production amplitudes in the Roper region can be explained by an interplay of intermediate Δ or σ states. Classification of resonances can be facilitated by looking at the density as a function of inter-quark distance. The renormalization of singular potentials with one-meson exchange still pose problems. The electromagnetic form-factors of baryons, the "gravitational" form-factor of the pion, the restoration of chiral symetry and the spin structure of baryons continue to attract our attention.

New resonances in the charmonium spectrum present many puzzles and model descriptions of their decay channels are not yet consistent. However, admixtures of higher configurations in baryons gain more and more credit; the excess of $\bar{d}$ over $\bar{u}$, for example, seems to require that. The four resonances studied at Belle were presented from the tetraquark point of view.

What topics should we tackle next year? We have not yet decided. There are many puzzles and secret wishes hidden in your and our minds. We are exploring the "market" and we are also awaiting your suggestions.

Ljubljana, November 2009

M. Rosina
B. Golli
S. Širca

Workshops organized at Bled

- *What Comes beyond the Standard Model* (June 29–July 9, 1998), Vol. **0** (1999) No. 1
- *Hadrons as Solitons* (July 6–17, 1999)
- *What Comes beyond the Standard Model* (July 22–31, 1999)
- *Few-Quark Problems* (July 8–15, 2000), Vol. **1** (2000) No. 1
- *What Comes beyond the Standard Model* (July 17–31, 2000)
- *Statistical Mechanics of Complex Systems* (August 27–September 2, 2000)
- *Selected Few-Body Problems in Hadronic and Atomic Physics* (July 7–14, 2001), Vol. **2** (2001) No. 1
- *What Comes beyond the Standard Model* (July 17–27, 2001), Vol. **2** (2001) No. 2
- *Studies of Elementary Steps of Radical Reactions in Atmospheric Chemistry*
- *Quarks and Hadrons* (July 6–13, 2002), Vol. **3** (2002) No. 3
- *What Comes beyond the Standard Model* (July 15–25, 2002), Vol. **3** (2002) No. 4
- *Effective Quark-Quark Interaction* (July 7–14, 2003), Vol. **4** (2003) No. 1
- *What Comes beyond the Standard Model* (July 17–27, 2003), Vol. **4** (2003) Nos. 2-3
- *Quark Dynamics* (July 12–19, 2004), Vol. **5** (2004) No. 1
- *What Comes beyond the Standard Model* (July 19–29, 2004), Vol. **5** (2004) No. 2
- *Exciting Hadrons* (July 11–18, 2005), Vol. **6** (2005) No. 1
- *What Comes beyond the Standard Model* (July 18–28, 2005), Vol. **6** (2005) No. 2
- *Progress in Quark Models* (July 10–17, 2006), Vol. **7** (2006) No. 1
- *What Comes beyond the Standard Model* (September 16–29, 2006), Vol. **7** (2006) No. 2
- *Hadron Structure and Lattice QCD* (July 9–16, 2007), Vol. **8** (2007) No. 1
- *What Comes beyond the Standard Model* (July 18–28, 2007), Vol. **8** (2007) No. 2
- *Few-Quark States and the Continuum* (September 15–22, 2008), Vol. **9** (2008) No. 1
- *What Comes beyond the Standard Model* (July 15–25, 2008), Vol. **9** (2008) No. 2
- *Problems in Multi-Quark States* (June 29–July 6, 2009), Vol. **10** (2009) No. 1
- *What Comes beyond the Standard Model* (July 14–24, 2009), Vol. **10** (2009) No. 2

Also published in this series

- Book of Abstracts, *XVIII European Conference on Few-Body Problems in Physics*, Bled, Slovenia, September 8–14, 2002, Edited by Rajmund Krivec, Bojan Golli, Mitja Rosina, and Simon Širca, Vol. **3** (2002) No. 1–2

Bled Workshops
in Physics
Vol. 10, No. 1
p. 1

Proceedings of the Mini-Workshop
Problems in Multi-Quark States
Bled, Slovenia, June 29 - July 6, 2009

Nambu–Jona-Lasinio model from QCD

B. A. Arbuzov

Skobeltsyn Institute of Nuclear Physics of MSU, 119992 Moscow, Russia

The NJL model [1–3] proves to be effective in description of low-energy hadron physics. The model starts with effective chiral invariant Lagrangian

$$\frac{G_1}{2}\left(\bar{\psi}\tau^b\gamma_5\psi\,\bar{\psi}\tau^b\gamma_5\psi\,-\,\bar{\psi}\,\psi\,\bar{\psi}\,\psi\right), \tag{1}$$

where ψ is the light quark doublet $(u,\,d)$. This interaction is non-renormalizable, so one is forced to introduce an ultraviolet cut-off Λ. Thus we have at least two arbitrary parameters

$$G_1\,;\quad \Lambda_1\,;$$

to be adjusted by comparison with real physics. It comes out that after such adjustment (and similar procedure for the vector sector and for the s-quark terms) we obtain satisfactory description of light mesons and their low-energy interactions.

However, the problem how to calculate the parameters G_i and Λ_i from the fundamental QCD was not solved for a long time. The main problem here is to find a method to obtain effective interactions from fundamental gauge interactions, *e.g.* QCD.

There are also non-local variants of the NJL model, in which one introduces a form-factor $F(q_i)$ into the effective interaction of the type (1) instead of a cut-off Λ. In this case again there was no regular method to obtain this function F and one has to make an arbitrary assumption for the choice.

Our goal is to formulate a regular approach, which allows to obtain a unique solution for the form-factors and other necessary quantities of the effective interactions. In particular we apply this approach to the NJL effective interaction.

The approach is based on the Bogoliubov compensation principle [4,5].

The main principle of the approach is to check if an effective interaction could be generated in a chosen variant of a renormalizable theory.

In previous works [6–12] the Bogoliubov compensation principle was applied to studies of spontaneous generation of effective non-local interactions in renormalizable gauge theories. In view of this one performs an "add and subtract" procedure for the effective interaction with a form-factor. Then one assumes the presence of the effective interaction in the interaction Lagrangian and the same term with the opposite sign is assigned to the newly defined free Lagrangian.

The QCD Lagrangian with two light quarks is (u and d)

$$L = \sum_{k=1}^{2}\left(\frac{\imath}{2}\left(\bar{\psi}_k\gamma_\mu\partial_\mu\psi_k - \partial_\mu\bar{\psi}_k\gamma_\mu\psi_k\right) - m_0\bar{\psi}_k\psi_k + g_s\bar{\psi}_k\gamma_\mu t^a A^a_\mu\psi_k\right) - \frac{1}{4}\left(F^a_{\mu\nu}F^a_{\mu\nu}\right). \tag{2}$$

Let us assume that a non-local NJL interaction is spontaneously generated in this theory. We use the Bogoliubov "add and subtract" procedure to check the assumption. We have

$$\begin{aligned} L &= L_0 + L_{int}\,,\\ L_0 &= \frac{\imath}{2}\left(\bar{\psi}\gamma_\mu\partial_\mu\psi - \partial_\mu\bar{\psi}\gamma_\mu\psi\right) - m_0\bar{\psi}\,\psi + \frac{G_1}{2}\left(\bar{\psi}\tau^b\gamma_5\psi\,\bar{\psi}\tau^b\gamma_5\psi \;-\; \bar{\psi}\,\psi\,\bar{\psi}\,\psi\right)\\ &\quad + \frac{G_2}{2}\left(\bar{\psi}\tau^b\gamma_\mu\psi\,\bar{\psi}\tau^b\gamma_\mu\psi + \bar{\psi}\tau^b\gamma_5\gamma_\mu\psi\bar{\psi}\tau^b\gamma_5\gamma_\mu\psi\right) - \frac{1}{4}F^a_{0\,\mu\nu}F^a_{0\,\mu\nu}\,, \qquad (3)\\ L_{int} &= g_s\,\bar{\psi}\gamma_\mu t^a A^a_\mu\psi \;-\frac{G_1}{2}\left(\bar{\psi}\tau^b\gamma_5\psi\,\bar{\psi}\tau^b\gamma_5\psi - \bar{\psi}\,\psi\,\bar{\psi}\,\psi\right)\\ &\quad - \frac{G_2}{2}\left(\bar{\psi}\tau^b\gamma_\mu\psi\,\bar{\psi}\tau^b\gamma_\mu\psi + \bar{\psi}\tau^b\gamma_5\gamma_\mu\psi\bar{\psi}\tau^b\gamma_5\gamma_\mu\psi\right)\\ &\quad - \frac{1}{4}\left(F^a_{\mu\nu}F^a_{\mu\nu} - F^a_{0\,\mu\nu}F^a_{0\,\mu\nu}\right). \qquad (4) \end{aligned}$$

Here the notation *e.g.* $\frac{G_1}{2}\bar{\psi}\,\psi\,\bar{\psi}\,\psi$ means the corresponding non-local vertex in the momentum space

$$\imath(2\pi)^4 G_1\,\bar{u}^a(p)\,u_a(q)\,\bar{u}^b(k)\,u_b(t)\,F(p,q,k,t)\,\delta(p+q+k+t)\,, \tag{5}$$

where $F(p,q,k,t)$ is a form-factor, p, q, k, t are respectively incoming momenta and a, b are isotopic indices of corresponding quarks.

Let us consider expression (3) as the new **free** Lagrangian L_0, whereas expression (4) is the new **interaction** Lagrangian L_{int}. The compensation equation demands fully connected four-fermion vertices, following from Lagrangian L_0, to be zero. The equation has evidently

1. a perturbative trivial solution $G_i = 0$;
2. but it might also have a non-perturbative non-trivial solution, which we shall look for.

In the first approximation we use the following assumptions.

1. Loop numbers 0, 1, 2. For one-loop case only a trivial solution exists.
2. Procedure of linearizing over form-factor, which leads to linear integral equations.
3. Intermediate UV cut-off Λ, results not depending on the value of this cut-off.
4. IR cut-off at the lower limit of integration by momentum squared q^2 at value m^2.

5. Only the first two terms of the $1/N$ expansion ($N = 3$).
6. We look for a solution with the following simple dependence on all four variables:

$$F(p_1, p_2, p_3, p_4) = F\left(\frac{p_1^2 + p_2^2 + p_3^2 + p_4^2}{2}\right). \tag{6}$$

Then we come to the following integral equation (see [8])

$$\begin{aligned}
&F_1(x) = A + \frac{3\,G_2}{8\pi^2}\left(2\Lambda^2 + x\log\frac{x}{\Lambda^2} - \frac{3}{2}x - \frac{\mu^2}{2x}\right) - \frac{(G_1^2 + 6G_1G_2)N}{32\,\pi^4}\times\\
&\left(\frac{1}{6\,x}\int_\mu^x (y^2 - 3\mu^2)F_1(y)\,dy + \frac{3}{2}\int_\mu^x yF_1(y)\,dy + \frac{x^2 - 3\mu^2}{6}\int_x^\infty \frac{F_1(y)}{y}dy + \right.\\
&\log x\int_\mu^x yF_1(y)\,dy + x\log x\int_\mu^x F_1(y)\,dy + \int_x^\infty y\log y\,F_1(y)\,dy +\\
&x\int_x^\infty \left(\log y + \frac{3}{2}\right)F_1(y)dy + \left(2\Lambda^2 - \frac{3}{2}x\right)\int_\mu^\infty F_1(y)\,dy - \frac{3}{2}\int_\mu^\infty yF_1(y)\,dy -\\
&\left.\log\Lambda^2\left(\int_\mu^\infty yF_1(y)\,dy + x\int_\mu^\infty F_1(y)\,dy\right)\right);\ \mu = m_0^2;\ x = p^2;\ y = q^2; \qquad (7)\\
&A = \frac{G_1N\Lambda^2}{2\pi^2}\left(1 + \frac{1}{4N} - \frac{G_1N}{2\pi^2}\left(1 + \frac{1}{2N}\right)\int_\mu^\infty F_1(y)\,dy\right).
\end{aligned}$$

The equation has the following solution decreasing at infinity

$$\begin{aligned}
F_1(z) &= C_1\,G_{06}^{40}\left(z|1, \frac{1}{2}, \frac{1}{2}, 0, a, b\right) + C_2\,G_{06}^{40}\left(z|1, \frac{1}{2}, b, a, \frac{1}{2}, 0, \right)\\
&\quad + C_3\,G_{06}^{40}\left(z|1, 0, b, a, \frac{1}{2}, \frac{1}{2}\right), \qquad (8)\\
a &= -\frac{1 - \sqrt{1 - 64u_0}}{4}, \qquad b = -\frac{1 + \sqrt{1 - 64u_0}}{4},
\end{aligned}$$

where $x = p^2$, $y = q^2$ are respectively external momentum squared and inegration momentum squared,

$$G_{pq}^{mn}\left(z|^{a_1, \dots, a_p}_{b_1, \dots, b_q}\right)$$

is a Meijer G-function [13],

$$\beta = \frac{(G_1^2 + 6G_1G_2)N}{16\pi^4}, \quad z = \frac{\beta x^2}{2^6}, \quad u_0 = \frac{\beta\mu^2}{64}, \quad F_1(u_0) = 1.$$

The constants C_i are defined by the boundary conditions

$$\frac{3\,G_2}{8\pi^2} - \frac{\beta}{2}\int_{m_0^2}^\infty F_1(y)\,dy = 0, \quad \int_{m_0^2}^\infty y\,F_1(y)\,dy = 0, \quad \int_{m_0^2}^\infty y^2\,F_1(y)\,dy = 0. \tag{9}$$

These conditions and the condition $A = 0$ lead to the cancellation of all terms in equation (7) being proportional to Λ^2 and $\log\Lambda^2$. So we have the unique solution. The values of the parameter u_0 and the ratio of two constants G_i are also fixed

$$u_0 = 1.92\cdot 10^{-8} \simeq 2\cdot 10^{-8}, \quad G_1 = \frac{6}{13}\,G_2. \tag{10}$$

We would draw attention to a natural appearance of a small quantity u_0. So G_1 and G_2 are both defined in terms of m_0.

Thus we have the unique non-trivial solution of the compensation equation, which contains no additional parameters. It is important that the solution exists only for positive G_2 and due to (10) for positive G_1 as well.

Now we have the non-trivial solution, which lead to the following effective Lagrangian

$$\begin{aligned} L = & \frac{i}{2}\left(\bar\psi\gamma_\mu\partial_\mu\psi - \partial_\mu\bar\psi\gamma_\mu\psi\right) - \frac{1}{4}F^a_{\mu\nu}F^a_{\mu\nu} - m_0\bar\psi\,\psi \\ & + g_s\,\bar\psi\gamma_\mu t^a A^a_\mu\psi - \frac{1}{4}F^a_{\mu\nu}F^a_{\mu\nu} \\ & - \frac{G_1}{2}\left(\bar\psi\tau^b\gamma_5\psi\bar\psi\tau^b\gamma_5\psi - \bar\psi\psi\bar\psi\psi\right) \\ & - \frac{G_2}{2}\left(\bar\psi\tau^b\gamma_\mu\psi\bar\psi\tau^b\gamma_\mu\psi + \bar\psi\tau^b\gamma_5\gamma_\mu\psi\bar\psi\tau^b\gamma_5\gamma_\mu\psi\right). \end{aligned} \tag{11}$$

Here $g_s^2/4\pi = \alpha_s(q^2)$ is the running constant depending on the momentum variable. We need this constant in the low-momenta region. We assume that in this region $\alpha_s(q^2)$ may be approximated by its average value α_s. The possible range of values of α_s is from 0.40 up to 0.75.

Thus we come to the effective non-local NJL interaction which we use to obtain the description of low-energy hadron physics [7,8,11]. In this way we obtain expressions for all quantities under study.

Analysis shows that the optimal set of low-energy parameters corresponds to $\alpha_s = 0.67$ and $m_0 = 20.3\,MeV$. We present a set of calculated parameters for these conditions including the quark condensate,the parameters of the σ-meson as well as the parameters of ρ and a_1-mesons:

$$\begin{aligned} \alpha_s &= 0.673\,; \qquad m_0 = 20.3\,MeV\,; \\ m_\pi &= 135\,MeV\,; \quad m_\sigma = 492\,MeV\,; \quad \Gamma_\sigma = 574\,MeV \\ f_\pi &= 93\,MeV\,; \quad m = 295\,MeV\,; \quad <\bar q\,q> = -(222\,MeV)^3\,; \\ G_1 &= \frac{1}{(244\,MeV)^2}\,; \qquad g = 3.16\,. \\ M_\rho &= 926.3\,MeV(771.1 \pm 0.9); \quad \Gamma_\rho = 159.5\,MeV(149.2 \pm 0.7); \\ M_{a_1} &= 1174.8\,MeV(1230 \pm 40); \quad \Gamma_{a_1} = 350\,MeV(250 - 600); \\ \Gamma(a_1 \to \sigma\pi)/\Gamma_{a_1} &= 0.23\,(0.188 \pm 0.043). \end{aligned}$$

The upper line here is our input, while all other quantities are calculated from these two fundamental parameters. The overall accuracy may be estimated to be on the order of 10 – 15%. The worst accuracy occurs in the value of M_ρ (20%). It seems that the vectors and the axials need further study.

Important result: average value of $\alpha_s \simeq 0.67$ agrees with calculated low-energy α_s [9]. So we have consistent description of low-energy hadron physics with only one dimensional parameter, e.g. m_0 or f_π.

References

1. Y. Nambu and G. Jona-Lasinio, Phys. Rev. **122**, 345 (1961); **124**, 246 (1961).
2. T. Eguchi, Phys. Rev. D **14**, 2755 (1976).
3. M. K. Volkov and D.Ebert, Yad. Fiz. **36**, 1265 (1982).
4. N. N. Bogoliubov. Physica Suppl. **26**, 1 (1960).
5. N. N. Bogoliubov, *Quasi-averages in problems of statistical mechanics.* Preprint JINR D-781, (Dubna: JINR, 1961).
6. B. A. Arbuzov, Theor. Math. Phys. **140**, 1205 (2004).
7. B. A. Arbuzov, Phys. Atom. Nucl. **69**, 1588 (2006).
8. B. A. Arbuzov, M. K. Volkov, I. V. Zaitsev. J. Mod. Phys. A, **21**, 5721 (2006).
9. B.A. Arbuzov, Phys.Lett. **B656**, 67 (2007).
10. B.A. Arbuzov, Proc. International Seminar on Contemporary Problems of Elementary Particle Physics, Dubna, January 17-18, 2008, Dubna, JINR, 2008, p. 156.
11. B. A. Arbuzov, M. K. Volkov, I. V. Zaitsev. J. Mod. Phys. A, **24**, 2415 (2009).
12. B. A. Arbuzov, Eur. Phys. Journal C **61**, 51 (2009).
13. H. Bateman and A. Erdélyi, *Higher transcendental functions*, Vol. 1. New York, Toronto, London: McGraw-Hill, 1953.

BLED WORKSHOPS
IN PHYSICS
VOL. 10, NO. 1
p. 6

Proceedings of the Mini-Workshop
Problems in Multi-Quark States
Bled, Slovenia, June 29 - July 6, 2009

Renormalization and universality of NN interactions in Chiral Quark and Soliton Models ⋆

E. Ruiz Arriola and A. Calle Cordón

Departamento de Física Atómica, Molecular y Nuclear, Universidad de Granada, E-18071 Granada, Spain

Abstract. We use renormalization as a tool to extract universal features of the NN interaction in quark and soliton nucleon models, having the same long distance behaviour but different short distance components. While fine tuning conditions in the models make difficult to fit NN data, the introduction of suitable renormalization conditions supresses the short distance sensitivity. Departures from universality are equivalent to extracting information on the model nucleon structure.

1 Introduction

The meson exchange picture has played a key role in the development of Nuclear Physics [1,2]. However, the traditional difficulty has been a practical need to rely on short distance information which is hardly accessible directly but becomes relevant when nucleons are placed off-shell. From a theoretical point of view this is unsatisfactory since one must face uncertainties not necessarily linked to our deficient knowledge at long distances and which are difficult to quantify. On the other hand, the purely field theoretical derivation yields potentials which present short distance singularities, thereby generating ambiguities even in the case of the widely used One Boson Exchange (OBE) potential. Consider, for instance, the venerable One Pion Exchange (OPE) $NN \to NN$ potential which for $r \neq 0$ reads

$$V^{1\pi}_{NN,NN}(r) = \tau_1 \cdot \tau_2 \sigma_1 \cdot \sigma_2 W^{1\pi}_S(r) + \tau_1 \cdot \tau_2 S_{12} W^{1\pi}_T(r)\,, \tag{1}$$

where the tensor operator $S_{12} = 3\sigma_1 \cdot \hat{x}\sigma_2 \cdot \hat{x} - \sigma_1 \cdot \sigma_2$ has been introduced and

$$W^{1\pi}_S(r) = \frac{m_\pi}{3}\frac{f^2_{\pi NN}}{4\pi} Y_0(m_\pi r) \quad , \qquad W^{1\pi}_T(r) = \frac{m_\pi}{3}\frac{f^2_{\pi NN}}{4\pi} Y_2(m_\pi r)\,. \tag{2}$$

Here $Y_0(x) = e^{-x}/x$ and $Y_2(x) = e^{-x}/x(1 + 3/x + 3/x^2)$ and $f_{\pi NN} = m_\pi g_{\pi NN}/(2M_N)$; $f^2_{\pi NN}/(4\pi) = 0.07388$ for $g_{\pi NN} = 13.08$. As we see, the OPE potential presents a $1/r^3$ singularity, but it can be handled unambiguously mathematically and with successful deuteron phenomenology [3]. Nonetheless, the standard way out to *avoid* the singularities in this and the more general OBE case is to implement vertex functions for the meson-baryon-baryon coupling (mAB) in the OBE

⋆ Talk delivered by E. Ruiz Arriola

potentials. This correspondins to a folding in coordinate space which in momentum space becomes the multiplicative replacement

$$V_{mAB}(q) \to V_{mAB}(q) \left[\Gamma_{mAB}(q^2)\right]^2 . \tag{3}$$

where $q^2 = q_0^2 - \mathbf{q}^2$ is the 4-momentum. Standard choices are to take form factors of the mono-pole [1] and exponential [2] parameterizations

$$\Gamma^{mon}_{mNN}(q^2) = \frac{\Lambda^2 - m^2}{\Lambda^2 - q^2}, \quad \Gamma^{exp}_{mNN}(q^2) = \exp\left[\frac{q^2 - m^2}{\Lambda^2}\right], \tag{4}$$

fulfilling the normalization condition $\Gamma_{mNN}(m^2) = 1$. Due to an extreme fine-tuning of the interaction, mainly in the $^1S_0$ channel, OBE potential models have traditionally needed a too large $g_{\omega NN}$ to overcome the mid range attraction implying one of the largest ($\sim 40\%$) $SU(3)$ violations known to date. In our recent works [4–9] we discuss how this problem may be circumvented with the help of renormalization ideas which upon imposing short distance insensitivity sidestep the fine tuning problem and allow natural $SU(3)$ values to be adopted in such a way that form factors and heavy mesons play a more marginal role. Contrarily to what one might naively think, renormalization *reduces* the short distance dependence provided, of course, removing the cut-off and the imposed renormalization conditions are mutually compatible operations.

Of course, the extended character of the nucleon as a composite and bound state of three quarks has motivated the use of microscopic models of the nucleon to provide an understanding of the short range interaction besides describing hadronic spectroscopy; quark or soliton models endow the nucleon with its finite size and incorporate basic requirements from the Pauli principle at the quark level or as dictated by the equivalent topology [10–13]. While much effort has been invested into determining the short range interactions, there is a plethora of models and related approximations; it is not obvious *what* features of the model are being actually tested. In fact, NN studies set the most stringent nucleon size oscillator constant value $b_N = 0.518$fm [13] from S-waves and deuteron properties which otherwise could be in a wider range $b_N = 0.4 - 0.6$fm. This shows that quark models also suffer from a fine tuning problem. In this contribution we wish to focus on the common and universal patterns of the various approaches and to show how these fine tunings can be reduced to a set of renormalization conditions.

2 The relevant scales

From a fundamental point of view the NN interaction should be obtained as a natural solution of the 6-q system. However, in order to describe the NN interaction it is far more convenient to study two 3-q clusters with nucleon quantum numbers, a procedure also applied in recent lattice QCD investigations of the nuclear force [14,15]. NN scattering in the elastic region corresponds to resolve distances about the minimal de Broglie wavelength associated to the first inelastic pion

production threshold, $NN \to NN\pi$, and corresponds to take $2E_{CM} = 2M_N + m_\pi$ yielding $p_{CM} = \sqrt{m_\pi M_N} = 360\text{MeV}$ which means $\lambda_{\min} \sim 1/\sqrt{m_\pi M_N} = 0.5\text{fm}$. This scale is smaller than 1π and 2π exchange (TPE) with Compton wavelengths 1.4 and 0.7fm respectively. Other length scales in the problem are comparable and even shorter namely 1) Nucleon size, 2) Correlated meson exchanges and 3) Quark exchange effects. All these effects are of similar range and, to some extent, redundant. In a quark model the constituent quark mass is related to the Nucleon and vector meson masses through $M_q = M_N/N_c = M_V/2$ which for $N_c = 3$ colours gives the estimate $M_q = 310 - 375\text{MeV}$. Exchange effects due to e.g. One-Gluon-Exchange are $\sim e^{-2M_q r}$ since they correspond to the probability of finding a quark in the opposite baryon. This follows from complete Vector Meson Dominance (for a review see e.g. [16]), which for the isoscalar baryon density, $\rho_B(r)$, and assuming independent particle motion yields

$$\int d^3x e^{iq\cdot x}\langle N|\rho_B(x)|N\rangle = 4\pi\int_0^\infty dr\, r^2|\phi(r)|^2 j_0(qr) \sim \frac{M_V^2}{M_V^2+q^2} \tag{5}$$

suggesting a spectroscopic factor $\phi(r) \sim e^{-M_V r/2}M_V/\sqrt{4\pi r}$ at large distances. As we have said and we will discuss below these effects are somewhat marginal but if they ought to become visible they should reflect the correct asymptotic behaviour. In the constituent quark model the CM motion can be easily extracted assuming harmonic oscillator wave functions, $\phi(r) \sim e^{-b^2r^2/2}$ [10,11,13] which yield Gaussian form factors falling off *much faster* than the experimental ones. Skyrme models without vector mesons yield instead topological Baryon densities $\rho_B(r) \sim e^{-3m_\pi r}/r^7$[12] corresponding to the outer pion cloud contributions which are longest range but pressumably yield *only* a fraction of the radius. In any case quark-exchange looks very much like direct vector meson exchange potential which is $\sim e^{-M_V r}$.

3 Chiral quark soliton model

Most high precision NN potentials providing $\chi^2/\text{DOF} < 1$ need to incorporate universally the One-Pion-Exchange (OPE) potential (including charge symmetry breaking effects) while the shorter range is described by many and not so similarly looking interactions [17]. This is probably a confirmation that chiral symmetry is spontaneously broken at longer distances than confinement, since hadronization has already taken place. It also suggests that in a quark model aiming at describing NN interactions the pion must be effectively included. Chiral quark models accomplish this explicitly under the assumption that confinement is not crucial for the binding of π, N and Δ. Pure quark models including confinement or not have to face in addition the problem of recovering the pion from quark-gluon dynamics. In between, hybrid models have become practical and popular [10,11,13]. As mentioned, all these scales around the confinement scale are mixed up. Because these effects are least understood and trigger side effects such as spurious colour Van der Waals forces arising from Hidden color singlet states $[\mathbf{88}]_A$ states [18,19] in the (presumably doubtful) adiabatic approximation, we will cavalierly ignore the difficulties by remaining in a regime where

confinement is not expected to play a role and stay with standard chiral quark models.

While both the constituent chiral quark model and the Skyrme soliton model look very disparate the Chiral Quark Soliton Model embeds both models in the small and the large soliton limit respectively [1]. We analyze the intuitive non-relativistic chiral quark model (NRCQM) explicitly and comment on the soliton case where similar patterns emerge. The comparison stresses common aspects of the quark soliton model pictures which could be true features of QCD. While the long distance universality between both NRCQM and Skyrme soliton model NN calculations may appear somewhat surprising this is actually so because in a large N_c framework both models are just different realizations of the contracted spin-flavour symmetry [23].

4 The non-relativistic chiral quark model

To fix ideas it is instructive to consider the chiral-quark model which corresponds to the Gell-Mann–Levy sigma model Lagrangean at the quark level [24] (the non-linear version suggested in Ref. [25] will be discussed below),

$$\mathcal{L} = \bar{q}\left(i\partial\!\!\!/ - g_{\pi qq}(\sigma + i\gamma_5\tau\cdot\pi)\right)q + \frac{1}{2}\left[(\partial^\mu\sigma)^2 + (\partial^\mu\boldsymbol{\pi})^2\right] - U(\sigma,\pi)\,, \qquad (6)$$

where $U(\sigma,\boldsymbol{\pi}) = \lambda^2(\sigma^2+\boldsymbol{\pi}^2-v^2)^2/8 - f_\pi m_\pi^2\sigma$ is the standard Mexican hat potential implementing both spontaneous breaking of chiral symmetry as well as PCAC yielding the Goldberger-Treiman relation $M_q = g_{\pi qq}f_\pi = g_{\sigma qq}f_\pi$ at the constituent quark level. When this model is interpreted from a gradient expansion of the NJL model quarks are regarded as valence quarks whereas kinetic meson terms arise from the polarization of the Dirac sea and $m_\sigma^2 = 4M_q^2 + m_\pi^2$, which for $M_q = M_N/3 = M_V/2$ yields $m_\sigma = 650 - 770$MeV. In the heavy constituent quarks limit the model implies 1π and 1σ exchange potentials,

$$V^{1\pi}_{qq'}(\mathbf{r}) = -\frac{g^2_{\pi qq}}{4M_q^2}\tau_q\cdot\tau'_q\int\frac{d^3p}{(2\pi)^3}e^{i\mathbf{p}\cdot\mathbf{r}}\frac{(\sigma_q\cdot p)(\sigma_{q'}\cdot p)}{p^2+m_\pi^2}\,,$$
$$V^{1\sigma}_{qq'}(\mathbf{r}) = g^2_{\pi qq}\int\frac{d^3p}{(2\pi)^3}e^{i\mathbf{p}\cdot\mathbf{r}}\frac{1}{p^2+m_\sigma^2} = -\frac{g^2_{\pi qq}}{4\pi}\frac{e^{-m_\sigma r}}{r}\,, \qquad (7)$$

whence baryon properties can be obtained by solving the Hamiltonian

$$H = \sum_{i=1}^{N_c}\left[\frac{p_i^2}{2M_q} + M_q\right] + \sum_{i<j}V(x_i-x_j) = \frac{P^2}{2M} + N_cM_q + H_{\rm int}\,, \qquad (8)$$

[1] Within the large N_c framework the difference corresponds to a saddle point approximation around a trivial or non-trivial background. The question *which* regime is the appropriate one is a dynamical issue [20,21]. Likewise, when the soliton is large, quarks are deeply bound and the topological soliton picture of Skyrme sets in, giving the appearance of a confined state (where colour Van der Waals forces cannot take place). The soliton of the Spectral Quark model does not allow this interpretation as baryon charge is never topological [22].

where the total momentum $P = \sum_{i=1}^{N_c} p_i/N_c$ and the intrinsic Hamiltonian have been introduced. Due to Galilean invariance the wave function of a moving baryon can be factorized

$$\Psi_B(x_1,\ldots,x_{N_c}) = \phi(\xi_1,\ldots,\xi_{N_c-1})e^{iP\cdot R}\,, \tag{9}$$

with $R = \sum_{i=1}^{N_c} x_i/N_c$ the CM of the cluster and $\xi_i = x_i - R/N_c$ intrinsic coordinates, $\sum_i \xi_i = 0$. We will assume that this complicated problem has been solved already Ref. [26]. For large N_c the Hartree mean field approximation $\Psi_B(x_1,\ldots,x_{N_c}) = \prod_{i=1}^{N_c}\phi_{\alpha_i}(x_i)\chi_c$ might be used [27]). For separated hadrons the interaction between quark clusters A and B can be written as sum of pairwise interactions which, for elementary πqq and σqq vertices, reads

$$\begin{aligned} V_{\rm int}(\mathbf{x}_1,\ldots,\mathbf{x}_{N_c};\mathbf{y}_1,\ldots,\mathbf{y}_{N_c}) &= \sum_{i,j} V_{ij}^{\sigma+\pi}(\mathbf{x}_i-\mathbf{y}_j) \\ &= \int \frac{d^3q}{(2\pi)^3}\sum_{i,j} V_{ij}^{\sigma+\pi}(q)e^{i\mathbf{q}\cdot(\mathbf{x}_i-\mathbf{y}_j)}\,. \end{aligned} \tag{10}$$

Switching to intrinsic coordinates variables $\mathbf{x}_i = \boldsymbol{\xi}_i + \mathbf{R}/2$ and $\mathbf{y}_j = \boldsymbol{\eta}_j - \mathbf{R}/2$ with $\sum_i \xi_i = \sum_j \eta_j = 0$ where R is the distance between the CM of each cluster, we have

$$V_{1\pi}(\mathbf{R}) = \frac{g_{\pi qq}^2}{M_q^2}\int \frac{d^3q}{(2\pi)^3}e^{iq\cdot R}\,\frac{q_k q_k}{q^2+m_\pi^2}G_A^{ka}(q)G_B^{ka}(q)^*\,, \tag{11}$$

$$V_{1\sigma}(\mathbf{R}) = g_{\pi qq}^2\int \frac{d^3q}{(2\pi)^3}e^{iq\cdot R}\,\frac{1}{q^2+m_\sigma^2}\rho_A(q)\rho_B(q)^*\,, \tag{12}$$

where the spin-isospin density and scalar densities are given by (e.g. cluster A)

$$G_A^{ka}(q) = \frac{1}{2}\sum_{i=1}^{N_c}\sigma_i^k\tau_i^a e^{i\xi_i\cdot q}\,, \qquad \rho_A(q) = \frac{1}{N_c}\sum_{i=1}^{N_c}e^{i\xi_i\cdot q}\,, \tag{13}$$

respectively. Note that the scalar and Baryon densities as well as the pseudoscalar and axial densities coincide unlike the relativistic case. That means that *within* the approximations one should have $M_S = M_V$. Thus, the total Hamiltonian is written as

$$H = H_{A,\rm int} + H_{B,\rm int} + V_{\rm int}(R) + \frac{P^2}{2M_T} + \frac{p^2}{2\mu}\,. \tag{14}$$

Galilean invariance implies that *inertial masses* are $M_T = 2N_cM_q$ and $\mu = N_cM_q/2$. Introducing the two independent cluster complete states $H_{A,\rm int}\phi_{A,n} = M_{A,n}\phi_{A,n}$ and $H_{B,\rm int}\phi_{B,m} = M_{B,m}\phi_{B,m}$ the two-clusters CM frame unperturbed wave function is just a product

$$\Psi^{(0)}_{A_n,B_m}(1,2,3;4,5,6) = \phi_{A,n}(1,2,3;R/2)\phi_{B,m}(4,5,6;-R/2)e^{iQ\cdot R}\,, \tag{15}$$

where Q is the relative momentum between the two clusters. The above problem is usually handled by Resonating Group Methods [10,11,13,28]. We analyze

this coupled channel scattering problem perturbatively where the transition potentials, defined as $V_{A_nB_m;A_kB_l}(R) = \langle\phi_{A,n}\phi_{B,m}|V_{\rm int}|\phi_{A,k}\phi_{B,l}\rangle$, have a familiar folding structure which in the case of the pion reads

$$V^{1\pi}_{A_nB_m;A_kB_l}(R) = \frac{g^2_{\pi qq}}{M_q^2}\int\frac{d^3q}{(2\pi)^3}\frac{q_iq_j}{q^2+m_\pi^2}e^{iq\cdot R}\langle A_n|G_{ia}(q)|A_k\rangle\langle B_m|G_{ja}(-q)|B_l\rangle\,. \tag{16}$$

5 Long distance limit and the need for renormalization

At long distances the leading singularities $q = im_\pi$ and $q = im_\sigma$ dominate [29,30]. Using that $|\langle N|\rho(q)|N\rangle|^2$ is an even function of q we get the structure for the NN $\to$ NN potentials

$$\begin{aligned} V_\sigma(\mathbf{R}) &= g^2_{\pi qq}N_c^2\int\frac{d^3q}{(2\pi)^3}e^{iq\cdot R}\frac{|\langle N|\rho(im_\sigma)|N\rangle|^2}{q^2+m_\sigma^2} + C_0\,\delta^{(3)}(R) \\ &\quad + C_2(-\nabla^2+m_\sigma^2)\delta^{(3)}(R) + \ldots \\ &= -\frac{g^2_{\sigma NN}}{4\pi}\frac{e^{-m_\sigma r}}{r} + \text{distributions} \end{aligned} \tag{17}$$

and Eq. (1) for the OPE contribution. Here, the couplings are given by $g_{\sigma NN} = N_c g_{\sigma qq}|\rho(im_\sigma)|$ and $g_{\pi NN} = N_c g_A g_{\pi qq}|\rho(im_\pi)|$ where $g_A = (N_c+2)/3$ [31]. Assuming $|\rho(im_\pi)| \sim |\rho(0)| = 1$ one has the Goldberger-Treiman relation $g_A M_N = g_{\pi NN} f_\pi$ at the nucleon level. Thus, at long distances finite size effects are represented as an infinite sum of delta functions and derivatives thereof. However, any finite truncation will produce a negligible contribution at any non-vanishing distance. In a sense, this result is reminiscent of the Gauss theorem for charged objects with a sharp non-overlapping boundary; the interaction is mainly due to the total charge and regardless on the density profiles of the system. Only an infinite number of terms may yield a finite size effect. Note that the coefficients of the contact interactions are *fixed* numbers having a meaning perturbatively. However, if one tries to play with them to characterize finite resolution effects (nucleon size and potential range) in a model independent way non-perturbatively (solving e.g. the Schrödinger equation) important restrictions arise. Unlike the δ's, the OPE short distance $1/r^3$ singularity is not located in a compact region, i.e. is not killed by taking a finite support test function, and contributes to all arbitrarily small distances. Thus, one can effectively drop the derivatives of distributions. This simple-minded argument was advanced in Ref. [32] and explicitly verified in momentum space by taking C_0 and C_2 as *real* counterterms in the Lippmann-Schwinger equation in Ref. [29]; either C_2 becomes irrelevant or the scattering amplitude does not converge. Therefore, we represent C_0 as an energy independent boundary condition. The renormalization procedure in coordinate space generally corresponds to 1) fix some low energy constants such as e.g. the scattering length for s-waves, α_0, at zero energy as an *independent* variable of the potential, 2) integrate in down to an arbitrarily small cut-off radius r_c, 3) construct an orthogonal finite energy state by matching log-derivatives at r_c and 4)

integrating out generating a phase-shift $\delta_0(p)$ with a *prescribed* scattering length α_0. This prescription is the *renormalization condition* and the procedure of integrating in and out corresponds to evolving along the renormalization trajectory. The crucial aspect is that short distance insensitivity is implemented. The $\pi+\sigma$ model and OBE extensions are analyzed in detail in Refs. [4,5,9] where form factors *after renormalization* are found to be marginal.

6 Renormalization of Spin-flavour Van der Waals forces

The non-linear chiral quark model [25] corresponds to take $m_\sigma \to \infty$, reducing to just OPE. The results for the phase shifts in the lowest partial waves are presented in Fig. 1. Note the bad ${}^1S_0$ phase. To improve on this the long distance OPE transition potential is taken

$$V_{AB;CD}(R) = (\boldsymbol{\tau}_{AB}\cdot\boldsymbol{\tau}_{CD})\Big\{\sigma_{AB}\cdot\sigma_{CD}[W_S^{1\pi}]_{AB;CD}(R) + [S_{12}]_{AB;CD}[W_T^{1\pi}]_{AB;CD}(R)\Big\}, \tag{18}$$

where the tensor term is defined as $S_{12} = 3(\sigma_{AB}\cdot\hat{R})(\sigma_{CD}\cdot\hat{R}) - \sigma_{AB}\cdot\sigma_{CD}$ and

$$[W_{S,T}^{1\pi}]_{AB;CD}(R) = \frac{m_\pi}{3}\frac{f_{\pi AC}f_{\pi BD}}{4\pi}Y_{0,2}(m_\pi R) \tag{19}$$

Note that also here there is a $1/r^3$ singularity. In this particular form the resulting potential is model independent [33] [2]. In general, this requires solving a coupled channel problem [34,35] but if we are interested in the elastic channel with $T_{CM} = m_\pi < \Delta \equiv M_\Delta - M_N = 293\text{MeV}$ we may take into account the effect of the closed channels as sub-threshold effects in perturbation theory. We neglect the exponentially $\sim e^{-2M_q r}$ suppressed quark exchange contribution. In obvious operator-matrix notation and restricting to the two particle ground $|0\rangle = |NN\rangle$ and excited $|n\rangle = |N\Delta\rangle, |\Delta N\rangle, |\Delta\Delta\rangle$ in-going and out-going channels and resolvent $G_{0,k}(E) = (E - H_{0,k})^{-1}$ with $H_{0,k} = P^2/(2\mu_k) + E_k$, we get for the T-matrix

$$(T)_{nm} = (V)_{nm} + \sum_k (V)_{nk}G_{0,k}(V)_{k,m} + \mathcal{O}(V^3), \tag{20}$$

with $E_0 = 2M_N$,$E_{1,2} = M_N + M_\Delta$ and $E_3 = 2M_\Delta$ the corresponding thresholds. Thus, separating the elastic term $k = 0$ explicitly from the sum we get the effective potential in the elastic scattering channel corresponding to higher pion exchanges, wich, when iterated to second order yields the elastic scattering amplitude T_{00}. Specifically, defining the momentum space potential $V_{nm}(k' - k) \equiv$

[2] The corresponding couplings are $f_{\pi AB} = |F_{\pi AB}(im_\pi)|$ where the transition form factors are defined as $F_{\pi AB}(q^2)\chi_A^\dagger T^a S^i \chi_B = \langle A|G^{ia}(q)|B\rangle$. In the $SU(4)\otimes SU_c(N_c)$ quark model [31] and in the chiral limit they fulfill $f_{\pi\Delta\Delta}/f_{\pi NN} = 1/5$ and $f_{\pi N\Delta}/f_{\pi NN} = 3[(N_c-1)(N_c+5)/2]^{\frac{1}{2}}/(N_c+2)$. The $\Delta \to N\pi$ width in the Born approximation yields $f_{\pi N\Delta}^2/(4\pi) = 0.324$.

$\langle k', n|V|k, m\rangle = \int d^3R V_{nm}(R) e^{i(k-k')\cdot R}$ we get

$$\bar{V}_{00}(k'-k, E) = V_{00}(k'-k) + \sum_{n\neq 0}\int \frac{d^3q}{(2\pi)^3}\frac{V_{0n}(k'-q)V_{n0}(q-k)}{E - q^2/2\mu_n - E_n} + \mathcal{O}(V^3) \quad (21)$$

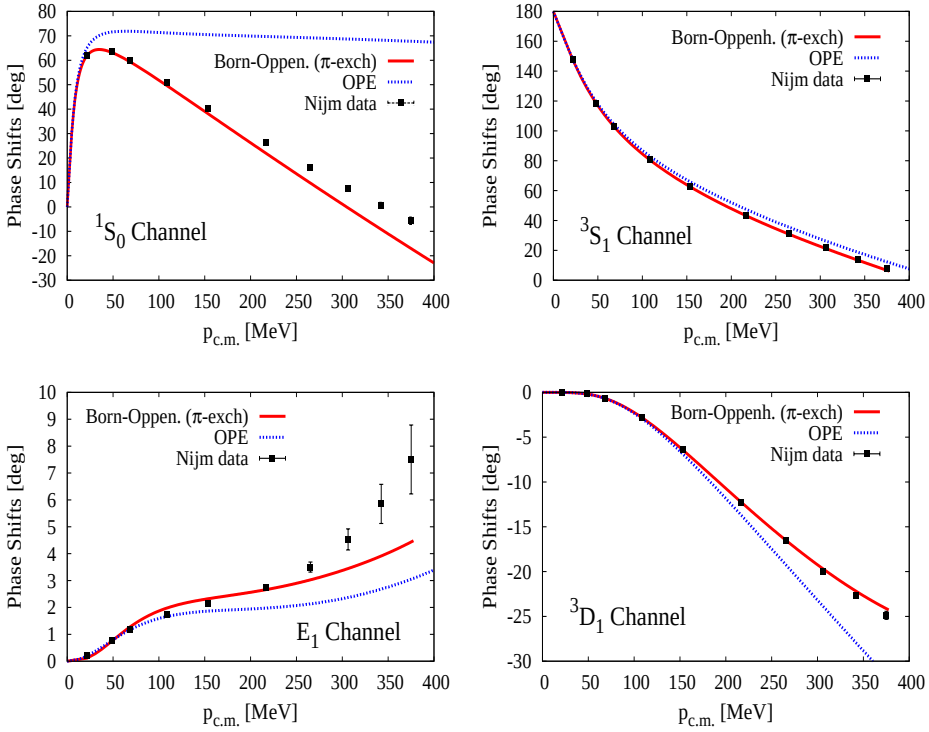

Fig. 1. Renormalized (eigen) phase shifts for the OPE and Δ-Born-Oppenheimer potentials as a function of the CM np momentum p in the spin singlet ${}^1S_0$ (one counterterm) and triplet ${}^3S_1 - {}^3D_1$ (three counterterms) channels compared to averaged Nijmegen potentials [17]. We take $f^2_{\pi NN}/4\pi = 0.07388$[17] and $f_{\pi N\Delta}/f_{\pi NN} = 6\sqrt{2}/5$.

which, expectedly, depends on the energy. Evaluating on-shell at $E = E_0 + p^2/2\mu_0$, assuming a large splitting $p \ll \sqrt{\Delta M_\Delta} = 600$MeV and neglecting the kinetic energy piece in the NΔ cannel, we get the perturbative and local optical potential in coordinate space

$$\bar{V}^{1\pi+2\pi+\cdots}_{NN;NN}(R) = V^{1\pi}_{NN,NN}(R) + \frac{2|V^{1\pi}_{NN,N\Delta}(R)|^2}{M_N - M_\Delta} + \mathcal{O}(V^3) \quad (22)$$

which is the Born-Oppenheimer approximation to second order which generates more complicated spin-isospin structures than just OPE *including* a central force, all of them $\sim e^{-2m_\pi R}$ and resembling TPE. Note that only the intermediate NΔ

state contributes. The above result implies an attractive and short distance singular potential since $V^{1\pi}_{NN,N\Delta}(R) \sim g_A^2/(f_\pi^2 R^3)$ and hence the potential becomes singular $\bar{V}_{NN,NN} \sim -g_A^4/(\Delta f_\pi^4 R^6)$. Actually, Eq. (22) was evaluated in the Skyrme soliton model within the Heitler-London approximation, i.e. the product ansatz in the coupled channel space [36,37] providing the long sought mid range attraction [12]. [3] We reproduce the same results in the quark model calculation. The potential found using Feynman graph techniques [39] looks very similar with identical short distance singular behaviour identifying $h_A/g_A = f_{\pi N\Delta}/2f_{\pi NN}$. Note that we leave out background πN scattering which correspond to triangle and box TPE diagrams at the quark level. The renormalization procedure as well as the necessary counterterms in the general coupled channel singular potentials has been explained in much detail in Ref. [32,40]. The results for the phase shifts using Eq. (22) in the lowest partial waves are depicted in Fig. 1. In any case the description looks extremely similar (including deuteron properties) to the renormalization [41] of more sophisticated field theoretical potentials [39]. Convergence is achieved already at $r_c \sim 0.5$fm.

The multiplicative structures of Eq. (22) reflect spin-flavour excitations and remind of the analogous Van der Waals forces in atomic systems. They hold literally even after inclusion of form factors with folded potentials (although $\Lambda_{\pi NN}$, $\Lambda_{\pi N\Delta}$ and $\Lambda_{\pi\Delta\Delta}$ are not necessarily identical) which remove the singularity. This is *not* equivalent to regularize the effective potential as a whole through subtractions. We have checked that form factors *after renormalization* become marginal in agreement with the OBE analysis [9].

7 Wigner SU(4) as a long distance symmetry

If the tensor force component of the qq potential, Eq. (7), is neglected one has invariance under the spin-isospin $SU(4)$ group with the quarks in the fundamental **4**-dimensional representation, $q = (u\uparrow, u\downarrow, d\uparrow, d\downarrow)$. In the three quark system we have the spin-flavour states $\mathbf{4}\otimes\mathbf{4}\otimes\mathbf{4} = \mathbf{4}_A \oplus \mathbf{20}_S \oplus \mathbf{20}_{M_1} \oplus \mathbf{20}_{M_2}$. Due to colour antisymmetry only the symmetric state survives which spin-isospin, (S,T), decomposition is $\mathbf{20}_S = (\frac{1}{2},\frac{1}{2}) \oplus (\frac{3}{2},\frac{3}{2}) = N \oplus \Delta$ yielding $N-\Delta$ degeneracy. Since $M_\Delta - M_N$ is large at nuclear scales, one might still treat the Nucleon quartet $N = (p\uparrow, p\downarrow, n\uparrow, n\downarrow)$ as the fundamental rep. of the old Wigner-Hund $SU(4)$ symmetry which implies spin independence, in particular that $V_{^1S_0}(r) = V_{^3S_1}(r)$ at *all distances* suggesting that phases $\delta_{^1S_0}(p) = \delta_{^3S_1}(p)$ in contradiction to data (see e.g. Fig. 1). The amazing finding of Ref. [6] was that assuming identical potentials $V_{^1S_0}(r) = V_{^3S_1}(r)$ for $r > r_c \to 0$ one has

$$p\cot\delta_{^1S_0}(p) = \frac{\alpha_{^1S_0}\mathcal{A}(p) + \mathcal{B}(p)}{\alpha_{^1S_0}\mathcal{C}(p) + \mathcal{D}(p)}, \quad p\cot\delta_{^3S_1}(p) = \frac{\alpha_{^3S_1}\mathcal{A}(p) + \mathcal{B}(p)}{\alpha_{^3S_1}\mathcal{C}(p) + \mathcal{D}(p)}, \quad (23)$$

where the functions $\mathcal{A}(p)$, $\mathcal{B}(p)$, $\mathcal{C}(p)$ and $\mathcal{D}(p)$ are *identical* in both channels, but the experimentally different scattering lengths $\alpha_{^1S_0} = -23.74$fm and $\alpha_{^3S_1} =$

[3] Molecular methods used in the Skyrme model [36,37,12] are replaced by evaluating model form factor yielding regularized Meson Exchange potentials [38] where the only remnant of the model is in the meson-form factors.

5.42fm yield quite different phase shifts with a fairly good agreement. Thus, Wigner symmetry is broken by very short distance effects and hence corresponds to a *long distance symmetry* (a symmetry broken only by counterterms). Moreover, large N_c [23] suggests that Wigner symmetry holds only for *even* L, a fact verified by phase shift sum rules [6]. In Refs. [7,8] we analyze further the relation to the old Serber symmetry which follows from vanishing P-waves in $S = 1$ channels, showing how old nuclear symmetries are unveiled by coarse graining the NN interaction via the V_{lowk} framework [42] and with testable implications for Skyrme forces in mean field calculations [43].

The chiral quark model is supposedly an approximate non-perturbative description, but *perturbative* gluons may be introduced by standard minimal coupling [13], $i\partial\!\!\!/ \to i\partial\!\!\!/ + gA\!\!\!/^a \cdot \lambda_a^c/2$ with λ_a^c the $N_c^2 - 1$ Gell-Mann *colour* matrices. A source of $SU(4)$ breaking is the contact one gluon exchange which yields spin-colour chromo-magnetic interactions (S_{ij} is the tensor operator),

$$V^{OGE} = \frac{1}{4}\alpha_s \sum_{i<j} (\lambda_i^c \cdot \lambda_j^c) \left\{ \frac{1}{r_{ij}} - \frac{\pi}{4m_i m_j} \left[1 + \frac{2}{3}\sigma_i \cdot \sigma_j \right] \delta^{(3)}(\mathbf{r}_{ij}) - \frac{3}{4m_i m_j r_{ij}} S_{ij} \right\} \tag{24}$$

breaking the $\Delta - N$ degeneracy. This short distance terms break *also* the $^1S_0$ and $^3S_1$ degeneracy of the NN system providing an understanding of the long distance character of Wigner symmetry. Taking the Wigner symmetric zero energy state and perturbing around it, the previous argument suggests that $1/\alpha_{^3S_1} - 1/\alpha_{^1S_0} = \mathcal{O}(M_\Delta - M_N)$ with a computable coefficient.

8 Conclusions

Chiral Quark and Soliton models while quite different in appearance provide some universal behaviour regarding NN interactions. If the asymptotic potentials coincide, the main differences in describing the scattering data are due to a few low energy constants which in some cases are subjected to extreme fine tuning of the model parameters. The success of the model at finite energy is mainly reduced to reproducing these low energy parameters.

One of us (E.R.A.) warmly thanks M. Rosina, B. Golli and S. Širca for the invitation and D. R. Entem, F. Fernandez, M. Pavón Valderrama and J. L. Goity for discussions. This work is supported by the Spanish DGI and FEDER funds with grant FIS2008-01143/FIS, Junta de Andalucía grant FQM225-05, and EU Integrated Infrastructure Initiative Hadron Physics Project contract RII3-CT-2004-506078.

References

1. R. Machleidt, K. Holinde and C. Elster, Phys. Rept. 149 (1987) 1.

2. M.M. Nagels, T.A. Rijken and J.J. de Swart, Phys. Rev. D17 (1978) 768.
3. M. Pavon Valderrama and E. Ruiz Arriola, Phys. Rev. C72 (2005) 054002.
4. E. Ruiz Arriola, A. Calle Cordon and M. Pavon Valderrama, (2007), 0710.2770.
5. A. Calle Cordon and E. Ruiz Arriola, AIP Conf. Proc. 1030 (2008) 334.
6. A. Calle Cordon and E. Ruiz Arriola, Phys. Rev. C78 (2008) 054002.
7. A. Calle Cordon and E. Ruiz Arriola, Phys. Rev. C80 (2009) 014002.
8. E. Ruiz Arriola and A. Calle Cordon, (2009), 0904.4132.
9. A. Calle Cordon and E. Ruiz Arriola, (2009), 0905.4933.
10. M. Oka and K. Yazaki, Int. Rev. Nucl. Phys. 1 (1984) 489.
11. R.F. Alvarez-Estrada, F. Fernandez, J. L. Sanchez-Gomez and V. Vento, Lect. Notes Phys. 259 (1986) 1.
12. T.S. Walhout and J. Wambach, Int. J. Mod. Phys. E1 (1992) 665.
13. A. Valcarce, H. Garzilazo, F. Fernandez and P. Gonzalez, Rept. Prog. Phys. 68 (2005) 965.
14. N. Ishii, S. Aoki and T. Hatsuda, Phys. Rev. Lett. 99 (2007) 022001.
15. S. Aoki, T. Hatsuda and N. Ishii, (2009), 0909.5585.
16. H.B. O'Connell et al., Prog. Part. Nucl. Phys. 39 (1997) 201.
17. V.G.J. Stoks et al., Phys. Rev. C49 (1994) 2950.
18. M.B. Gavela et al., Phys. Lett. B82 (1979) 431.
19. O.W. Greenberg and H.J. Lipkin, Nucl. Phys. A370 (1981) 349.
20. C.V. Christov et al., Prog. Part. Nucl. Phys. 37 (1996) 91.
21. H. Weigel, Lect. Notes Phys. 743 (2008) 1.
22. E. Ruiz Arriola, W. Broniowski and B. Golli, Phys. Rev. D76 (2007) 014008.
23. D.B. Kaplan and A.V. Manohar, Phys. Rev. C56 (1997) 76.
24. M.C. Birse and M.K. Banerjee, Phys. Lett. B136 (1984) 284.
25. A. Manohar and H. Georgi, Nucl. Phys. B234 (1984) 189.
26. L.Y. Glozman and D.O. Riska, Phys. Rept. 268 (1996) 263.
27. J.L. Goity, Phys. Atom. Nucl. 68 (2005) 624.
28. D. Bartz and F. Stancu, Phys. Rev. C63 (2001) 034001.
29. D. R. Entem, E. Ruiz Arriola, M. Pavon Valderrama and R. Machleidt, Phys. Rev. C77 (2008) 044006.
30. M.T. Fernandez-Carames, P. Gonzalez and A. Valcarce, Phys. Rev. C77 (2008) 054003.
31. G. Karl and J.E. Paton, Phys. Rev. D30 (1984) 238.
32. M. Pavon Valderrama and E. Ruiz Arriola, Phys. Rev. C74 (2006) 054001.
33. A.M. Green, Rept. Prog. Phys. 39 (1976) 1109.
34. G.H. Niephaus, M. Gari and B. Sommer, Phys. Rev. C20 (1979) 1096.
35. R.B. Wiringa, R.A. Smith and T.L. Ainsworth, Phys. Rev. C29 (1984) 1207.
36. N.R. Walet, R.D. Amado and A. Hosaka, Phys. Rev. Lett. 68 (1992) 3849.
37. N.R. Walet and R.D. Amado, Phys. Rev. C47 (1993) 498.
38. G. Holzwarth and R. Machleidt, Phys. Rev. C55 (1997) 1088.
39. N. Kaiser, S. Gerstendorfer and W. Weise, Nucl. Phys. A637 (1998) 395.
40. M. Pavon Valderrama and E. Ruiz Arriola, Annals Phys. 323 (2008) 1037.
41. M. Pavon Valderrama and E. Ruiz Arriola, Phys. Rev. C79 (2009) 044001.
42. S. K. Bogner, T. T. S. Kuo and A. Schwenk, Phys. Rept. 386 (2003) 1
43. M. Zalewski, J. Dobaczewski, W. Satula and T. R. Werner, Phys. Rev. C77 (2008) 024316

Bled Workshops
in Physics
Vol. 10, No. 1
p. 17

Proceedings of the Mini-Workshop
Problems in Multi-Quark States
Bled, Slovenia, June 29 - July 6, 2009

Electro-magnetic meson form-factor from a relativistic coupled-channels approach*

E. P. Biernat[a], W. Schweiger[b], K. Fuchsberger[b], and W. H. Klink[c]

[a] Institut für Physik, Universität Graz, A-8010 Graz, Austria
[b] BE-OP Division, CERN, CH-1211 Geneve 23, Switzerland
[c] Department of Physics and Astronomy, University of Iowa, Iowa City, Iowa, USA

We calculate the electromagnetic form factor of a confined quark-antiquark pair within the framework of relativistic point-form quantum mechanics. The idea is to treat elastic electromagnetic scattering of an electron by a meson as a relativistic two-channels problem for a Bakamjian-Thomas type mass operator [1] such that the dynamics of the exchanged photon is taken explicitly into account.

On the hadronic level the structure of the meson is encoded in a phenomenological form factor which is not known a priori. Similarly, on the constituents level we can consider electromagnetic scattering of an electron by a confined quark-antiquark pair as a two-channels problem. The quark and the antiquark are assumed to interact via a spontaneous confining potential. Elimination of the channel containing the photon gives in both cases an eigenvalue equation for the eM and $eq\bar{q}$ channels on the hadronic and constituent levels, respectively, which contains the one-photon-exchange optical potential. In order to work within the Bakamjian-Thomas framework one has to resort to the approximation that the total four-velocity of the system is conserved at electromagnetic vertices [2]. By comparison of matrix elements of the optical potential on the hadronic and the constituent levels the electromagnetic meson form factor can be read off [3,4].

The form factor obtained in this way depends on all Lorentz invariants of the electron-meson system, i.e. on the momentum-transfer and on the total invariant mass of the electron-meson system. The dependence on the invariant mass is related to the violation of cluster separability. If, however, the invariant mass is chosen large enough this dependence becomes negligible. In the limit of an infinitely large invariant mass the optical potential separates into an electron and a meson current which are connected via the usual photon propagator. The expression for the form factor becomes then [5]

$$F\left(Q^2\right) = \int d^3\tilde{k}'_q \sqrt{\frac{m_{q\bar{q}}}{m'_{q\bar{q}}}} \mathcal{S}\, \Psi^*\left(\tilde{\mathbf{k}}'_q\right) \Psi\left(\tilde{\mathbf{k}}_q\right). \tag{1}$$

Here $Q^2 = \mathbf{q^2}$ is the momentum transfer squared with $\mathbf{q} = \mathbf{k}'_\mathbf{q} - \mathbf{k}_\mathbf{q} = \mathbf{k}'_\mathbf{M} - \mathbf{k}_\mathbf{M}$ and $m^2_{q\bar{q}} = (E_q + E_{\bar{q}})^2 - \mathbf{k}^2_\mathbf{M}$ is the invariant mass of the quark-antiquark pair.

* Talk delivered by E. P. Biernat

Quantities without a tilde refer to the electron-meson center-of-mass and quantities with a tilde refer to the meson rest system. $\mathcal{S}$ is a spin-rotation factor which takes into account the substantial effect of the quark spin on the form factor. By an appropriate change of variables the integral for the form factor Eq. (1) takes the same form as the integral for the pion form factor from front form calculations [6,7]. This remarkable result means that relativity is treated in an equivalent way and the physical ingredients are the same in both approaches.

For a simple two-parameter harmonic-oscillator wave function with the parameterization taken from [6,7] our result for the pion electromagnetic form factor provides a reasonable fit to the data as shown in Fig. 1.

The generalization of this multichannel approach to electroweak form factors for an arbitrary bound few-body system is quite obvious. By an appropriate extension of the Hilbert space this approach is also able to accommodate exchange-current effects.

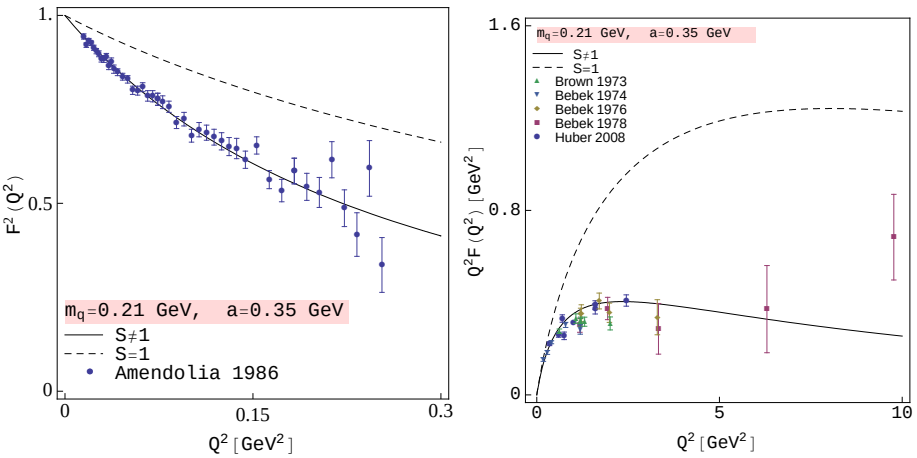

Fig. 1. Q^2-dependence of the pion form factor with (solid) and without (dashed) spin-rotation factor $\mathcal{S}$. Values for the quark mass m_q and the oscillator parameter a are taken from [6,7] and data are taken from [8–13].

References

1. B. Bakamjian and L. H. Thomas, Phys. Rev. **92**, 1300 (1953).
2. W. H. Klink, Nucl. Phys. **A716**, 123 (2003).
3. K. Fuchsberger, Master's thesis, Karl–Franzens–Universität Graz (2007).
4. E. P. Biernat, K. Fuchsberger, W. Schweiger, and W. H. Klink, Few Body Syst. **44**, 311 (2008).
5. E .P. Biernat, W. Schweiger, K. Fuchsberger, and W. H. Klink, Phys. Rev. **C79**, 055203 (2009).
6. P. L. Chung, F. Coester, and W. N. Polyzou, Phys. Lett. **B205**, 545 (1988).
7. F. Coester, W. N. Polyzou, Phys. Rev. **C71**, 028202 (2005).
8. S. R. Amendolia *et al.*, Nucl. Phys. **B277**, 168 (1986)
9. C. N. Brown *et al.*, Phys. Rev. **D8**, 92 (1973)
10. C. J. Bebek *et al.*, Phys. Rev. **D9**, 1229 (1974)

11. C. J. Bebek *et al.*, Phys. Rev. **D13**, 25 (1976)
12. C. J. Bebek *et al.*, Phys. Rev. **D17**, 1693 (1978)
13. G. M. Huber *et al.*, Phys. Rev. **C78**, 045203 (2008)

Bled Workshops
in Physics
Vol. 10, No. 1
p. 20

Proceedings of the Mini-Workshop
Problems in Multi-Quark States
Bled, Slovenia, June 29 - July 6, 2009

Gravitational, electromagnetic, and transition form factors of the pion*

Wojciech Broniowski[a] and Enrique Ruiz Arriola[b]

[a] The H. Niewodniczański Institute of Nuclear Physics PAN, PL-31342 Kraków and Institute of Physics, Jan Kochanowski University, PL-25406 Kielce, Poland
[b] Departamento de Física Atómica, Molecular y Nuclear, Universidad de Granada, E-18071 Granada, Spain

Abstract. Results of the Spectral Quark Model for the gravitational, electromagnetic, and transition form factors of the pion are discussed. In this model both the parton distribution amplitude and the parton distribution function are flat, in agreement with the transverse lattice calculations at low renormalization scales. The model predictions for the gravitational form factor are compared to the lattice data, with good agreement. We also find a remarkable relation between the three form factors, holding within our model, which besides reproducing the anomaly, provides a relation between radii which is reasonably well fulfilled. Comparison with the CELLO, CLEO, and BaBar data for the transition form factor is also considered. While asymptotically the model goes above the perturbative QCD limit, in qualitative agreement with the BaBar data, it fails to accurately reproduce the data at intermediate momenta.

The low-energy behavior of the pion is determined by the spontaneous breakdown of the chiral symmetry. This fact allows for modeling the soft matrix elements in a genuinely dynamical way [1–25]. This talk is based on Refs. [26,27] and employs the Spectral Quark Model (SQM) [28] in the analysis of several high-energy processes and their partonic interpretation. This model satisfies *a priori* consistency conditions [28] between open quark lines and closed quark lines, which becomes crucial in the analysis of high-energy processes and enables an unambiguous identification of parton distribution functions and amplitudes. This is not necessarily the feature of other versions of chiral quark models, such as the Nambu–Jona–Lasinio (NJL) model, as was spelled out already in Ref. [1]. For these reasons SQM is particularly well suited for the presented study.

The general theoretical framework is set by the Generalized Parton Distributions (GPDs) [29–37]. These objects arise formally, *e.g.*, from deeply virtual Compton scattering (DVCS) on a hadronic target, effectively opening up the quark lines joining the currents. In local quark models usually the one-loop divergences appear and a regularization is needed. One may either compute the *regularized* DVCS and take the high-energy limit, or compute directly the *regularized* GPD.

* Talk delivered by W. Broniowski

Besides the requirements of gauge invariance and energy-momentum conservation, this apparently innocuous issue sets a non-trivial consistency condition on admissible regularizations which SQM fulfills satisfactorily.

For the case of the pion, the GPD for the non-singlet channel is defined as

$$\epsilon_{3ab}\,\mathcal{H}^{q,NS}(x,\zeta,t)=\int\frac{dz^-}{4\pi}e^{ixp^+z^-}\langle\pi^b(p')|\bar\psi(0)\gamma^+\psi(z)\,\tau_3|\pi^a(p)\rangle\big|_{z^+=0,z^\perp=0}\,,$$

with similar expressions for the singlet quarks and gluons. We omit the gauge link operators $[0,z]$, absent in the light-cone gauge. The kinematics is set by $p'=p+q$, $p^2=p'^2=m_\pi^2$, $q^2=-2p\cdot q=t$. The variable $\zeta=q^+/p^+$ denotes the momentum fraction transferred along the light cone. Formal properties of GPDs can be elegantly written in the symmetric notation involving the variables $\xi=\frac{\zeta}{2-\zeta}$, $X=\frac{x-\zeta/2}{1-\zeta/2}$:

$$H^{I=0}(X,\xi,t)=-H^{I=0}(-X,\xi,t),\;\; H^{I=1}(X,\xi,t)=H^{I=1}(-X,\xi,t).$$

For $X\geq 0$ one has $\mathcal{H}^{I=0,1}(X,0,0)=q^{S,NS}(X)$, where $q(x)^i$ are the standard parton distribution functions (PDFs). In QCD all these objects are subjected to radiative corrections, as they carry anomalous dimensions, and become scale-dependent, *i.e.* they undergo a suitable QCD evolution. This raises an important question: what is the scale Q_0 of the quark model when matching to QCD is performed? The momentum-fraction sum rule fixes this scale to be admittedly very low, $Q_0=313^{+20}_{-10}$ MeV, for $\Lambda_{QCD}=226$ MeV. Remarkably, but also perhaps unexpectedly, this choice, followed by the leading-order evolution, provides a rather impressive agreement with the high energy data, as well as the Euclidean and transverse-lattice simulations (see Ref. [26] for a detailed summary).

The following *sum rules* hold for the moments of the GPDs:

$$\int_{-1}^{1}dX\,H^{I=1}(X,\xi,t)=2F_V(t),\;\int_{-1}^{1}dX\,X\,H^{I=0}(X,\xi,t)=2\theta_2(t)-2\xi^2\theta_1(t),$$

where $F_V(t)$ denotes the *vector form factor*, while $\theta_1(t)$ and $\theta_2(t)$ stand for the *gravitational form factors* [38]. Other important features are the *polynomiality* conditions [29], the *positivity bounds* [39,40], and a low-energy theorem [41]. We stress that all these properties required on formal grounds are satisfied in our quark-model calculation [26]. Unlike GPDs, the form factors of conserved currents do not undergo the QCD evolution.

In the chiral limit we have the following identity in SQM relating the gravitational and electromagnetic form factor,

$$\frac{d}{dt}\,[t\,\theta_i(t)]=F_V(t)\,,\quad (i=1,2)\,,\tag{1}$$

from which the identity between the two gravitational form factors $\theta_1(t)=\theta_2(t)\equiv\Theta(t)$ follows.

Since there is no data for the full kinematic range for the GPDs of the pion, we present here the results for the generalized form factors only, in particular for

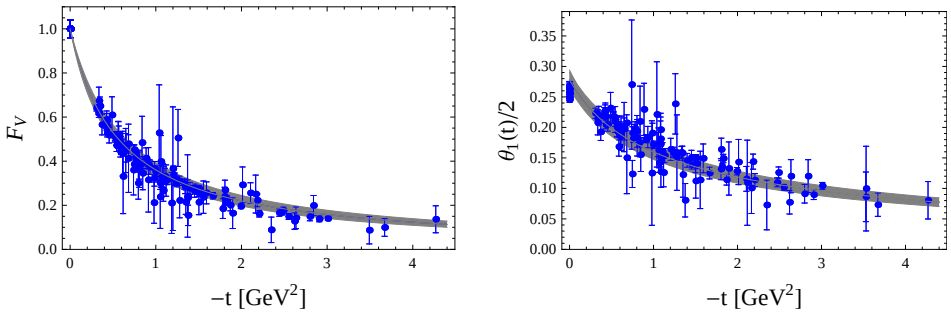

Fig. 1. Form factors of the pion vs. lattice data. Left: the electromagnetic form factor. Right: the quark part of the gravitational form factor, $\theta_1(t)/2$, computed in the Spectral Quark Model and compared to the lattice data from Ref. [42]. The band around the model curves indicates the uncertainty in the model parameters.

the gravitational ones. It is well known that the data for the electromagnetic form factor are well parameterized with the monopole form, which by construction is reproduced in SQM, where the vector meson dominance is built in. The gravitational form factors are available from the lattice QCD simulations [42,43]. In Fig. 1 the electromagnetic form factor and the quark part of the gravitational form factor are compared to the lattice data. We note a very good agreement. In SQM one has the relation

$$m_\rho^2 = 24\pi^2 f^2/N_c, \tag{2}$$

where f is the pion weak decay constant in the chiral limit. This relation works within a few percent phenomenologically. The expressions for the form factors in SQM are very simple,

$$F_V(t) = \frac{m_\rho^2}{m_\rho^2 - t}, \quad \theta_{1,2}(t)/\theta_{1,2}(0) = \frac{m_\rho^2}{t}\log\left(\frac{m_\rho^2}{m_\rho^2 - t}\right). \tag{3}$$

We note the longer tail of the gravitational form factor in the momentum space, meaning a more compact distribution of energy-momentum in the coordinate space. Explicitly, we find a quark-model formula

$$2\langle r^2\rangle_\theta = \langle r^2\rangle_V. \tag{4}$$

The two previous processes regard two pions and either one photon or one graviton in the corresponding three-point vertex function. An apparently disparate object is given by the pion-photon *transition distribution amplitude* (TDA) [44,45]

$$\int \frac{dz^-}{2\pi}\, e^{ixp^+z^-}\langle\gamma(p',\varepsilon)|\bar\psi(0)\gamma^\mu\frac{\tau^a}{2}\psi(z)|\pi^b(p)\rangle\Big|_{\substack{z^+=0\\ z_T=0}} = \frac{ie}{p^+ f}\epsilon^{\mu\nu\alpha\beta}\varepsilon_\nu p_\alpha q_\beta V^{ab}(x,\zeta,t), \tag{5}$$

Here the photon carries momentum $p' = p + q$ and has polarization ε. As before, the presence of the gauge link operators is understood in Eq. (5) to guarantee the

gauge invariance of the bilocal operators. We consider here the *isovector* quark bilinears. Since the photon couples to the quark through a combination of the isoscalar and isovector couplings, *i.e.* the quark charge is $Q = 1/(2N_c) + \tau^3/2$, one has the isospin decomposition

$$V^{ab}(x,\zeta,t) = \delta^{ab} V_{I=0}(x,\zeta,t) + i\epsilon^{abc} V_{I=1}(x,\zeta,t). \tag{6}$$

The isoscalar form factor is related to the pion-photon *transition form factor* by the sum rule

$$F_{\pi\gamma\gamma^*}(t) = \frac{2}{f}\int dx V^{I=0}(x,\zeta,t), \tag{7}$$

where the factor of 2 comes fom the fact, that either of the photons can be isoscalar. The form factor in SQM was obtained directly in Ref. [28] and later on from the integration of the pion-photon isoscalar transition distribution amplitude (TDA) yielding [21] a ζ-independent function (as required by polynomiality),

$$F_{\pi\gamma\gamma}(t,A) = \frac{2f}{N_c}\left[\frac{2m_\rho^2}{m_\rho^4 - t m_\rho^2 + (1-A^2)t^2} + \frac{1}{At}\log\left(\frac{2m_\rho^2 - (1-A)t}{2m_\rho^2 - (1+A)t}\right)\right], \tag{8}$$

where $A = (q_1^2 - q_2^2)/(q_1^2 + q_2^2)$ is the photon asymmetry parameter. For $A = 1$ we have

$$F_{\pi\gamma\gamma^*}(t) = \frac{1}{12\pi^2 f}\left[\frac{2m_\rho^2}{m_\rho^2 - t} + \frac{m_\rho^2}{t}\log\left(\frac{m_\rho^2}{m_\rho^2 - t}\right)\right], \tag{9}$$

where relation (2) has been used. We read out from this formula the corresponding rms radius to be $\langle r^2\rangle^{1/2}_{\pi\gamma\gamma^*} = \sqrt{5}/m_\rho = 0.57$ fm for $m_\rho = 770$ MeV. Equivalently, one may use the slope parameter $b_\pi = \frac{d}{dt}F_{\pi^0\gamma\gamma^*}(t)/F_{\pi^0\gamma\gamma^*}(t)\Big|_{t=0}$. SQM gives $b_\pi = 5/(6m_\rho^2) = 1.4\,\mathrm{GeV}^{-2}$, in a very reasonable agreement with the experimental value $b_\pi = (1.79 \pm 0.14 \pm 14)\mathrm{GeV}^{-2}$, originally reported by CELLO [46]. A comparison of Eq. (8,9) to the CLEO [47] and BaBar [48] data is presented in the right panel of Fig. 2. The solid line corresponds to the model calculation with $A = 1$, while the dashed line is for $A = 0.95$. We note that the experiment does not produce strictly real photons, thus the observed sensitivity to the value of A is a relevant effect. We note that while at $|A| = 1$ the model asymptotics for the transition form factor is $(2f/N_c)\log(-t/m_\rho^2)/(-t)$, at $|A| \neq 1$ it becomes $(2f/N_c)\log[(1+A)/(1-A)]/(-At)$. The behavior is clearly seen in Fig. 2. As we notice, in the intermediate range of Q SQM overshoots the data.

The recent BaBar measurements [48] have predated the long-standing perturbative QCD prediction [49,50] that $-tF_{\pi\gamma\gamma^*}(t)$ goes asymptotically to a constant value of $2f$. Some authors [51,52] have pointed out that the key to this unexpected behavior hints for a flat pion PDA and the end-point singularities and switched-off QCD evolution. The flatness of the PDA at low renormalization scales has been originally found in the Nambu–Jona-Lasinio model [10] and in SQM [28].

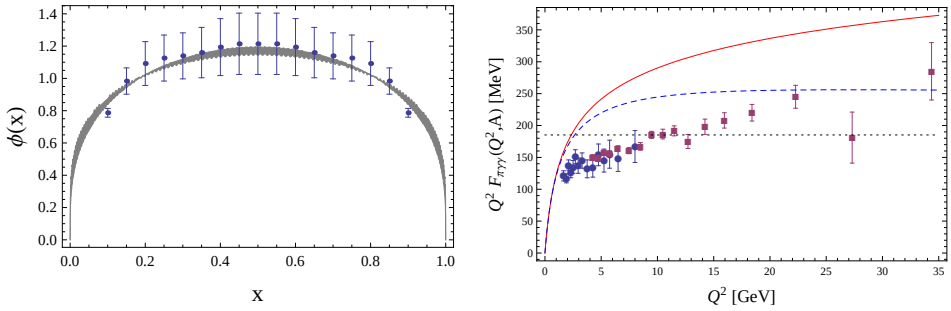

Fig. 2. Left: chiral quark model prediction for the pion DA evolved to the scale of 0.5GeV (band) and compared to the transverse lattice data [54]. Right: the pion trantition form factor compared to the CLEO [47] and BaBar [48] data. Solid (dashed) lines are the SQM prediction at $A = 1$ ($A = 0.95$). The dotted line is the perturbative QCD prediction.

We note in passing that a constant PDA is also found in the Regge model [53].

Remarkably, an almost flat PDA is also found non-perturbatively on the transverse lattice [54] (see the left panel of Fig. 2). Actually, the non-vanishing of the PDA at the end points (at the quark-model scale) is not only a consequence of local quark models. Nonlocal models correctly implementing the chiral Ward-Takahashi identity also get such a feature [18]. A trend to flatness is observed in contrast to calculations violating the chiral symmetry constraints. However, the corresponding transition form factor in non-local models does not show a steep rise [55] as suggested by the BaBar data. The calculation in Ref. [56,57], which reproduces the CLEO and BaBar data, requires, unfortunately, a much too small constituent quark mass, which is incompatible with other sectors of the pion phenomenology. The apparent inconsistency of the BaBar data with the QCD convolution scheme is also addressed in Ref. [58,59].

Let us remind the reader that according to the conventional perturbative QCD approach, the radiative corrections are computed order by order in the twist expansion. Most often this is in practice possible only for the leading-twist contribution. Actually, this is the only way to identify the PDA within a non-perturbative scenario or quark model calculations. In fact, the chiral quark models require a low scale not only by fixing the second Gegenbauer coefficient a_2 of the PDA. As already mentioned, the same conclusion is reached independently by fixing the momentum fraction of the valence quarks to its natural 100% value at the quark-model scale, where the quarks constitute the only degrees of freedom.

On a more methodological level, it is worth mentioning that the conventional NJL model does not share some of the virtues of SQM, particularly the interplay between chiral anomaly and factorization, a subtle point which was discussed at length in Ref. [11] for the NJL case. The $\pi\gamma\gamma$ triangle graph is linearly divergent, and thus a regularization must generally be introduced. If one insists on preserving the vector gauge invariance, the regulator must preserve that symmetry, but

then the axial current is not conserved, generating the standard chiral anomaly. The obvious question arises whether the limit $Q^2 \to \infty$ must be taken before or after removing the cut-off. If one takes the sequence $Q^2 > \Lambda^2$, a constant PDA is obtained in agreement with our low energy calculation. For the opposite sequence factorization does not hold in NJL. The good feature of SQM is that the spectral regularization does not make any difference between the two ways. This illustrates in a particular case the above-mentioned general consistency requirement between regularized open and closed quark lines (see e.g. [60]).

Finally, by combining Eq. (3) and Eq. (9) we get the remarkable relation among the electromagnetic, gravitational and transition form factors, holding in SQM:

$$F_{\pi\gamma\gamma^*}(t) = \frac{1}{12\pi^2 f}\left[2F_V(t) + \Theta(t)\right] , \tag{10}$$

whence

$$3\langle r^2\rangle_{\pi\gamma\gamma^*} = 2\langle r^2\rangle_V + \langle r^2\rangle_\Theta . \tag{11}$$

The previous relation is not fulfilled in the conventional NJL model. Of course, it would be interesting to test the relation Eq. (10) against the future data or lattice QCD.

In conclusion, we note that while the description of the pion transition form factor in a genuinely dynamical way remains a challenge, the Spectral Quark Model offers many attractive features which are required from theoretical consistency. It satisfies the chiral anomaly and the factorization property. The vector and gravitational form factors describe experimental and/or lattice-QCD data satisfactorily. A remarkable model relation among the gravitational, electromagnetic and transition form factors has also been deduced. Finally, for the latter, we have also displayed a hitherto unnoticed sensitivity to the photon momentum asymmetry parameter A which might be relevant for other studies.

This research is supported in part by the Polish Ministry of Science and Higher Education, grants N202 034 32/0918 and N202 249235, Spanish DGI and FEDER funds with grant FIS2008-01143/FIS, Junta de Andalucía grant FQM225-05, and the EU Integrated Infrastructure Initiative Hadron Physics Project, contract RII3-CT-2004-506078.

References

1. R.M. Davidson and E. Ruiz Arriola, Phys. Lett. B348 (1995) 163.
2. A.E. Dorokhov and L. Tomio, (1998), hep-ph/9803329.
3. M.V. Polyakov and C. Weiss, Phys. Rev. D59 (1999) 091502, hep-ph/9806390.
4. M.V. Polyakov and C. Weiss, Phys. Rev. D60 (1999) 114017, hep-ph/9902451.
5. A.E. Dorokhov and L. Tomio, Phys. Rev. D62 (2000) 014016.
6. I.V. Anikin et al., Nucl. Phys. A678 (2000) 175.
7. I.V. Anikin et al., Phys. Atom. Nucl. 63 (2000) 489.
8. E. Ruiz Arriola, (2001), hep-ph/0107087.

9. R.M. Davidson and E. Ruiz Arriola, Acta Phys. Polon. B33 (2002) 1791, hep-ph/0110291.
10. E. Ruiz Arriola and W. Broniowski, Phys. Rev. D66 (2002) 094016, hep-ph/0207266.
11. E. Ruiz Arriola, Acta Phys. Polon. B33 (2002) 4443, hep-ph/0210007.
12. M. Praszalowicz and A. Rostworowski, (2002), hep-ph/0205177.
13. B.C. Tiburzi and G.A. Miller, Phys. Rev. D67 (2003) 013010, hep-ph/0209178.
14. B.C. Tiburzi and G.A. Miller, Phys. Rev. D67 (2003) 113004, hep-ph/0212238.
15. L. Theussl, S. Noguera and V. Vento, Eur. Phys. J. A20 (2004) 483, nucl-th/0211036.
16. W. Broniowski and E. Ruiz Arriola, Phys. Lett. B574 (2003) 57, hep-ph/0307198.
17. M. Praszalowicz and A. Rostworowski, Acta Phys. Polon. B34 (2003) 2699, hep-ph/0302269.
18. A. Bzdak and M. Praszalowicz, Acta Phys. Polon. B34 (2003) 3401, hep-ph/0305217.
19. S. Noguera and V. Vento, Eur. Phys. J. A28 (2006) 227, hep-ph/0505102.
20. B.C. Tiburzi, Phys. Rev. D72 (2005) 094001, hep-ph/0508112.
21. W. Broniowski and E.R. Arriola, Phys. Lett. B649 (2007) 49, hep-ph/0701243.
22. A. Courtoy and S. Noguera, Phys. Rev. D76 (2007) 094026, 0707.3366.
23. A. Courtoy and S. Noguera, Prog. Part. Nucl. Phys. 61 (2008) 170, 0803.3524.
24. A.E. Dorokhov and W. Broniowski, Phys. Rev. D78 (2008) 073011, 0805.0760.
25. P. Kotko and M. Praszalowicz, (2008), 0803.2847.
26. W. Broniowski, E.R. Arriola and K. Golec-Biernat, Phys. Rev. D77 (2008) 034023, 0712.1012.
27. W. Broniowski and E.R. Arriola, Phys. Rev. D78 (2008) 094011, 0809.1744.
28. E. Ruiz Arriola and W. Broniowski, Phys. Rev. D67 (2003) 074021, hep-ph/0301202.
29. X.D. Ji, J. Phys. G24 (1998) 1181, hep-ph/9807358.
30. A.V. Radyushkin, (2000), hep-ph/0101225.
31. K. Goeke, M.V. Polyakov and M. Vanderhaeghen, Prog. Part. Nucl. Phys. 47 (2001) 401, hep-ph/0106012.
32. A.P. Bakulev et al., Phys. Rev. D62 (2000) 054018, hep-ph/0004111.
33. M. Diehl, Phys. Rept. 388 (2003) 41, hep-ph/0307382.
34. X.D. Ji, Ann. Rev. Nucl. Part. Sci. 54 (2004) 413.
35. A.V. Belitsky and A.V. Radyushkin, Phys. Rept. 418 (2005) 1, hep-ph/0504030.
36. T. Feldmann, Eur. Phys. J. Special Topics 140 (2007) 135.
37. S. Boffi and B. Pasquini, Riv. Nuovo Cim. 30 (2007) 387, 0711.2625.
38. J.F. Donoghue and H. Leutwyler, Z. Phys. C52 (1991) 343.
39. B. Pire, J. Soffer and O. Teryaev, Eur. Phys. J. C8 (1999) 103, hep-ph/9804284.
40. P.V. Pobylitsa, Phys. Rev. D65 (2002) 077504, hep-ph/0112322.
41. M.V. Polyakov, Nucl. Phys. B555 (1999) 231, hep-ph/9809483.
42. D. Brommel, Pion structure from the lattice, PhD thesis, University of Regensburg, Regensburg, Germany, 2007, DESY-THESIS-2007-023.
43. D. Brommel et al., PoS LAT2005 (2006) 360, hep-lat/0509133.
44. J.P. Lansberg, B. Pire and L. Szymanowski, Phys. Rev. D73 (2006) 074014, hep-ph/0602195.
45. J.P. Lansberg, B. Pire and L. Szymanowski, (2007), 0709.2567.
46. CELLO, H.J. Behrend et al., Z. Phys. C49 (1991) 401.
47. CLEO, J. Gronberg et al., Phys. Rev. D57 (1998) 33, hep-ex/9707031.
48. The BABAR, B. Aubert et al., Phys. Rev. D80 (2009) 052002, 0905.4778.
49. A.V. Efremov and A.V. Radyushkin, Phys. Lett. B94 (1980) 245.
50. G.P. Lepage and S.J. Brodsky, Phys. Lett. B87 (1979) 359.
51. A.V. Radyushkin, (2009), 0906.0323.
52. M.V. Polyakov, (2009), 0906.0538.
53. E. Ruiz Arriola and W. Broniowski, Phys. Rev. D74 (2006) 034008, hep-ph/0605318.

54. S. Dalley and B. van de Sande, Phys. Rev. D67 (2003) 114507, hep-ph/0212086.
55. P. Kotko and M. Praszalowicz, (2009), 0907.4044.
56. A.E. Dorokhov, (2009), 0905.4577.
57. A.E. Dorokhov, (2009), 0909.5111.
58. S.V. Mikhailov and N.G. Stefanis, Nucl. Phys. B821 (2009) 291, 0905.4004.
59. S.V. Mikhailov and N.G. Stefanis, (2009), 0909.5128.
60. E.R. Arriola, W. Broniowski and B. Golli, Phys. Rev. D76 (2007) 014008, hep-ph/0610289.

BLED WORKSHOPS
IN PHYSICS
VOL. 10, NO. 1
p. 28

Proceedings of the Mini-Workshop
Problems in Multi-Quark States
Bled, Slovenia, June 29 - July 6, 2009

Axial charges of nucleon resonances*

Ki-Seok Choi, W. Plessas, and R.F. Wagenbrunn

Theoretical Physics, Institute of Physics, University of Graz, Universitätsplatz 5, A-8010 Graz, Austria

Recently, first results have become available from lattice quantum chromodynamics (QCD) for two of the nucleon excitations, namely, the negative-parity $N^*(1535)$ and $N^*(1650)$ resonances [1]. The axial charge of the nucleon ground state had been studied before by different lattice-QCD groups in quenched calculations and with dynamical quarks [2–7]. In some of these works one has used chiral extrapolations (for a recent discussion of the associated problems see Ref. [8]), and the bulk of results obtained for g_A of the nucleon varies between about $1.10 \sim 1.40$.

Lately, the issue of axial constants of N^* resonances has become debated a lot due to the suggestion of chiral-symmetry restoration in the higher hadron spectra [9,10]. According to this scenario there should appear chiral doublets of positive- and negative-parity states and as a further consequence their axial charges should became small or almost vanishing. The first parity partners above the nucleon ground state are supposed to be the $N^*(1440)-N^*(1535)$, the next ones the $N^*(1710)-N^*(1650)$. The axial charges of the negative-parity partners in these pairs have been calculated in lattice QCD to be $\sim$0.00 and $\sim$0.55, respectively [1]; for the positive-parity states no results are yet available.

We have performed a study of the axial charges of N^* resonances in the framework of the relativistic constituent quark model (RCQM). Specifically we have extended a previous investigation of the nucleon axial form factors [11,12] to the first $J^P = \frac{1}{2}^{\pm}$ nucleon excitations. Our approach relies on solving the eigenvalue problem of the Poincaré-invariant mass operator in the framework of relativistic quantum mechanics. The axial current operator is chosen according to the spectator model (SM) [13]. For the RCQM we employed in the first instance the extended Goldstone-boson exchange (EGBE) RCQM [14], as it produces the most elaborate nucleon and N^* wave functions.

In Table 1 we present a selection of results for the axial charges g_A of the nucleon and the $N^*(1440)$, $N^*(1710)$, $N^*(1535)$, as well as $N^*(1650)$ resonances in case of the EGBE RCQM. It is immediately evident that the EGBE RCQM produces reasonable values for the axial charges in all instances without any further fittings. In the cases where a comparison is possible it produces the same pattern as lattice QCD. The g_A of the nucleon and of $N^*(1440)$ are practically of the same size, with the theoretical result for the nucleon being quite close to the experi-

* Talk delivered by Ki-Seok Choi

mental value of g_A=1.2695±0.0029 [15]. The nonrelativistic calculations cannot produce this value, neither in the simplistic $SU(6) \times O(3)$ quark model nor in the nonrelativistic limit of the RCQM. For the negative-parity $N^*(1535)$ resonance the g_A is predicted to be compatible with 0, while for the negative-parity $N^*(1650)$ resonance it is 0.51; both cases agree with the lattice-QCD results of Ref. [1]. Accidentally, the g_A value of the nonrelativistic $SU(6) \times O(3)$ quark model is similar in the $N^*(1650)$ case but the nonrelativistic limit of the EGBE RCQM shows deviations for both of the $\frac{1}{2}^-$ resonances. At this time nothing is known from lattice QCD for the $\frac{1}{2}^+$ resonances. For the latter, it would also be most interesting to check our results against lattice QCD, and we look forward to corresponding calculations.

Table 1. Predictions for axial charges g_A of the EGBE in comparison to available lattice QCD results [1-7], the values calculated by Glozman and Nefediev [9] within the $SU(6) \times O(3)$ nonrelativistic quark model, and the nonrelativistic limit from the EGBE RCQM.

State	J^P	EGBE	Lattice QCD	$SU(6) \times O(3)$ QM	EGBE nonrel
N(939)	$\frac{1}{2}^+$	1.15	1.10~1.40	1.66	1.65
N(1440)	$\frac{1}{2}^+$	1.16	–	1.66	1.61
N(1535)	$\frac{1}{2}^-$	0.02	~0.00	-0.11	-0.20
N(1710)	$\frac{1}{2}^+$	0.35	–	0.33	0.42
N(1650)	$\frac{1}{2}^-$	0.51	~0.55	0.55	0.64

It is particularly satisfying to find the RCQM predictions for the axial charges of the $N^*(1535)$ and $N^*(1650)$ resonances in agreement with the lattice-QCD results. We may thus be confident that at least for zero momentum-transfer processes the mass eigenstates of these nucleon excitations as produced especially with EGBE RCQM are quite reasonable. The latter is supposed to model the SBχS property of low-energy QCD. This type of hyperfine interaction, which also introduces an explicit flavor dependence, has been remarkably successful in describing a number of phenomena in low-energy baryon physics. Most prominently, it produces the correct level orderings of the positive- and negative-parity N^* resonances and simultaneously the ones in the other hyperon spectra, notably the Λ spectrum. The RCQM with GBE dynamics does not have any mechanism for chiral-symmetry restoration built in. As such it cannot be expected to produce parity doublets due to this reason. Nevertheless the EGBE RCQM describes the N^* resonance masses with good accuracy (mostly within the experimental error bars or at most exceeding them by 4%).

Acknowledgments K-S. C. is grateful to the organizers of the Mini-Workshop for the invitation and for creating such a lively working atmosphere. This work was supported by the Austrian Science Fund (through the Doctoral Program on *Hadrons in Vacuum, Nuclei, and Stars*; FWF DK W1203-N08).

References

1. T. T. Takahashi and T. Kunihiro, Phys. Rev. D **78**, 011503 (2008).
2. D. Dolgov *et al.* [LHPC collaboration and TXL Collaboration], Phys. Rev. D **66**, 034506 (2002).
3. R. G. Edwards *et al.* [LHPC Collaboration], Phys. Rev. Lett. **96**, 052001 (2006).
4. A. A. Khan *et al.*, Phys. Rev. D **74**, 094508 (2006).
5. T. Yamazaki *et al.* [RBC+UKQCD Collaboration], Phys. Rev. Lett. **100**, 171602 (2008).
6. H. W. Lin, T. Blum, S. Ohta, S. Sasaki and T. Yamazaki, Phys. Rev. D **78**, 014505 (2008).
7. C. Alexandrou *et al.*, PoS(LATTICE 2008), 139 (2008); arXiv:0811.0724 [hep-lat].
8. V. Bernard, Prog. Part. Nucl. Phys. **60**, 82 (2008).
9. L. Y. Glozman, Phys. Rept. **444**, 1 (2007).
10. L. Y. Glozman and A. V. Nefediev, Nucl. Phys. A **807**, 38 (2008).
11. L. Y. Glozman, M. Radici, R. F. Wagenbrunn, S. Boffi, W. Klink and W. Plessas, Phys. Lett. B **516**, 183 (2001).
12. S. Boffi, L. Y. Glozman, W. Klink, W. Plessas, M. Radici and R. F. Wagenbrunn, Eur. Phys. J. A **14**, 17 (2002).
13. T. Melde, L. Canton, W. Plessas and R. F. Wagenbrunn, Eur. Phys. J. A **25**, 97 (2005).
14. K. Glantschnig, R. Kainhofer, W. Plessas, B. Sengl and R. F. Wagenbrunn, Eur. Phys. J. A **23**, 507 (2005).
15. C. Amsler *et al.* [Particle Data Group], Phys. Lett. B **667**, 1 (2008).

Bled Workshops
in Physics
Vol. 10, No. 1
p. 31

Proceedings of the Mini-Workshop
Problems in Multi-Quark States
Bled, Slovenia, June 29 - July 6, 2009

Nucleon axial couplings and $[(\frac{1}{2},0)\oplus(0,\frac{1}{2})]$–$[(1,\frac{1}{2})\oplus(\frac{1}{2},1)]$ chiral multiplet mixing*

V. Dmitrašinović[a], A. Hosaka[b], K. Nagata[c]

[a] Vinča Institute of Nuclear Sciences, lab 010, P.O.Box 522, 11001 Beograd, Serbia
[b] Research Center for Nuclear Physics, Osaka University, Mihogaoka 10-1, Osaka 567-0047, Japan
[c] Research Institute for Information Science and Education, Hiroshima University, Higashi-Hiroshima 739-8521, Japan

Abstract. Three-quark nucleon interpolating fields in QCD have well-defined, $U_A(1)$ and $SU_L(2)\times SU_R(2)$ chiral transformation properties: mixing of the $[(1,\frac{1}{2})\oplus(\frac{1}{2},1)]$ chiral multiplet with one (of four available) $[(\frac{1}{2},0)\oplus(0,\frac{1}{2})]$, or $[(0,\frac{1}{2})\oplus(\frac{1}{2},0)]$ fields can be used to fit the isovector axial coupling $g_A^{(1)}$ and thus predict the isoscalar axial coupling $g_A^{(0)}$ of the nucleon, in reasonable agreement with experiment. We also use a chiral meson-baryon interaction to calculate the masses and one-pion-interaction terms of $J=\frac{1}{2}$ baryons belonging to the $[(0,\frac{1}{2})\oplus(\frac{1}{2},0)]$ and $[(1,\frac{1}{2})\oplus(\frac{1}{2},1)]$ chiral multiplets and fit two of the diagonalized masses to the lowest-lying nucleon resonances thus predicting the third $J=\frac{1}{2}$ resonance at 2030 MeV, not far from the (one-star PDG) state $\Delta(2150)$.

1 Introduction

Almost 40 years ago Weinberg [1] considered mixing of chiral multiplets in the broken symmetry phase. In general such representation mixing may be complicated, but if only a few states are mixed, it may have predictive power. For instance, Weinberg used the mixing of $[(\frac{1}{2},0)\oplus(0,\frac{1}{2})]$ and $[(1,\frac{1}{2})\oplus(\frac{1}{2},1)]$ to explain the nucleon's isovector axial coupling constant $g_A^{(1)}=1.23$, its value at the time (the present value being 1.267). Weinberg's idea predated QCD and did not even invoke the existence of quarks, but it may still be viable in QCD. Indeed, this idea was revived in the early 1990's, since when it has been known by the name of mended symmetry [2].

The nucleon also has an isoscalar axial coupling $g_A^{(0)}$, which has been estimated from spin-polarized lepton-nucleon DIS data as $g_A^{(0)}=0.28\pm0.16$ [3], or the more recent value $0.33\pm0.03\pm0.05$ [4]. The question is if the same chiral mixing angle can also explain the anomalously low value of this coupling? The answer manifestly depends on the $U_A(1)$ chiral transformation properties of the two admixed nucleon fields.

* Talk delivered by V. Dmitrašinović

In this paper we address this question using the $U_A(1)$ chiral transformation properties of nucleon fields [6,7] as derived from the three-quark nucleon interpolating fields in QCD. If the answer to our question turns out in the positive, we may speak about Weinberg's idea being viable in QCD. To test the present idea, besides the phenomenological study, we also investigate an extended linear sigma model containing baryon resonances, where we evaluate the axial couplings using baryon masses as input.

2 Three-quark nucleon interpolating fields

We start by summarizing the transformation properties of various quark trilinear forms with quantum numbers of the nucleon as shown in Refs. [6,7]. It turns out that every nucleon, i.e., spin- and isospin 1/2 field, besides having same non-Abelian transformation properties, comes in two varieties: one with "mirror" and another with "triple-naive" Abelian chiral properties.

In Table 1 we show the Abelian and non-Abelian chiral properties of the nucleon interpolating fields in QCD, Ref. [6,7]. Here we shall use those results as the theoretical input into our calculations. This constitutes a minimal assumption, as one has no other guide to the chiral representations of the nucleon. In Refs. [5–7] the local (non-derivative) spin $\frac{1}{2}$ baryon operators

$$N_1 = \epsilon_{abc}(\tilde{q}_a q_b) q_c, \tag{1}$$

$$N_2 = \epsilon_{abc}(\tilde{q}_a \gamma^5 q_b)\gamma^5 q_c, \tag{2}$$

were classified according to their Lorentz, chiral $SU_L(2) \times SU_R(2)$ (so-called "naive" chiral multiplet, whose axial charge is positive) and $U_A(1)$ group representations. Here we have introduced the "tilde-transposed" quark field $\tilde{q}$ as $\tilde{q} = q^T C\gamma_5(i\tau_2)$, where $C = i\gamma_2\gamma_0$ is the Dirac field charge conjugation operator, τ_2 is the second isospin Pauli matrix. Once one allows for the presence of one derivative, such as the so-called "mirror" $(0, \frac{1}{2}) \oplus (\frac{1}{2}, 0)$, whose axial charge is negative, Ref.[8],

$$N'_1 = \epsilon_{abc}(\tilde{q}_a q_b) i\partial_\mu \gamma^\mu q_c, \tag{3}$$

$$N'_2 = \epsilon_{abc}(\tilde{q}_a \gamma^5 q_b) i\partial_\mu \gamma^\mu \gamma^5 q_c. \tag{4}$$

and the $(1, \frac{1}{2}) \oplus (\frac{1}{2}, 1)$ nucleon chiral representation

$$N'_3 = i\partial_\mu(\tilde{q}\gamma_\nu q)\Gamma^{\mu\nu}_{3/2}\gamma_5 q, \tag{5}$$

$$N'_4 = i\partial_\mu(\tilde{q}\gamma_\nu\gamma_5\tau^i q)\Gamma^{\mu\nu}_{3/2}\tau^i q, \tag{6}$$

also become Pauli allowed, see Table 1. Here $\Gamma^{\mu\nu}_{3/2} = g^{\mu\nu} - \frac{1}{4}\gamma^\mu\gamma^\nu$. We found that indeed, as Gell-Mann and Levy [9] had postulated, the lowest-twist (non-derivative) J= $\frac{1}{2}$ nucleon field(s) form a $(\frac{1}{2}, 0)$ chiral multiplet, albeit there are two such independent fields. There is only one set of J= $\frac{1}{2}$ Pauli-allowed subleading-twist (one-derivative) interpolating fields that form a $(1, \frac{1}{2})$ chiral multiplet, however.

Table 1. The Abelian and the non-Abelian axial charges (+ sign indicates "naive", − sign "mirror" transformation properties) and the non-Abelian chiral mutiplets of $J^P = \frac{1}{2}$, Lorentz representation $(\frac{1}{2}, 0)$ nucleon fields. The field denoted by 0 belongs to the $(1, \frac{1}{2}) \oplus (\frac{1}{2}, 1)$ chiral multiplet and is the basic nucleon field that is mixed with various $(\frac{1}{2}, 0)$ nucleon fields in Eq. (7).

case	field	$g_A^{(0)}$	$g_A^{(1)}$	$SU_L(2) \times SU_R(2)$
I	$N_1 - N_2$	-1	$+1$	$(\frac{1}{2}, 0) \oplus (0, \frac{1}{2})$
II	$N_1 + N_2$	$+3$	$+1$	$(\frac{1}{2}, 0) \oplus (0, \frac{1}{2})$
III	$N_1^{'} - N_2^{'}$	$+1$	-1	$(0, \frac{1}{2}) \oplus (\frac{1}{2}, 0)$
IV	$N_1^{'} + N_2^{'}$	-3	-1	$(0, \frac{1}{2}) \oplus (\frac{1}{2}, 0)$
0	$N_3^{'} + \frac{1}{3} N_4^{'}$	$+1$	$+\frac{5}{3}$	$(1, \frac{1}{2}) \oplus (\frac{1}{2}, 1)$

3 Mixing of two chiral representations

Next consider the mixing of one of the fundamental chiral representations, as shown in Table 1 and the "higher" representation $(1, \frac{1}{2})$ for the nucleon,

$$\begin{aligned} g_{A\ \mathrm{mix.}}^{(1)} &= g_{A,\,\alpha}^{(1)} \cos^2\theta + g_{A\ (1,\frac{1}{2})}^{(1)} \sin^2\theta, \\ &= g_{A,\,\alpha}^{(1)} \cos^2\theta + \frac{5}{3} \sin^2\theta = 1.267. \end{aligned} \tag{7}$$

Here the suffix α corresponds to one of I-IV and the corresponding values of $g_{A,\,\alpha}^{(1)}$ are given in Table 1. We have also used the fact that $g_{A\ (1,\frac{1}{2})}^{(1)} = \frac{5}{3}$, see Ref. [1,7].

This provides a possible solution to the nucleon's axial coupling problem in QCD. Three-quark nucleon interpolating fields in QCD have well-defined two-fold $U_A(1)$ chiral transformation properties, see Table 1, that can be used to (naively) predict the isoscalar axial coupling $g_{A\ \mathrm{mix.}}^{(0)}$ as follows

$$g_{A\ \mathrm{mix.}}^{(0)} = g_{A,\,\alpha}^{(0)} \cos^2\theta + g_{A\ (1,\frac{1}{2})}^{(0)} \sin^2\theta, \tag{8}$$

together with the mixing angle θ extracted from Eq. (7). Note, however, that due to the different (bare) non-Abelian $g_A^{(1)}$ and Abelian $g_A^{(0)}$ axial couplings, see Table 1, the mixing formulae Eq. (8) give substantially different predictions from one case to another, see Table 2. We can see in Table 2 that the two candidates are cases I and IV, with $g_A^{(0)} = -0.2$ and $g_A^{(0)} = 0.4$, respectively, the latter being within 1-σ of the measured value $g_A^{(0)} = 0.33 \pm 0.08$. The nucleon field in case I is the well-known "Ioffe current", which reproduces the nucleon's properties in QCD lattice and sum rules calculations. The nucleon field in case IV is a "mirror" opposite of the orthogonal complement to the Ioffe current, an interpolating field that, to our knowledge, has not been used in QCD thus far.

3.1 A Simple Model

The next step is to try and reproduce this phenomenological mixing starting from a model interaction, rather than *per fiat*. As the first step in that direction we

Table 2. The values of the baryon isoscalar axial coupling constant predicted from the naive mixing and $g_{A\ \mathrm{expt.}}^{(1)} = 1.267$; compare with $g_{A\ \mathrm{expt.}}^{(0)} = 0.33 \pm 0.03 \pm 0.05$.

case	$(g_A^{(1)}, g_A^{(0)})$	$g_{A\ \mathrm{mix.}}^{(1)}$	θ	$g_{A\ \mathrm{mix.}}^{(0)}$	$g_{A\ \mathrm{mix.}}^{(0)}$
I	$(+1,-1)$	$\frac{1}{3}(4-\cos 2\theta)$	$\pm 39.3^o$	$-\cos 2\theta$	-0.20
II	$(+1,+3)$	$\frac{1}{3}(4-\cos 2\theta)$	$\pm 39.3^o$	$2+\cos 2\theta$	2.20
III	$(-1,+1)$	$\frac{1}{3}(1-4\cos 2\theta)$	$\pm 67.2^o$	1	1.00
IV	$(-1,-3)$	$\frac{1}{3}(1-4\cos 2\theta)$	$\pm 67.2^o$	$-(1+2\cos 2\theta)$	0.40

must look for a dynamical source of mixing. One such mechanism is the simplest chirally symmetric *non-derivative* one-(σ,π)-meson interaction Lagrangian, which induces baryon masses via its σ-meson coupling. We shall show that only the mirror fields couple to the $(1,\frac{1}{2})$ baryon chiral multiplet by non-derivative terms; the naive ones require one (or odd number of) derivative. This is interesting, as we have already pointed out that the mixing case IV seems a preferable one from the phenomenological consideration of axial couplings.

We use the projection method of Ref. [10] to construct the chirally invariant diagonal and off-diagonal meson-baryon-baryon interactions involving the "mirror" baryon $B_1 \in (0,\frac{1}{2})$, the $(B_2,\Delta) \in (1,\frac{1}{2})$ baryon and one $(\sigma,\pi) \in (\frac{1}{2},\frac{1}{2})$ meson chiral multiplets. Here all baryons have spin $1/2$, while the isospin of B_1 and B_2 is $1/2$ and that of Δ is $3/2$. The Δ field is then represented by an isovector-isospinor field Δ^i, $(i = 1,2,3)$. We found that for non-derivative mixing interaction the following chirally invariant combination

$$\mathcal{L}_3 = -g_3\left[\bar{B}_1(\sigma + \frac{i}{3}\gamma_5\tau\cdot\pi)B_2 + 4\bar{B}_1 i\gamma_5\pi^i\Delta^i + \mathrm{h.c.}\right], \tag{9}$$

with the coupling constant g_3 induces an off-diagonal term in the baryon mass matrix after spontaneous symmetry breaking $\langle\sigma\rangle_0 \to f_\pi$ via its σ-meson coupling. Of course this is in addition to the conventional diagonal interactions:

$$\mathcal{L}_1 = -g_1\bar{B}_1\,(\sigma - i\gamma_5\tau\cdot\pi)\,B_1, \tag{10}$$

$$\mathcal{L}_2 = -\frac{2}{3}g_2\Big[\bar{B}_2(\sigma + \frac{5}{3}i\gamma_5\tau\cdot\pi)B_2 - 2\bar{\Delta}^i(\sigma + i\gamma_5\tau\cdot\pi)\Delta^i - \frac{1}{\sqrt{3}}\bar{B}_2\tau^i(\sigma + i\gamma_5\tau\cdot\pi)\Delta^i + \mathrm{h.c.}\Big], \tag{11}$$

In writing down the Lagrangians (9,10,11), we have implicitly assumed that the parities of B_1, B_2 and Δ are the same. In principle, their parities are arbitrary, except for the parity of the ground state nucleon, which must be even. For instance, if B_2 has odd parity, the first term in the interaction Lagrangian Eq. (9) must include another γ_5 matrix. Here we consider all possible cases for the parities of B_2 and Δ.

Having established the mixing interaction Eq. (9), as well as the diagonal terms Eqs. (10),(11), we calculate the masses of the baryon states, as functions of the pion decay constant/chiral order parameter and (as yet undetermined)

Born approximation coupling constants. We diagonalize the mass matrix and express the mixing angle in terms of diagonalized masses. We find the following double-angle formulas for the mixing angles $\theta_{1,\ldots,4}$, in the four different parities scenarios

$$\tan 2\theta_1 = \frac{\sqrt{(2N+\Delta)(2N^{*-}-\Delta)}}{(\Delta - N + N^{*-})}, \tag{12}$$

$$\tan 2\theta_2 = \frac{\sqrt{(\Delta-2N)(2N^{*+}-\Delta)}}{(N + N^{*+} - \Delta)} \tag{13}$$

$$\tan 2\theta_3 = \frac{\sqrt{(2N-\Delta)(2N^{*-}+\Delta)}}{(\Delta - N + N^{*-})}, \tag{14}$$

$$\tan 2\theta_4 = \frac{\sqrt{-(\Delta+2N)(2N^{*+}+\Delta)}}{(N + N^{*+} + \Delta)}, \tag{15}$$

where N is the nucleon ground state mass (940 MeV) and $N^{*\pm}, \Delta$ are the masses of the nucleon excited state, where $\pm$ indicates the parity of the N^* state. These angles correspond to the two (variable) parities as follows $\theta_1 \leftrightarrow (N^{*-}, \Delta^+)$, $\theta_2 \leftrightarrow (N^{*+}, \Delta^-)$, $\theta_3 \leftrightarrow (N^{*-}, \Delta^-)$, $\theta_4 \leftrightarrow (N^{*+}, \Delta^+)$, where $\pm$ indicates the parity of the state. Note that the angle θ_4 is necessarily imaginary so long as the Δ, N^* masses are physical (positive), and that the reality of the mixing angle(s) imposes stringent limits on the Δ, N^* resonance masses in other three cases, as well. Next, we use (some of) the observed resonance masses to determine the mixing angle(s) and thence calculate the axial couplings.

3.2 Results

Direct prediction

The four lowest-lying (besides the $N(940)$) candidate states in the PDG tables are: $R(1440)$, $N(1535)$, $\Delta(1620)$, $\Delta(1910)$, we use them to fit the free coupling constants. Of the two "mass allowed" scenarios, however, none survive the axial coupling test. Perhaps our choice of input resonances is inadequate. Note that one may "invert" this procedure, however, and use the isovector axial coupling to predict one of the baryon masses, say the Δ's, having fixed the other two, in this case the nucleon's $N(940)$ and $N^*(1440)$ or $N^*(1535)$.

Inverse prediction

Next, we use the double-angle formulas Eqs. (12)-(15) for the mixing angles $\theta_{1,\ldots,4}$ together with the two observed nucleon masses to predict the Δ masses shown in the Table 3. We see that only the (N^{*+}, Δ^-) parity case leads to a realistic prediction: The difference between the observed (one-star) $S_{31}(2150)$ [11] Δ resonance mass and the predicted 2030 MeV may be neglected in view of the uncertainties and typical widths of states at such (high) energies. We shall not attach undue significance to this proximity in view of the rather uncertain status of this resonance, at least not until it is confirmed by another experiment. This choice of resonances leads to a reasonable πNN coupling constant (14.2 vs. 13.6 expt.) and predicts a set of as yet not measured π-baryon couplings.

Table 3. The values of the Δ baryon masses predicted from the isovector axial coupling $g_{A\ \mathrm{mix.}}^{(1)} = g_{A\ \mathrm{expt.}}^{(1)} = 1.267$ and $g_{A\ \mathrm{mix.}}^{(0)} = 0.4$ vs. $g_{A\ \mathrm{expt.}}^{(0)} = 0.33 \pm 0.08$.

$(N^{*P}, \Delta^{P'})$	$(N,\ N^*)$	Δ (MeV)	expt.
$(-,+)$	N(940), R(1535)	2330	1910
$(+,-)$	N(940), R(1440)	2030,2730	1620,2150
$(-,-)$	N(940), R(1535)	1140	1620,2150

A comment about the comparatively high value of the Δ mass seems to be in order now: In the mid-1960-s Hara [12] noticed that the chiral transformation rules for a $(1, \frac{1}{2})$ multiplet impose a strict and seemingly improbable mass relation among its two members: $m_\Delta = 2m_N$. The mixing with the $(\frac{1}{2}, 0)$ multiplet modifies this mass relation for the worse, i.e. it makes the Δ even heavier. For this reason, the lowest-lying Δ's of either parity cannot be the chiral partners of the nucleon ground state, as we initially assumed in our "direct prediction".

4 Three-field mixing

A linear superposition of yet another field (except for the mixture of cases II and III above) ought to give a perfect fit to both experimental values. Such an admixture introduces new free parameters (besides the two already introduced mixing angles, e.g. θ_1 and θ_4, we have the relative/mutual mixing angle θ_{14}, as the two nucleon fields I and IV may also mix). One may subsume/redefine the sum and the difference of the two angles θ_1 and θ_4 into the new angle θ, whereas one may define $\theta_{14} \doteq \varphi$ (this relationship depends on the precise definition of the mixing angles θ_1, θ_4 and θ_{14}); thus we find two equations with two unknowns of the general form:

$$\frac{5}{3}\sin^2\theta + \cos^2\theta\ \left(g_A^{(1)}\cos^2\varphi + g_A^{(1)\prime}\sin^2\varphi\right) = 1.267 \tag{16}$$

$$\sin^2\theta + \cos^2\theta\ \left(g_A^{(0)}\cos^2\varphi + g_A^{(0)\prime}\sin^2\varphi\right) = 0.33 \tag{17}$$

The values of the mixing angles obtained from this simple fit to the two baryon axial coupling constants are shown in Table 4. This, however, is not just a mere fit: when extending to the $SU_L(3) \times SU_R(3)$ symmetry, chiral transformation properties of the nucleon fields differ: $N_1 - N_2 \in [(\bar{3}, 3) \oplus (3, \bar{3})]$, $N_1 + N_2 \in [(8, 1) \oplus (1, 8)]$ and $(N_3' + \frac{1}{3}N_4') \in [(6, 3) \oplus (3, 6)]$, see Ref. [13]. From these chiral $SU_L(3) \times SU_R(3)$ symmetry assignment we can also predict the F and D couplings (un-corrected for the explicit $SU_F(3)$ symmetry breaking) in Table 4, which can be compared with the experimental numbers. We have not calculated the $SU_F(3)$ symmetry breaking corrections, as yet, so we have not taken into account the "error bars" on the mixing angle(s), which remains a task for the future. At any rate, it should be clear that the predicted values are "in the right ball park" for most of the scenarios considered here. Thus, the chiral multiplet mixing remains a viable theoretical scenario for the explanation of the nucleon isoscalar axial couplings.

Table 4. The values of the mixing angles obtained from the fit to the baryon axial coupling constants and the predicted values of axial F and D couplings. Experimental values have evolved from F=0.459 $\pm$ 0.008 and D=0.798 $\pm$ 0.008 in Ref. [14] to F=0.477 $\pm$ 0.001 and D=0.835 $\pm$ 0.001 in Ref. [15]. Note that the new values are more than 2-σ away from the old ones, and that the new F,D add up to F+D = 1.312 $\neq$ 1.269 $\pm$ 0.002.

case	$g_{A\ expt.}^{(0)}$	$g_{A\ expt.}^{(1)}$	θ	φ	F	D
I-II	1.267	0.33	39.3°	26.6°	0.399	0.868
I-III	1.267	0.33	49.6°	23.9°	0.333	0.934
I-IV	1.267	0.33	63.2°	53.9°	0.399	0.868

5 Summary and Discussion

We have shown that one can reproduce, within 1-σ uncertainty, the (unexpectedly small) isoscalar axial coupling of the nucleon by mixing (only) two (out of five independent) nucleon interpolating fields [1] by fitting the isovector- axial coupling. This solution to the nucleon spin problem does not invoke exotica such as a) hidden strangeness; or b) polarized gluon components in the nucleon wave function, in agreement with recent results of the COMPASS experiment [16],[17]. This scenario is quantitatively reproduced in a simple dynamical model which then predicts the existence of the S_{31} resonance at 2160 MeV, in agreement with the PDG tables [11]. By mixing three nucleon interpolating field chiral multiplets one may simultaneously fit both the isovector and the isoscalar axial couplings and predict the SU(3) F and D couplings, which have the correct size within the expected $\mathcal{O}(20\%)$ SU(3) symmetry breaking corrections.

References

1. S. Weinberg, Phys. Rev. **177**, 2604 (1969).
2. S. Weinberg, Phys. Rev. Lett. **65**, 1177 (1990).
3. B. W. Filippone and X. D. Ji, Adv. Nucl. Phys. **26**, 1 (2001) [arXiv:hep-ph/0101224].
4. S. D. Bass, "*The Spin structure of the proton*," World Scientific, 2007. (ISBN 978-981-270-946-2 and ISBN 978-981-270-947-9). 212 p.
5. V. Dmitrašinović, K. Nagata, and A. Hosaka, "Does nucleon parity doubling imply $U_A(1)$ symmetry restoration?", p. 17 - 23, Proceedings of the Mini-Workshop "Hadron structure and lattice QCD", "Bled Workshops in Physics", Vol. 8, No. 8, ed. B. Golli, M. Rosina and S. Širca, DMFA-Založništvo, Ljubljana, Slovenia, (2007).
6. V. Dmitrašinović, K. Nagata, and A. Hosaka, Mod. Phys. Lett. A **23**, 2381 (2008) [arXiv:0705.1896 [hep-ph]].
7. K. Nagata, A. Hosaka and V. Dmitrašinović, Eur. Phys. J. C **57** (2008) 557.
8. D. Jido, M. Oka and A. Hosaka, Prog. Theor. Phys. **106**, 873 (2001)
9. M. Gell-Mann and M. Levy, Nuovo Cim. **16**, 705 (1960).
10. K. Nagata, A. Hosaka and V. Dmitrašinović, Phys. Rev. Lett. **101**, 092001 (2008) [arXiv:0804.3185 [hep-ph]].
11. W. M. Yao *et al.* [Particle Data Group], J. Phys. G **33** (2006) 1.

[1] or equivalently relativistic component in the nucleon's Bethe-Salpeter wave function

12. Y. Hara, Phys. Rev. 139, B**134** (1965).
13. H. X. Chen, V. Dmitrašinović, A. Hosaka, K. Nagata and S. L. Zhu, Phys. Rev. D **78**, 054021 (2008) [arXiv:0806.1997 [hep-ph]].
14. P. G. Ratcliffe, Phys. Lett. B **242**, 271 (1990).
15. T. Yamanishi, Phys. Rev. D **76**, 014006 (2007) [arXiv:0705.4340 [hep-ph]].
16. E. S. Ageev *et al.* [Compass Collaboration], Phys. Lett. B **647**, 330 (2007) [arXiv:hep-ex/0701014].
17. M. Alekseev *et al.* [COMPASS Collaboration], arXiv:0802.3023 [hep-ex].

BLED WORKSHOPS
IN PHYSICS
VOL. 10, NO. 1
p. 39

Proceedings of the Mini-Workshop
Problems in Multi-Quark States
Bled, Slovenia, June 29 - July 6, 2009

Quadrupole polarizabilities of the pion in the Nambu–Jona-Lasinio model*

Brigitte Hiller[a], Wojciech Broniowski[b,c], Alexander A. Osipov[a,d], Alex H. Blin[a]

[a] Centro de Física Computacional, Departamento de Física da Universidade de Coimbra, 3004-516 Coimbra, Portugal
[b] The H. Niewodniczański Institute of Nuclear Physics, Polish Academy of Sciences, PL-31342 Cracow, Poland
[c] Institute of Physics, Jan Kochanowski University, PL-25406 Kielce, Poland
[d] Dzhelepov Laboratory of Nuclear Problems, JINR, 141980 Dubna, Russia

Abstract. We present the results for the pion electromagnetic quadrupole polarizabilities, calculated within the Nambu–Jona-Lasinio model. We obtain the sign and magnitude in agreement with the respective experimental analysis based on the Dispersion Sum Rules. At the same time the dipole polarizabilities are well reproduced. Comparison is also made with the results from the Chiral Perturbation Theory.

The neutral and charged pion dipole and quadrupole polarizabilities have been recently analyzed using the Dispersion Relations (DR) and the Dispersion Sum Rules (DSR) [1,2], as displayed in Tables 2 and 3, together with the results of the Chiral Perturbation Theory (χPT) [3–5]. The first row shows our results based on the Nambu–Jona-Lasinio model (NJL) [6] model; for that purpose we have extended [7] the study of Ref. [8], where the dipole polarizabilities have been calculated, to the quadrupole case. We refer to these papers for details.

Our leading-N_c calculations are done according to the Feynman diagrams of Fig. 1. The amplitude is a function of the Mandelstam variables related to the $\gamma(p_1,\epsilon_1)+\gamma(p_2,\epsilon_2)\to\pi^a(p_3)+\pi^b(p_4)$ reaction for the on-shell pions and photons,

$$T(p_1,p_2,p_3)=e^2\epsilon_1^\mu\epsilon_2^\nu T_{\mu\nu},\quad T_{\mu\nu}=A(s,t,u)\mathcal{L}_1^{\mu\nu}+B(s,t,u)\mathcal{L}_2^{\mu\nu},$$

with the Lorentz tensors

$$\mathcal{L}_1^{\mu\nu}=p_2^\mu p_1^\nu-\frac{1}{2}sg^{\mu\nu},\qquad \mathcal{L}_2^{\mu\nu}=-\left(\frac{1}{2}u_1t_1g^{\mu\nu}+t_1p_2^\mu p_3^\nu+u_1p_3^\mu p_1^\nu+sp_3^\mu p_3^\nu\right).$$

Terms that vanish upon the conditions $\epsilon_1\cdot p_1=\epsilon_2\cdot p_2=0$ are omitted and the notation $\xi_1=\xi-m_\pi^2$, $\xi=s,t,u$ is used. The scalar quantities A and B enter the amplitudes $H_{++}=-(A+m_\pi^2B)$ and $H_{+-}=(u_1t_1/s-m_\pi^2)B$ for the equal-helicity and helicity-flipped photons. The dipole, α_1^i, β_1^i, and quadrupole,

* Talk delivered by Brigitte Hiller

α_2^i, β_2^i, polarizabilities are obtained in the t-channel and extracted from the first two coefficients of the Taylor expansion of the amplitudes $\alpha A^i(s,t,u)/(2m_\pi)$ and $-\alpha m_\pi B^i(s,t,u)$ around $s=0$ with $u=t=m_\pi^2$ [9],

$$\frac{\alpha}{2m_\pi}\left(A^i(0,m_\pi^2,m_\pi^2)+s\frac{d}{ds}A^i(0,m_\pi^2,m_\pi^2)\right)=\beta_1^i+\frac{s}{12}\beta_2^i,$$
$$-\alpha m_\pi\left(B^i(0,m_\pi^2,m_\pi^2)+s\frac{d}{ds}B^i(0,m_\pi^2,m_\pi^2)\right)=(\alpha_1+\beta_1)^i+\frac{s}{12}(\alpha_2+\beta_2)^i,$$

where the superscripts $i=N,C$ denote the neutral and charged pions, respectively, and $\alpha\simeq 1/137$ is the fine structure constant. The Born term, arising in the case of the charged pion, is removed from the amplitudes.

The NJL Lagrangian used in this work contains pseudoscalar isovector and scalar isoscalar four-quark interactions and is minimally coupled to the electromagnetic field.

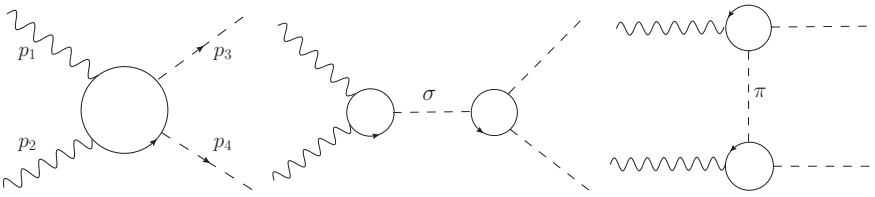

Fig. 1. Leading-N_c quark-loop diagrams for the $\gamma\gamma\to\pi\pi$ amplitude. The crossed terms are not displayed.

The diagrams of Fig. 1 provide polarizabilities which scale as N_c^0. Besides the quark one-loop diagrams, it is expected that the pion loops yield important contributions, mainly in the case where the tree-level results are absent (in the NJL model the chiral counting of meson tree-level results are classified in Refs. [8,10]). We include the lowest model-independent pion-loop diagram at the p^4 order, calculated within χPT in Refs. [11–13], and known to be the only non-vanishing contribution to the amplitude A at this order in the neutral channel. The pion loop in the charged mode contributes only to the quadrupole polarizabilities, with half the strength of the neutral quadrupole case. The pion loop as well as the σ-exchange diagram of Fig. 1 enter only the amplitude A.

The amplitude B for the neutral (charged) mode is completely determined by the quark box (quark box + pion exchange) diagrams, starting from the p^6 order for the dipole and from the p^8 order for the quadrupole polarizabilities. Thus the combinations $(\alpha_j+\beta_j)^i$, $(j=1,2)$, to which the B amplitude leads, provide a genuine test of the dynamical predictions of the NJL model at the leading order in $1/N_c$, as they are insensitive to the lowest-order χPT corrections.

All quark one-loop integrals are regularized using the Pauli-Villars prescription with one regulator Λ and two subtractions, which is consistent with the requirements of gauge invariance.

Table 1. The NJL model parameters for the charged and neutral channels, with the input marked by * and $f_\pi^* = 93.1$ MeV.

M^* [MeV]	m_π^* [MeV]	m [MeV]	G [GeV^{-2}]	Λ [MeV]
300	139	7.5	13.1	827
300	136	7.2	13.1	827

Table 2. The dipole (in units of 10^{-4}fm^3) and quadrupole (in units of 10^{-4}fm^5) neutral pion polarizabilities. The first row shows our model prediction at $M = 300$ MeV.

	$(\alpha_1+\beta_1)_{\pi^0}$	$(\alpha_1-\beta_1)_{\pi^0}$	$(\alpha_2+\beta_2)_{\pi^0}$	$(\alpha_2-\beta_2)_{\pi^0}$
$M = 300$ MeV	0.73	-1.56	-0.14	36.1
DR fit [1]	0.98 ± 0.03	-1.6 ± 2.2	-0.181 ± 0.004	39.70 ± 0.02
DSR [1]	0.802 ± 0.035	-3.49 ± 2.13	-0.171 ± 0.067	39.72 ± 8.01
χPT [5,3]	1.1 ± 0.3	-1.9 ± 0.2	0.037 ± 0.003	37.6 ± 3.3

Table 3. Same as in Table 2 for the dipole and quadrupole charged pion polarizabilities.

	$(\alpha_1+\beta_1)_{\pi^\pm}$	$(\alpha_1-\beta_1)_{\pi^\pm}$	$(\alpha_2+\beta_2)_{\pi^\pm}$	$(\alpha_2-\beta_2)_{\pi^\pm}$
$M = 300$ MeV	0.19	9.4	0.20	17.5
DR fit [2]	$0.18^{+0.11}_{-0.02}$	$13.0^{+2.6}_{-1.9}$	0.133 ± 0.015	$25.0^{+0.8}_{-0.3}$
DSR [2]	0.166 ± 0.024	13.60 ± 2.15	0.121 ± 0.064	25.75 ± 7.03
χPT [5,4]	0.16	5.7 ± 1.0	-0.001	16.2

In Table 1 we collect the model parameters, obtained by fitting the physical pion mass and the weak decay constant. The parameters of the model are the four-quark coupling constant G, the cutoff Λ, and the current quark mass m. These are determined by the choice of $f_\pi = 93.1$ MeV, $m_\pi = 139$ MeV (charged mode) or $m_\pi = 136$ MeV (neutral mode), and the constituent quark mass, M. In Table 4 we present the anatomy of our result for the case $M = 300$ MeV. We display separately all the gauge invariant contributions to the polarizabilities: the box (for neutral polarizabilities), box + pion exchange diagram (for the charged polarizabilities), the σ exchange, and the pion loop. The pion exchange diagram arises only for the charged channel and builds together with the box a gauge invariant amplitude. Let us first comment on the channels involving the difference of the electric and magnetic polarizabilities:

• $(\alpha_1 - \beta_1)_{\pi^0}$: here the box contribution is largely canceled by the scalar exchange. At the p^4-order of the chiral counting they cancel exactly [8]. The higher-order contributions have a slow convergence rate, at p^8-order one reaches only about 50% of the full sum.

• $(\alpha_1 - \beta_1)_{\pi^\pm}$: contrary to the neutral channel, the size of the σ-exchange diagram for this combination is about an order of magnitude larger than the box + pion exchange diagram, and it becomes the most important contribution. The pion loops are absent.

Table 4. Contribution of various diagrams for $M = 300$ MeV. Units as in Table 2.

	box + π-exchange	σ-exchange	pion-loop	total
$(\alpha_1+\beta_1)_{\pi^0}$	0.73	0	0	0.73
$(\alpha_1-\beta_1)_{\pi^0}$	-11.13	10.57	-1.0	-1.56
$(\alpha_2+\beta_2)_{\pi^0}$	-0.144	0	0	-0.144
$(\alpha_2-\beta_2)_{\pi^0}$	5.09	9.07	21.97	36.13
$(\alpha_1+\beta_1)_{\pi^\pm}$	0.189	0	0	0.189
$(\alpha_1-\beta_1)_{\pi^\pm}$	-0.977	10.36	0	9.39
$(\alpha_2+\beta_2)_{\pi^\pm}$	0.198	0	0	0.198
$(\alpha_2-\beta_2)_{\pi^\pm}$	-1.63	8.87	10.29	17.54

• $(\alpha_2-\beta_2)_{\pi^\pm}$: the pattern observed for the charged dipole difference repeats itself for the quadrupole polarizabilities. However in this case the subleading in the $1/N_c$ counting pion-loop diagram has the same magnitude as the σ-exchange term.

• $(\alpha_2-\beta_2)_{\pi^0}$: the pion loop dominates, $\sim 2\times$ σ-exchange.

• Finally, regarding the sums of polarizabilities, we stress that the values (including the overall signs) of $(\alpha_2+\beta_2)_{\pi^0,\pi^\pm}$ are totally determined by the gauge-invariant quark box or the box + pion exchange contribution. This is a key result of the presented calculation. The sign is stable when the model parameters are changed. The magnitude depends on the value chosen for the constituent quark mass, but the best overall fit to the other empirical data, typically yielding $M \sim 300$ MeV, also yields the optimum values for the polarizabilities [7]. Moreover, the main part of the box contribution comes from the first non-vanishing p^8-order term in the chiral expansion. Based on this fact we expect that the contact term of the p^8 3-loop calculation in χPT may also play an important role in reversing the signs of the 2-loop order results for these quantities.

Acknowledgement We are very grateful to the organizers of the "Mini-Workshop Bled 2009: Problems in multi-quark states", for the kind invitation to present this work. This research is supported by the Polish Ministry of Science and Higher Education, grants N202 034 32/0918 and N202 249235, by Fundação para a Ciência e Tecnologia, grants FEDER, OE, POCI 2010, CERN/FP/83510/2008, and by the European Community-Research Infrastructure Integrating Activity *Study of Strongly Interacting Matter* (Grant Agreement 227431) under the Seventh Framework Programme of the EU.

References

1. L. V. Fil'kov, V. L. Kashevarov, Phys. Rev. C 72 (2005) 035211.
2. L. V. Fil'kov, V. L. Kashevarov, Phys. Rev. C 73 (2006) 035210.
3. J. Gasser, M. A. Ivanov, M. E. Sainio, Nucl. Phys. B 728 (2005) 31.
4. J. Gasser, M. A. Ivanov, M. E. Sainio, Nucl. Phys. B 745 (2006) 84.
5. S. Bellucci, J. Gasser, M. E. Sainio, Nucl. Phys. B 423 (1994) 80; S. Bellucci, J. Gasser, M. E. Sainio, Nucl. Phys. B 431 (1994) 413, Erratum.

6. Y. Nambu, J. Jona-Lasinio, Phys. Rev. 122 (1961) 345; 124 (1961) 246.
7. B. Hiller, W. Broniowski, A. A. Osipov, A. H. Blin, arXiv:0908.0159 [hep-ph]
8. B. Bajc, A. H. Blin, B. Hiller, M. C. Nemes, A. A. Osipov, M. Rosina, Nucl. Phys. A 604 (1996) 406.
9. I. Guiasu, E. E. Radescu, Ann. Phys. 120 (1979) 145; I. Guiasu, E.E. Radescu, Ann. Phys. 122 (1979) 436.
10. V. Bernard, A. A. Osipov, U.-G. Meißner, Phys. Lett. B 285 (1992) 119.
11. J. Bijnens, F. Cornet, Nucl. Phys. B 296 (1988) 557.
12. J. F. Donoghue, B. R. Holstein, Y. C. Lin, Phys. Rev. D 37 (1988) 2423.
13. J. F. Donoghue, B. R. Holstein, Phys. Rev. D 48 (1993) 137.

BLED WORKSHOPS
IN PHYSICS
VOL. 10, NO. 1
p. 44

Proceedings of the Mini-Workshop
Problems in Multi-Quark States
Bled, Slovenia, June 29 - July 6, 2009

Extended NJL model with eight-quark interactions*

A. A. Osipov[a,b], B. Hiller[a], A. H. Blin[a], J. Moreira[a]

[a] Centro de Física Computacional, Departamento de Física da Universidade de Coimbra, 3004-516 Coimbra, Portugal
[b] Dzhelepov Laboratory of Nuclear Problems, JINR 141980 Dubna, Russia

Abstract. We present the results obtained in the three-flavour ($N_f = 3$) Nambu–Jona-Lasinio model which is extended by the $U_A(1)$ breaking six-quark 't Hooft interaction and eight-quark interactions. We address the problem of stability, and some phenomenological consequences of the models with multi-quark interactions.

A number of instructive models in low-energy QCD assume the existence of underlying multi-quark interactions and their importance for the physics of hadrons. They are efficient in the description of spontaneous chiral symmetry breaking (χSB), and in the study of the quark structure of light mesons. The Nambu–Jona-Lasinio (NJL) model [1] is a well-known example, where the local chiral symmetric four-fermion interactions under some conditions lead to the formation of fermion-antifermion bound states and as a result describe the χSB phenomenon. A modified form of these interactions has been widely considered to derive the QCD effective action at large distances [2]-[5].

One might ask if higher order multi-quark interactions are of importance. Indeed, along the lines suggested by an instanton-gas model, it can be argued [6] that there exists an infinite set of multi-quark terms in the effective quark Lagrangian starting from the NJL four-quark piece. In particular, the famous 't Hooft determinantal interaction [7] automatically appears if one keeps only the zero mode contribution in the mode expansion of the effective Lagrangian. This $2N_f$ multi-quark term manifestly violates the $U_A(1)$ axial symmetry of the QCD Lagrangian, offering a way out of the $U_A(1)$ problem.

The structure of QCD-motivated models at low energies with effective many-fermion interaction and a finite cutoff in the symmetry-breaking regime has been also considered in [8], where the authors, using the $1/N_c$ arguments and the fine-tuning condition in providing the scale invariance, classified the set of quasilocal vertices relevant for dynamical χSB. It has been found this way that in such effective models the vertices with four, six and eight fermions only should be retained in four-dimensional space-time.

Thus, it is tempting to consider the intuitive picture that describes the QCD vacuum based on a series of multi-quark interactions reflecting several tractable

* Talk delivered by A. A. Osipov

features of QCD, which include aspects of chiral symmetry and of the $1/N_c$ expansion. The bosonization of quark degrees of freedom leads then to the desirable effective Lagrangian with matter fields and a stable chiral asymmetric vacuum.

The NJL-type model with the $U_A(1)$ axial symmetry breaking by the 't Hooft determinant has been studied in the mean field approximation [9]-[14] for a long time. Numerous phenomenological applications show that the results of such an approach meet the expectations. Nevertheless, in this picture there is an apparent problem: the mean field potential is unbounded from below, and the 't Hooft term is the direct source of such an instability. A consistent approach requires obviously a stable hadronic vacuum.

To cure this disease of the model we consider the system of light quarks u, d, s with multi-fermion interactions described by the Lagrangian

$$\mathcal{L}_{\text{eff}} = \bar{q}(i\gamma^\mu\partial_\mu - m)q + \mathcal{L}_{4q} + \mathcal{L}_{6q} + \mathcal{L}_{8q}. \tag{1}$$

Here, the quark fields q have colour ($N_c = 3$) and flavour indices which are suppressed. We suppose that four-, six-, and eight-quark interactions $\mathcal{L}_{4q}$, $\mathcal{L}_{6q}$, $\mathcal{L}_{8q}$ are effectively local, for it is known that meson physics in the large N_c limit is described by a local Lagrangian of this type [15]. The interaction Lagrangians $\mathcal{L}_{4q}$ and $\mathcal{L}_{6q}$ of the model in the scalar and pseudoscalar channels is given by two terms

$$\mathcal{L}_{4q} = \frac{G}{2}\left[(\bar{q}\lambda_a q)^2 + (\bar{q}i\gamma_5\lambda_a q)^2\right], \tag{2}$$

$$\mathcal{L}_{6q} = \kappa(\det\bar{q}P_L q + \det\bar{q}P_R q). \tag{3}$$

The first one is the $U_L(3)\times U_R(3)$ chiral symmetric interaction specifying the local part of the effective four-quark Lagrangian in channels with quantum numbers $J^P = 0^+, 0^-$. The Gell-Mann flavour matrices λ_a, $a = 0, 1, \ldots, 8$, are normalized such that $\mathrm{tr}(\lambda_a\lambda_b) = 2\delta_{ab}$. The second term represents the 't Hooft determinantal interactions [7]. The matrices $P_{L,R} = (1 \mp \gamma_5)/2$ are projectors and the determinant is over flavour indices. The determinantal interaction breaks explicitly the axial $U_A(1)$ symmetry and Zweig's rule. The global chiral $SU(3)_L \times SU(3)_R$ symmetry of the Lagrangian (1) at $m = 0$ is spontaneously broken to the $SU(3)$ group, showing the dynamical instability of the fully symmetric solutions of the theory. In addition, the current quark mass m, being a diagonal matrix in flavour space with elements $\mathrm{diag}(m_u, m_d, m_s)$, explicitly breaks this symmetry down, retaining only the reduced $SU(2)_I \times U(1)_Y$ symmetries of isospin and hypercharge conservation, if $m_u = m_d \neq m_s$.

The eight-quark Lagrangian which describes the spin zero interactions contains two terms: $\mathcal{L}_{8q} = \mathcal{L}^{(1)}_{8q} + \mathcal{L}^{(2)}_{8q}$ [16], where

$$\mathcal{L}^{(1)}_{8q} = 8g_1\left[(\bar{q}_i P_R q_m)(\bar{q}_m P_L q_i)\right]^2, \tag{4}$$

$$\mathcal{L}^{(2)}_{8q} = 16g_2\left[(\bar{q}_i P_R q_m)(\bar{q}_m P_L q_j)(\bar{q}_j P_R q_k)(\bar{q}_k P_L q_i)\right]. \tag{5}$$

Here the sum is taken over flavour indices $i, j, m = 1, 2, 3$; $\mathcal{L}_{8q}$ is a $U_L(3)\times U_R(3)$ symmetric interaction with OZI-violating effects in $\mathcal{L}^{(1)}_{8q}$. The first term $\mathcal{L}^{(1)}_{8q}$ coincides with the OZI-violating eight-quark interactions considered in [17]. The

second term $\mathcal{L}_{8q}^{(2)}$ represents interactions without violation of Zweig's rule. $\mathcal{L}_{8q}$ is the most general Lagrangian which describes the spin zero eight-quark interactions without derivatives. It is the lowest order term in number of quark fields which is relevant to the case. We restrict our consideration to these forces, because in the long wavelength limit the higher dimensional operators are suppressed.

We view the main role of eight-quark forces considered as folows:
(i) They are of vital importance for the stability of the ground state built from four and six-quark interactions: the quark model considered follows the general trend of spontaneous breakdown of chiral symmetry and possesses a globally stable ground state, when relevant inequalities in terms of the coupling constants hold, $g_1 > 0, g_1 + 3g_2 > 0, Gg_1 > (\kappa/16)^2$ [16].
(ii) The low lying scalar and pseudoscalar mesonic spectra are almost insensitive to the eight-quark forces [18].
(iii) The 8q-interactions play an important role in determining the critical temperature, T_c, at which transitions occur from the dynamically broken chiral phase to the symmetric phase, lowering the value of T_c with growing strength of the 8q couplings [19].
(iv) The multi-quark interactions introduce new additional features to the catalysis of dynamical symmetry breaking by a constant magnetic field H in $3+1$ dimensions: the first minimum catalyzed by a constant magnetic field (that is, a slowly varying field) is then smoothed out with increasing H at the characteristic scale $H \sim 10^{19}$G. The reason is that multi-quark forces generate independently another local minimum associated with a larger dynamical fermion mass. This state may exist even for multi-quark interactions with a subcritical set of couplings and is globally stable with respect to a further increase of the magnetic field [20].
(v) The OZI-violating terms with coupling strength g_1 affect the mechanism of χSB: starting from some critical value of the coupling $g_1 = (g_1)_{crit}$ the χSB is induced by the 6q 'tH̃ooft interactions, as opposed to the 4q NJL forces at $g_1 < (g_1)_{crit}$ [18].
(vi) It turns out that the mesonic spectra built on the spontaneously broken vacuum induced by the 't Hooft interaction strength, as opposed to the commonly considered case driven by the four-quark coupling, undergo a rapid crossover to the unbroken phase with a slope and at a temperature which is regulated by the strength of the OZI violating eight-quark interactions. This strength g_1 can be adjusted in consonance with the four-quark coupling G (keeping the remaining model parameters fixed) and leaves the spectra unchanged, except for the sigma meson mass which decreases. A first order transition behavior is also a possible solution within the present approach at large g_1 [21].
(vii) They may be also of importance in decays and scattering, not considered so far.

We are very grateful to the organizers of the "Mini-Workshop Bled 2009: Problems in multi-quark states", for the kind invitation to present this work. Research supported by Fundação para a Ciência e Tecnologia, grants FEDER, OE, POCI 2010, CERN/FP/83510/2008, and by the European Community-Research

Infrastructure Integrating Activity Study of Strongly Interacting Matter (Grant Agreement 227431) under the Seventh Framework Programme of the EU.

References

1. Y. Nambu, J. Jona-Lasinio, Phys. Rev. 122 (1961) 345; 124 (1961) 246.
2. T. Eguchi, Phys. Rev. D 14 (1976) 2755; K. Kikkawa, Progr. Theor. Phys. 56 (1976) 947.
3. M.K. Volkov and D. Ebert, Sov. J. Nucl. Phys. 36 (1982) 736; D. Ebert and M.K. Volkov Z. Phys. C 16 (1983) 205.
4. M.K. Volkov, Ann. Phys. (N.Y.) 157 (1984) 282; A. Dhar and S. Wadia, Phys. Rev. Lett. 52 (1984) 959; A. Dhar, R. Shankar and S. Wadia, Phys. Rev. D31 (1985) 3256; D. Ebert and H. Reinhardt, Nucl. Phys. B271 (1986) 188.
5. J. Bijnens, C. Bruno, E. de Rafael, Nucl. Phys. B 390 (1993) 501.
6. Yu.A. Simonov, Phys. Lett. B 412 (1977) 371; Yu.A. Simonov, Phys. Rev. D 65 (2002) 094018.
7. G. 't Hooft, Phys. Rev. D 14 (1976) 3432; Erratum: *ibid* D 18 (1978) 2199.
8. A.A. Andrianov, and V.A. Andrianov, Int.J.Mod.Phys. A 8 (1993) No.11, 1981.
9. V. Bernard, R.L. Jaffe, U.-G. Meissner, Phys. Lett. B 198 (1987) 92; Nucl. Phys. B 308 (1988) 753.
10. H. Reinhardt, R. Alkofer, Phys. Lett. B 207 (1988) 482.
11. S. Klimt, M. Lutz, U. Vogl, W. Weise, Nucl. Phys. A 516 (1990) 429; U. Vogl, M. Lutz, S. Klimt, W. Weise, Nucl. Phys. A 516 (1990) 469; U. Vogl, W. Weise, Progr. Part. Nucl. Phys. 27 (1991) 195.
12. M. Takizawa, K. Tsushima, Y. Kohyama, K. Kubodera, Nucl. Phys. A 507 (1990) 611.
13. S.P. Klevansky, Rev. Mod. Phys. 64 (1992) 649.
14. T. Hatsuda, T. Kunihiro, Phys. Rep. 247 (1994) 221.
15. E. Witten, Nucl. Phys. B 160 (1979) 57.
16. A.A. Osipov, B. Hiller, J. da Providência, Phys. Lett. B 634 (2006) 48.
17. R. Alkofer and I. Zahed, Mod. Phys. Lett. A 4 (1989) 1737; R. Alkofer and I. Zahed, Phys. Lett. B 238 (1990) 149.
18. A.A. Osipov, B. Hiller, A.H. Blin, J. da Providência, Ann. Phys. 322 (2007) 2021.
19. A.A. Osipov, B. Hiller, J. Moreira, A.H. Blin, J. da Providência, Phys. Lett. B 646 (2007) 91.
20. A.A. Osipov, B. Hiller, A.H. Blin, J. da Providência, Phys. Lett. B 650 (2007) 262.
21. A.A. Osipov, B. Hiller, J. Moreira, A.H. Blin, Phys. Lett. B 659 (2008) 270.

BLED WORKSHOPS
IN PHYSICS
VOL. 10, NO. 1
p. 48

Proceedings of the Mini-Workshop
Problems in Multi-Quark States
Bled, Slovenia, June 29 - July 6, 2009

Meson-Baryon Interaction Vertices*

T. Melde[a], L. Canton[b], W. Plessas[a]

[a]Theoretical Physics, Institute of Physics, University of Graz, Universitätsplatz 5, A-8010 Graz, Austria
[b]Istituto Nazionale di Fisica Nucleare, Sezione di Padova, Via F. Marzolo 8, I-35131 Padova, Italy

We discuss predictions of the relativistic constituent-quark model (RCQM) for the structure of πNN as well as πNΔ strong interaction vertices. The results are put into perspective with strong meson-baryon form factors from lattice quantum chromodynamics (QCD) and phenomenological models.

Notions on the structure of meson-baryon interaction vertices are important in many areas of particle and nuclear physics. Often the corresponding strong form factors have been parametrized phenomenologically, especially in meson-baryon and baryon-baryon interaction models. Certainly, it is desirable to understand the structure of the hadronic interaction vertices on a microscopic level.

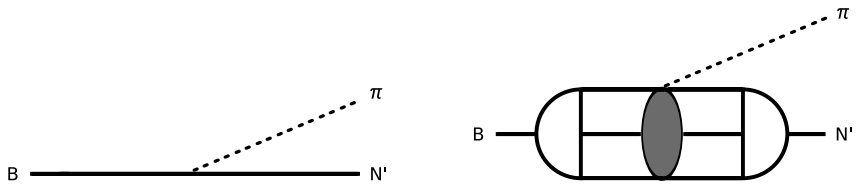

Fig. 1. Graphical representation of the meson-baryon vertex (a) and the corresponding amplitude in the RCQM (b).

We have recently performed a covariant study of the πNN and πNΔ interaction vertices within a relativistic constituent-quark model (RCQM) by considering the process of Fig. 1(a) resolved in the way as shown in Fig. 1(b) [1]. Predictions of the form factor dependences on the relativistic four-momentum transfer Q^2 have been obtained directly from the RCQM without introducing any fit parameters. The transition amplitudes from initial $|i\rangle$ to final $\langle f|$ states

$$F_{i\to f} = (2\pi)^4 \langle f| \mathcal{L}_I (0) |i\rangle \tag{1}$$

* Talk delivered by W. Plessas

with the πNN and πNΔ interaction Lagrangian densities

$$\mathcal{L}_I^N = -\frac{f_{\pi NN}}{m_\pi}\bar{\Psi}(x)\gamma_5\gamma^\mu T\Psi(x)\,\partial_\mu\Phi(x)\ , \tag{2}$$

$$\mathcal{L}_I^\Delta = -\frac{f_{\pi N\Delta}}{m_\pi}\bar{\Psi}(x)\,T\Psi^\mu(x)\,\partial_\mu\Phi(x) + h.c.\,, \tag{3}$$

where in obvious notation T represents the transition operator for the emission of the pion Φ from a nucleon Ψ or a delta Ψ^μ with couplings $f_{\pi NN}$ and $f_{\pi N\Delta}$, respectively, are thus identified with the matrix elements

$$F_{i\to f}^{RCQM} = \langle V', M', J', \Sigma'|\,\hat{D}_{rd}^{\pi}\,|V, M, J, \Sigma\rangle\ , \tag{4}$$

where the baryon states $|V, M, J, \Sigma\rangle$ are eigenstates of the RCQM invariant mass operator characterized by the four-velocity V, the invariant-mass eigenvalue M, and the intrinsic spin J with z-component Σ, and analogously for $\langle V', M', J', \Sigma'|$. These matrix elements are calculated within point-form (PF) relativistic quantum mechanics

$$\begin{aligned}
&\langle V', M', J', \Sigma'|\hat{D}_{rd}^{m}|V, M, J, \Sigma\rangle = \frac{2}{MM'}\sum_{\sigma_i\sigma_i'}\sum_{\mu_i\mu_i'}\int d^3\mathbf{k}_2 d^3\mathbf{k}_3 d^3\mathbf{k}_2' d^3\mathbf{k}_3' \\
&\times\sqrt{\frac{\left(\sum_i\omega_i'\right)^3}{\prod_i 2\omega_i'}}\Psi^\star_{M'J'M_{J'}T'M_{T'}}\left(\mathbf{k}_1', \mathbf{k}_2', \mathbf{k}_3'; \mu_1', \mu_2', \mu_3'\right)\prod_{\sigma_i'} D^{\star\frac{1}{2}}_{\sigma_i'\mu_i'}\{R_W[k_i'; B(V')]\} \\
&\times\langle p_1', p_2', p_3'; \sigma_1', \sigma_2', \sigma_3'|\,\hat{D}_{rd}^{m}\,|p_1, p_2, p_3; \sigma_1, \sigma_2, \sigma_3\rangle \\
&\times\prod_{\sigma_i} D^{\frac{1}{2}}_{\sigma_i\mu_i}\{R_W[k_i; B(V)]\}\sqrt{\frac{\left(\sum_i\omega_i\right)^3}{\prod_i 2\omega_i}}\Psi_{MJM_JTM_T}(\mathbf{k}_1, \mathbf{k}_2, \mathbf{k}_3; \mu_1, \mu_2, \mu_3)\,,
\end{aligned} \tag{5}$$

where the matrix element of the reduced transition operator $\hat{D}_{rd}^{\pi}$ between free three-quark states $|p_1, p_2, p_3; \sigma_1, \sigma_2, \sigma_3\rangle$ is taken according to the point-form spectator model (PFSM) [2]

$$\begin{aligned}
&\langle p_1', p_2', p_3'; \sigma_1', \sigma_2', \sigma_3'|\,\hat{D}_{rd}^{\pi}\,|p_1, p_2, p_3; \sigma_1, \sigma_2, \sigma_3\rangle = \\
&\qquad 3\mathcal{N}_S\frac{ig_{qqm}}{2m_1(2\pi)^{\frac{3}{2}}}\bar{u}(p_1', \sigma_1')\gamma_5\gamma_\mu\lambda_m u(p_1, \sigma_1)\,\tilde{q}^\mu \\
&\qquad\qquad\times 2p_{20}\delta(\mathbf{p}_2 - \mathbf{p}_2')\,2p_{30}\delta(\mathbf{p}_3 - \mathbf{p}_3')\,\delta_{\sigma_2\sigma_2'}\delta_{\sigma_3\sigma_3'}\,.
\end{aligned} \tag{6}$$

Here, the individual quark four-momenta k_i (k_i') and p_i (p_i') are connected through the boost transformations of the incoming and (outgoing) states, namely, $p_i = B(V)k_i$ (and analogously $p_i' = B(V')k_i'$). The normalization factor $\mathcal{N}_S$ as well as the momentum transfer $\tilde{q}^\mu = p_1^\mu - p_1'^\mu$ are specific for the PFSM and explicitly given in ref. [2], where also other details of the formalism/notation can be found. While there is a freedom in the choice of the normalization factor, which can cause minor influences on the results (cf. ref. [2]), it should be emphasized that $\tilde{q}^\mu$ is uniquely defined through the overall momentum conservation and the two spectator conditions. The off-shell extrapolation of the transition amplitude

is made by keeping all hadrons and quarks on their respective mass shells. Obviously it implies energy non-conservation in the transition process. By virtue of the pseudovector-pseudoscalar equivalence the above construction also guarantees that the pseudovector and pseudoscalar quark-meson couplings lead to the same transition amplitude.

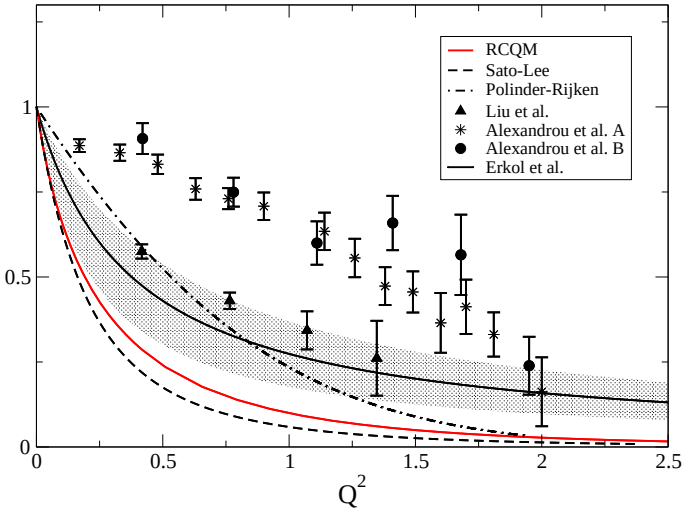

Fig. 2. Prediction of the strong form factor $G_{\pi NN}$, normalized to 1 at $Q^2 = 0$, by the GBE RCQM (solid/red line) in comparison to parametrizations from the dynamical meson-baryon models of Sato-Lee [5] and Polinder-Rijken [6,7] as well as results from three lattice QCD calculations [8–11] (cf. the legend); the shaded area around the result by Erkol *et al.* gives their theoretical error band.

The strong πNN and $\pi N\Delta$ form factors as dependent on the space-like momentum transfer $Q^2 = -q^2 > 0$ are then given by

$$G_{\pi NN}\left(Q^2\right) = \frac{1}{f_{\pi NN}} \frac{m_\pi \sqrt{2\pi}}{\sqrt{2M_N}} \frac{\sqrt{E'_N + M'_N}}{E'_N + M'_N + \omega} \frac{F^{RCQM}_{i\to f}}{Q_z}\,, \tag{7}$$

$$G_{\pi N\Delta}\left(Q^2\right) = -\frac{1}{f_{\pi N\Delta}} \frac{3\sqrt{2\pi}}{2} \frac{m_\pi}{\sqrt{E'_N + M'_N}\sqrt{2M_\Delta}} \frac{F^{RCQM}_{i\to f}}{Q_z}\,, \tag{8}$$

where the momentum transfer is taken into the z-direction. The results for the Goldstone-boson-exhange (GBE) RCQM [3,4] are shown in Figs. 2 and 3, where also a comparison is given to corresponding results from dynamical meson-baryon models and various lattice-QCD calculations. It is interesting to observe that the Q^2 dependence of both the $G_{\pi NN}$ and $G_{\pi N\Delta}$ form factors resulting directly and in a parameter-free manner from the RCQM qualitatively agrees with the parametrizations of the meson-baryon vertices in the Sato-Lee model [5]. In the case of $G_{\pi N\Delta}$ the RCQM result is also close to the Polinder-Rijken meson-baryon model [6,7]. On the other hand, the strong form factors from the lattice calculations show a

(sometimes much) slower fall off with increasing Q^2. Even for the smaller differences between our results (as well as the form factors of Sato-Lee) and the data sets by Liu *et al.* and Erkol *et al.* it remains to be seen if dressing effects can account for these differences. Regarding all of the lattice data by Alexandrou *et al.* one has also to keep in mind that they correspond to relatively large pion masses with no extrapolations applied.

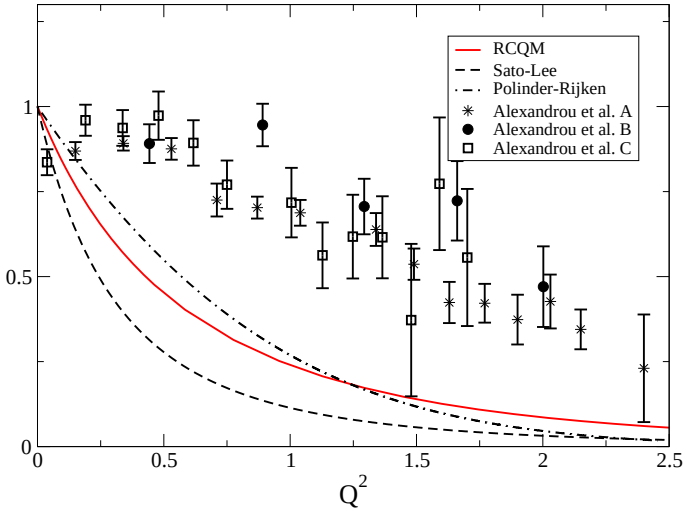

Fig. 3. Same as Fig. 2 but for the strong form factor $G_{\pi N\Delta}$.

As the vertex form factors represent an important input into a number of applications, we have also provided parametrizations in analytical forms as a function of the three-momentum transfer $\mathbf{q}^2$. It has turned out that an intermediate form between the usual monopole and dipole forms is most appropriate

$$G\left(\mathbf{q}^2\right) = \frac{1}{1+\left(\frac{q}{\Lambda_1}\right)^2+\left(\frac{q}{\Lambda_2}\right)^4}\,. \tag{9}$$

Our results in Figs. 2 and 3 are best reproduced with the parameter values given in Table 1.

Table 1. Coupling constants and cut-off parameters of the RCQM vertex form factors as parametrized according to the representation (9).

	$\frac{f_N^2}{4\pi}$	0.0691		$\frac{f_\Delta^2}{4\pi}$	0.188
N	Λ_1	0.451	Δ	Λ_1	0.594
	Λ_2	0.931		Λ_2	0.998

By this work we have obtained a parameter-free microscopic description of the strong πNN and πNΔ vertex form factors within a fully relativistic constituent quark model. Our study reveals that the structure of the πNΔ vertex is quite different from the πNN one, with cut-off parameters of up to 25% larger, contrary to what is often used in phenomenological models, where the πNN and πNΔ cut-offs are assumed of similar size [5–7] or even decreasing in the transition from πNN to πNΔ. Regarding the comparison with lattice-QCD results it will be most interesting, if the spread among them will be reduced by future calculations and how the final answer will turn out.

References

1. T. Melde, L. Canton and W. Plessas, Phys. Rev. Lett. **102**, 132002 (2009).
2. T. Melde, L. Canton, W. Plessas, and R. F. Wagenbrunn, Eur. Phys. J. A **25**, 97 (2005).
3. L. Y. Glozman, Z. Papp, W. Plessas, K. Varga, and R. F. Wagenbrunn, Phys. Rev. C **57**, 3406 (1998).
4. L. Y. Glozman, W. Plessas, K. Varga, and R. F. Wagenbrunn, Phys. Rev. D **58**, 094030 (1998).
5. T. Sato and T. S. H. Lee, Phys. Rev. C **54**, 2660 (1996).
6. H. Polinder and T. A. Rijken, Phys. Rev. C **72**, 065210 (2005).
7. H. Polinder and T. A. Rijken, Phys. Rev. C **72**, 065211 (2005).
8. C. Alexandrou, G. Koutsou, T. Leontiou, J. W. Negele, and A. Tsapalis, Phys. Rev. D **76**, 094511 (2007).
9. K. F. Liu, S. J. Dong, T. Draper, and W. Wilcox, Phys. Rev. Lett. **74**, 2172 (1995).
10. K. F. Liu *et al.*, Phys. Rev. D **59**, 112001 (1999).
11. G. Erkol, M. Oka and T. T. Takahashi, Phys. Rev. D **79**, 074509 (2009); arXiv:0805.3068.

BLED WORKSHOPS
IN PHYSICS
VOL. 10, NO. 1
p. 53

Proceedings of the Mini-Workshop
Problems in Multi-Quark States
Bled, Slovenia, June 29 - July 6, 2009

Multi-quark configurations in the baryons

D. O. Riska

Helsinki Institute of Physics, POB 64, 00014 University of Helsinki

Abstract. Several experiments have revealed the presence of antiquarks in the proton [1]. Extensive phenomenological studies of meson photoproduction on nucleons with unitary hadronic models with and without form factors have also revealed that the well known underproduction of the $N\Delta$ transition strengths by the conventional three quark model may be attributed to the missing "meson cloud" contributions [2]. The question thus arises of to what extent multi-quark configurations of the type $qqqq\bar{q}$, $qqqqq\bar{q}\bar{q}$, ... explicitly contribute to the observable of baryons. Here the contribution of the 5-quark configurations $qqqq\bar{q}$ to the magnetic moments and the axial form factors of the nucleon and the lowest resonances are considered. The two conclusions that emerge are that (a) a combination of at least three different $qqqq\bar{q}$ configurations are required for a satisfactory description of the nucleon properties and (b) that the vanishing of the axial form factor of the $N(1535)$ resonance is a natural consequence of the cancelation of the contributions of the qqq and $qqqq\bar{q}$ configurations [3].

1 The $qqqq\bar{q}$ configurations in the nucleon

The $qqqq$ subsystem of a $qqqq\bar{q}$ configuration has to be completely antisymmetric. As there are only 3 colors, the most "antisymmetric" qqqq color configuration is the mixed symmetry configuration $[211]_C$.

$$[211]_C : \begin{array}{|c|c|}\hline \multicolumn{1}{|c}{} & \multicolumn{1}{c|}{} \\ \hline \multicolumn{1}{|c}{} & \multicolumn{1}{c|}{} \\ \hline \multicolumn{1}{|c|}{} \\ \cline{1-1}\end{array}_C , \quad [31]_{XFS} : \begin{array}{|c|c|c|}\hline \multicolumn{1}{|c}{} & \multicolumn{1}{c}{} & \multicolumn{1}{c|}{} \\ \hline \multicolumn{1}{|c|}{} \\ \cline{1-1}\end{array} . \tag{1}$$

The complete antisymmetry of the $qqqq$ system therefore requires that the combined space-flavor-spin configuration has to have the (conjugate) mixed symmetry combination $[31]_{XFS}$ above. This can be achieved by either (1) choosing the spatial configuration to be completely symmetric $[4]_S$, with the flavor-spin configuration $[31]_{FS}$ or (2) by choosing the latter to be completely symmetric $[4]_{FS}$ and the former to have the mixed symmetry $[31]_X$:

$$(1) : \begin{array}{|c|c|c|c|}\hline \multicolumn{1}{|c}{} & \multicolumn{1}{c}{} & \multicolumn{1}{c}{} & \multicolumn{1}{c|}{} \\ \hline\end{array}_X \begin{array}{|c|c|c|}\hline \multicolumn{1}{|c}{} & \multicolumn{1}{c}{} & \multicolumn{1}{c|}{} \\ \hline \multicolumn{1}{|c|}{} \\ \cline{1-1}\end{array}_{FS} , \quad (2) : \begin{array}{|c|c|c|}\hline \multicolumn{1}{|c}{} & \multicolumn{1}{c}{} & \multicolumn{1}{c|}{} \\ \hline \multicolumn{1}{|c|}{} \\ \cline{1-1}\end{array}_X \begin{array}{|c|c|c|c|}\hline \multicolumn{1}{|c}{} & \multicolumn{1}{c}{} & \multicolumn{1}{c}{} & \multicolumn{1}{c|}{} \\ \hline\end{array}_{FS} . \tag{2}$$

In the first case positive parity demands that the antiquark $\bar{q}$ be in the $P-$state, while in the latter case, the antiquark has to be in the ground ($S-$) state. A pion

Table 1. Magnetic moments for the $qqqq\bar{q}$ configurations in the nucleon

$qqqq$ symmetry configuration	proton	neutron	
$[31]_X[4]_{FS}[22]_F[22]_S$	0	1/3	
$[31]_X[4]_{FS}[31]_F[31]_S$	2/9	-2/9	$qqqq : J = 1$
$[31]_X[4]_{FS}[31]_F[31]_S$	-1/3	0	$qqqq : J = 0$
$[4]_X[31]_{FS}[22]_F[31]_S$	7/27	-23/27	$\bar{q} : J = 3/2$
$[4]_X[31]_{FS}[22]_F[31]_S$	-4/27	0	$\bar{q} : J = 1/2$
$[4]_X[31]_{FS}[31]_F[22]_S$	-2/9	0	
$[4]_X[31]_{FS}[31]_F[31]_S$	-19/27	1/9	$\bar{q} : J = 3/2$
$[4]_X[31]_{FS}[31]_F[31]_S$	508/729	-95/729	$\bar{q} : J = 1/2$

loop configuration would correspond to the antiquark in the $P-$state. The configuration with the $\bar{q}$ in the $S-$state is, however, that which is consistent with a positive strangeness magnetic moment [4,5]. Note that if the antiquark is in the $P-$state the required $[31]_{XFS}$ configuration can also be obtained with $[31]_{FS}$ and $[22]_{FS}$ flavor-spin configurations of higher energy [20].

No $qqqq\bar{q}$ component alone can achieve the remarkable $-3/2$ ratio between the proton and the neutron magnetic moments, which is characteristic of the basic qqq configuration in both its nonrelativistic and relativistic versions [6]. This may be inferred from Table 1, where the nucleon magnetic moments for the 7 possible $qqqq\bar{q}$ configurations in the nucleons are listed. This may also inferred from the comprehensive attempt in ref.[7] to combine only the first of these $qqqq\bar{q}$ configurations with the basic qqq configuration.

The desired -3/2 ratio can however be obtained with a linear combination of the qqq and the first 3 configurations in the table:

$$\psi = \sqrt{P_3}\varphi_{[3][21][21]} + \sqrt{\frac{P_5}{\frac{11}{9}b_1 + \frac{5}{3}b_2}}\Big\{\sqrt{\frac{2}{9}b_1 + \frac{2}{3}b_2}\varphi_{[4][22][22]} + \sqrt{b_1}\varphi^{J=1}_{[4][31][31]} + \sqrt{b_2}\varphi^{J=0}_{[4][31][31]}\Big\}. \tag{3}$$

Here P_3 and P_5 are the probabilities for the qqq and (total) $qqqq\bar{q}$ components. The symmetry assignments [FS][F][S] in the wave functions represent flavor$\times$spin, flavor and spin respectively. The $\bar{q}$ components in the $qqqq\bar{q}$ wavefunctions is to be understood. A combination of the form (3) with 68 % qqq and 32 % of these $qqqq\bar{q}$ can in fact be arranged to yield the empirical value for $g_A(n \to p)$, eg by taking $b_1 = b_2$.

The identification of specific multi-quark contributions in the nucleon form factors is difficult because of their smooth behavior, which may be reproduced by a large variety of models. The prospective node in the region above $Q^2 \sim 6$

GeV^2 in G_E^p [8] does for example arise naturally already in the case of the qqq configuration if calculated with front form kinematics [9], although it also arises if a $qqqq\bar{q}$ component is included, the magnitude and form of which are set by the empirical values for G_E^n [10]. The electric form factor of the neutron G_E^n, which vanishes in the nonrelativistic qqq model, can in fact be brought into agreement with the empirical values by including a mixed symmetry S−state in the nucleon wave function with a probability of $1-2$ % [9].

2 The $qqqq\bar{q}$ configurations in the nucleon resonances

While it is possible to achieve a qualitative description of the lowest baryon resonances with the basic qqq model with spin and flavor dependent interactions [11], that model does not describe the systematics of the resonance decay widths. In the case of the $\Delta(1232)$ and the $N(1440)$ resonances it has been shown that the inclusion of a $qqqq\bar{q}$ component in the wave function makes it possible to overcome the underpredictions of the electromagnetic and strong decay widths [12–14]. Such calculations are however only qualitative in that the cross term matrix elements between the qqq and $qqqq\bar{q}$ components are very sensitive to the wave function models.

The cross terms between the qqq and the $qqqq\bar{q}$ configurations are large when the operator, which connects the annihilating $q\bar{q}$ pair and the meson or the γ ray involves the "large" components of the Dirac spinors. When the operator involves the small components, which is the case of the axial charge operator, the cross terms are suppressed.

In this context the recent lattice result that the axial charge of the $N(1535)$ is very small - if not 0 - is particularly interesting [15]. If the corresponding result for the (near) parity partner $N(1440)$ would also be close to 0, that might actually indicate the onset of restored chiral symmetry [16]. As the configuration mixing between the $N(1535)$ and the following $1/2^-$ resonance $N(1650)$ is expected to be small [17,18], these resonances may be considered separately.

The general expression for the axial charge of the $N(1535)$ is

$$g_A^* \simeq \sum_n A_n P_n\,, \quad n = 3, 5, .. \tag{4}$$

where n is the number of constituents ($(n+3)/2$ is the number of quarks and $(n-3)/2$ the number of antiquarks). Since the qqq model value for g_A^* is $-1/9$ [16], it follows that if indeed the axial charge of the $N(1535)$ vanishes, the multiquark configurations with $n > 3$ have to cancel that value.

Consideration of the $qqqq\bar{q}$ components indicates that this would be a very natural result [3]. In Table 2 all the possible $qqqq\bar{q}$ configurations in the $N(1535)$ and the corresponding coefficients A_n in the axial charge expression 4 are listed. These are listed in order of increasing energy under the assumption that the interaction between the quarks depend on spin and flavor or color.

Inclusion of these $qqqq\bar{q}$ components in addition to the qqq component leads to the axial charge expression,

$$g_A(N(1535)) = -\frac{1}{9}P_3 + \frac{5}{6}P_5^{(2)} - \frac{1}{9}P_5^{(3)} - \frac{4}{15}P_5^{(4)} + \frac{17}{18}P_5^{(5)}\,, \tag{5}$$

Table 2. The $qqqq\bar{q}$ configurations in the $N(1535)$ and the corresponding axial charge coefficient A_n (4) [19].

configuration	$qqqq$ flavor-spin	$qqqq$ color-spin	A_n
1	$[31]_{FS}[211]_F[22]_S$	$[31]_{CS}[211]_C[22]_S$	0
2	$[31]_{FS}[211]_F[31]_S$	$[31]_{CS}[211]_C[31]_S$	$+5/6$
3	$[31]_{FS}[22]_F[31]_S$	$[22]_{CS}[211]_C[31]_S$	$-1/9$
4	$[31]_{FS}[31]_F[22]_S$	$[211]_{CS}[211]_C[22]_S$	$-4/15$
5	$[31]_{FS}[31]_F[31]_S$	$[211]_{CS}[211]_C[31]_S$	$+17/18$

where the coefficients P indicate the corresponding probabilities. Because two of the $qqqq\bar{q}$ components have large positive coefficients, while the qqq contribution has a small negative coefficient it is possible to cancel the latter contribution altogether with only modest probabilities of the $qqqq\bar{q}$ components [19].

Combination of this result with the lattice calculation result for the axial charge of the $N(1650)$ resonance [15], which is close to the qqq quark model value $5/9$ [16], suggests the conclusion that the smallness of the axial charge of the $N(1535)$ is a natural consequence of its quark configuration and (possibly also) the cancelation between the contributions of the qqq and the $qqqq\bar{q}$ components [19] rather than an indication of restored chiral symmetry.

References

1. G.Garvey and J.C.Peng, Prog.Part.Nucl.Phys. **47**, 203 (2001)
2. B. Juliá-Díaz et al., Phys. Rev. **C 75**, 015205 (2007)
3. C. S. An and D. O. Riska, Eur.Phys.J **A37**, 263 (2008)
4. B. S. Zou and D. O. Riska, Phys. Rev. Lett. **95**, 072001 (2005)
5. J. Liu, R. D. McKeown and M. Ramsey-Musolf, Phys. Rev.**C 76**, 025202 (2007)
6. B. Juliá-Díaz and D. O. Riska, Nucl. Phys. **A 739**, 69 (2004)
7. C. S. An, Q. B. Li and D. O. Riska, Phys. Rev. **C 74**, 055207 (2006), **C 75**, 069901 (2007)
8. O. Gayou et al.. Phys. Rev. Lett. **88**, 092301 (2002)
9. B. Juliá-Díaz, D.O. Riska and F. Coester, Phys. Rev. **C 69**, 035212 (2004), **C75**, 069902 (2007)
10. Q. B. Li and D. O. Riska, Nucl.Phys. **A 791**, 406-421 (2007)
11. L. Ya. Glozman and D. O. Riska, Phys. Rept. **268**, 263 (1996)
12. Q. B. Li and D. O. Riska, Phys.Rev. **C 73**, 035201 (2006)
13. Q. B. Li and D. O. Riska, Nucl.Phys. **A 766**, 172 (2006)
14. Q. B. Li and D. O. Riska, Phys.Rev. **C 74**, 015202 (2006)
15. T. T. Takahashi and T. T. Kunihiro, Phys. Rev. **D 78**, 01150(R) (2008)
16. L. Ya. Glozman and A. V. Nefediev, Nucl. Phys. **A 807**, 38 (2008)
17. J. C. Nacher et al., Nucl. Phys. **A 678**, 187 (2000)
18. D. Pirjol and C. Schat, arXiv: 0906.0802 [hep-ph]
19. C. S. An and D. O. Riska, Eur.Phys.J. **A37**, 263-265 (2008)
20. C. Helminen and D. O. Riska, Nucl. Phys. **A699**, 624 (2002)

BLED WORKSHOPS
IN PHYSICS
VOL. 10, NO. 1
p. 57

Proceedings of the Mini-Workshop
Problems in Multi-Quark States
Bled, Slovenia, June 29 - July 6, 2009

Multiquark hadrons

Fl. Stancu

Institute of Physics, B5, University of Liège, Sart Tilman, 4000 Liège 1, Belgium

Abstract. The possible production of multiquark systems is very important for our understanding of hadrons. A considerable interest in such states started with Jaffe's work in 1977, demonstrating the role of the chromomagnetic interaction in the stability of light multiquarks. Since then, heavy quarks have also been included. A brief survey is presented regarding the evolution of the problem. Some of the recently observed resonances, named X,Y or Z, are discussed as possible candidates for tetraquarks.

1 Introduction

The multiquark hadrons studied so far are compact objects of type:

- Tetraquarks: $q^2\bar{q}^2$, $Q^2\bar{q}^2$, $Q\bar{Q}q\bar{q}$
- Pentaquarks: $q^4\bar{Q}$, $q^4\bar{q}$
- Hexaquarks: q^6 (the H-particle), q^5Q

where $q = u, d, s$ and $Q = c, b$. They are all color singlet objects described by the representation $[222]_c$. The possible existence of exotics has been mentioned in the literature [1,2] before the advent of QCD. Later on, their existence appeared natural in QCD inspired models. The interest started in 1977 with the work of Jaffe [3] who explained the stability of tetraquarks and hexaquarks (the H-particle) as due to the chromomagnetic interaction. Ten years later, independently, Gignoux et al. [4] and Lipkin [5] applied the same mechanism to charmed strange pentaquarks P, with explicit SU(3) breaking, finding more binding than for the H-particle. The status of the H-dibaryon is reviewed, for example, in Ref. [6]. In a review of the experimental searches for both H and P, Ashery [7] explained that the failure in observing the H-particle was the lack of sensitive measurements to small bindings. He also mentioned that the P search in charm hadroproduction at the Fermilab E791 experiment did not give a convincing evidence.

The criterion for stability was

$$\Delta E = E(q^m\bar{q}^n) - E_{threshold} < 0\,, \tag{1}$$

with q light or heavy.

The above theoretical studies were based on the OGE model which has a color-spin hyperfine interaction. Later on, the stability was also studied within the GBE (Goldstone boson exchange) model, which has a flavour-spin hyperfine

interaction [8]. A comparison of the stability results in the two models was given in Ref. [9]. In most cases, when the OGE interaction stabilizes a system, the GBE interaction destabilizes it and vice versa. For example, in Jaffe's calculations the H-particle is a bound $\Lambda\Lambda$ system, while the GBE interaction induces a strong short range repulsion in $\Lambda\Lambda$ [10], like in the NN system. The GBE model indicates that q^5Q is also highly unstable, despite the presence of a heavy quark [11]. Moreover the GBE interaction does not require strangeness in pentaquarks to better stabilize the system. The variational calculations of Ref. [12] predict a mass of about 2900 MeV for the $uudd\bar{c}$ system in its lowest state and the system is stable, the threshold energy being $M_N + M_{\bar{D}} = 2970$ MeV. Moreover the lowest state has a positive parity in contradistinction to the OGE model. The H1 Collaboration [13] observed a narrow resonance of mass M = 3099 MeV and width Γ = 12 MeV, which was interpreted as a $uudd\bar{c}$ pentaquark. This resonance was not confirmed by the CDF Collaboration.

2 Multiquark hadrons after 2002

After Jaffe's work there were several occasional waves of interest, some of them mentioned above. An impressive renaissance started in 2002, with the first observation by the LEPS Collaboration of a narrow baryon-like resonance in the nK^+ invariant mass spectrum produced in $\gamma n \to K^+K^-n$ reactions [14]. This was interpreted as a $uudd\bar{s}$ pentaquark. These results were supported by several experiments and contradicted by others, leading to a controversial situation. The LEPS Collaboration did however pursued its search to clarify the situation and some plausible explanations of the controversy together with new high statistics measurements can be found in Ref. [15].

Almost simultaneously several open charm D_s mesons with rather small widths were observed. The existing quark model calculations, based on the OGE interaction, failed to explain them as $c\bar{s}$ or $s\bar{c}$ pairs. For this reason, among others, a tetraquark interpretation has been proposed for $D_s(2317)$ [16]. The molecular picture [17] is more popular. Alternative explanations are: chiral partners of the ground state multiplet [18] or, simply, ordinary mesons with a proper spin-orbit interaction for unequal quark-antiquark masses [19], or $c\bar{s}$ states coupled to D^*K channels (for a review see *e.g.* [20]).

3 The hidden charm X,Y,Z resonances

The discovery of the charmonium-like resonances X,Y,Z starting with the first observation of X(3872) by the Belle Collaboration triggered a considerable interest in their interpretation as exotics, for example, $D\bar{D}$ molecules, tetraquarks, hybrids, etc. At the same time conventional options as $c\bar{c}$ pairs, threshold effects, etc., are being considered. A partial list of the newly observed hidden charm resonances is shown in Table 1. (For a more extensive list see [21].)

Table 1. Charmonium-like resonances

Resonance	Mass (MeV)	Width (MeV)	J^{PC}	Decay modes	Ref.
X(3872)	3871.4 ± 0.6	< 2.3	1^{++}	$\pi^+\pi^- J/\Psi, \gamma J/\Psi$	[22]
X(3940)	3942 ± 9	37^{+27}_{-17}	J^{P+}	$D\bar{D}^*$	[23]
Y(3940)	$3915\ ^{+4.3}_{-3.9}$	$34\ ^{+13}_{-9}$	J^{P+}	$\omega J/\Psi$	[24]
Z(3930)	3929 ± 5	29 ± 10	2^{++}	$D\bar{D}$	[25]
X(4160)	4156^{+29}_{-25}	139^{+113}_{-65}	J^{P+}	$D^*\bar{D}^*$	[23]
Y(4260)	4259 ± 8	88 ± 23	1^{--}	$\pi^+\pi^- J/\Psi$	[26]
$Z^+(4430)$	4433 ± 5	45^{+35}_{-18}	?	$\pi^+\Psi'$	[27]
$Z_1^+(4051)$	$4051 \pm 14^{+20}_{-41}$	82^{+21+47}_{-17-22}	?	$\pi^+\chi_{c1}$	[28]
$Z_2^+(4248)$	$4248\ ^{+44+180}_{-29-35}$	$177^{+54+316}_{-39-61}$	?	$\pi^+\chi_{c1}$	[28]
Y(4660)	4664 ± 12	48 ± 15	1^{--}	$\pi^+\pi^-\Psi'$	[29]
Y(4140)	4143 ± 3.14	$11.7^{+8.3}_{-5.0} \pm 3.7$	J^{P+}	$\phi J/\Psi$	[30]

After Belle, X(3782) has been confirmed by three other different collaborations [22]. The status of Y(3940), seen by BaBar [24], with M = 3915 ± 4 MeV, $\Gamma \approx 34$ MeV and that of X(3940), seen by Belle, with M = 3943 ± 17 MeV, $\Gamma = 87$ MeV $\pm$ 34 MeV [31], is being clarified. The Belle collaboration recently confirmed BaBar's results, as described in the recent overview by Olsen [32]. All the other resonances need confirmation.

Most of these resonances do not match well any of the unassigned charmonium levels. They can be candidates for exotics. In particular, a considerable amount of work has been devoted to the tetraquark or the molecular picture. In particular the best established and the narrowest resonance, X(3872), has been interpreted as a diquark-antidiquark state in a chromomagnetic model. The width was explained to be narrow due to its unnatural 1^{++} spin-parity, which forbids $D\bar{D}$ decay and estimated in a rearrangement of quarks and antiquarks process by Maiani et al. [33]. The mass was finally fitted. The diquark-antidiquark picture is useful in a relativistic framework [34]. In the tetraquark option, also with a chromomagnetic interaction, but without any correlated quark or antiquark pairs, it was found that the ground state $c\bar{c}q\bar{q}$ system has a mass of 3910 MeV, close to experiment and contains a tiny $J/\Psi + \rho$ or $J/\Psi + \omega$ component in the wave function, which can well explain the narrowness of its width [35]. The full spectrum of $c\bar{c}q\bar{q}$ was calculated within the same model in Ref. [36]. It contains twice more states than that of Maiani et al., because a complete color space was taken into account.

The X(3872) is also naturally interpreted as a loosely bound hadronic molecule, since its mass is close to $D^0\bar{D}^{*0}$ threshold, *e.* g. [37] or [38]. But this picture contradicts some experimental data. An ambiversion interpretation was recently proposed [39].

The spectrum of the $c\bar{c}s\bar{s}$ system was calculated [40] within the model of Ref. [35]. The structure of the states 1^{++} and 0^{++} suggests that they can decay

into $\phi J/\Psi$ with narrow widths. Thus they are good candidates for the resonance Y(4140), if this exists.

The charged Z^+ resonances from Table 1 are natural candidates for exotics because they have non-zero electric charge. In particular the $Z^+(4430)$ was interpreted as a $D^*(2010)\overline{D}_1(2420)$ molecule, for example in Ref. [41] or as a tetraquark [42].

4 Perspectives

Another type of tetraquarks, which have more chance to be bound are $QQ\bar{q}\bar{q}$. They have only one threshold $Q\bar{q} + Q\bar{q}$, while $Q\bar{Q} + q\bar{q}$, has two: $Q\bar{q} + Q\bar{q}$ and $Q\bar{Q} + q\bar{q}$. They are free of annihilation effects. Their study amounts to solve a four-body problem with a specific Hamiltonian. The interest started about two decades ago. Different variational methods have been proposed along the years as, for example, in Refs. [43–46]. A more complete list can be found in Ref. [47] where elaborate calculations are presented, both for S and P states. In the latter work as well as in Ref. [46], both $cc\bar{q}\bar{q}$ and $bb\bar{q}\bar{q}$ turn out to be bound, at least in the ground state. The possible experimental observation of $cc\bar{q}\bar{q}$ with present and future facilities is discussed in [47], complementing earlier studies [48]. There is hope that future generation experiments can lead to their observation.

5 Conclusion

The basic question is whether or not multiquark hadrons exist. The thoroughly searched H-particle, has not been seen so far. The evidence for heavy charmed pentaquarks $uuds\bar{c}$, $udds\bar{c}$ and $uudd\bar{c}$, is not convincing. The LEPS Collaboration still stubbornly searches for the pentaquark $uudd\bar{s}$ [15].

The number of X,Y,Z resonances is increasing every year and still more experimental work is necessary to confirm their existence, their quantum numbers, charged partners to neutral one, etc. It is plausible to believe that some of them, at least X(3872) or the Z^+ resonances, are exotics, in particular, they could have a tetraquark component at short range and behave as hadronic molecules at medium-longer range. Their theoretical interpretation is still a serious challenge. Less hastily studies are desired.

There is hope that future experiments will give evidence for $QQ\bar{q}\bar{q}$ states, found to be stable tetraquarks in quark model studies.

Acknowledgments I enjoyed the warm hospitality of the organizers of the Bled Workshop 2009. I gratefully acknowledge useful discussions with S. L. Olsen, regarding the experimental status of some charmonium-like resonances.

References

1. M. Gell-Mann, Phys. Lett. **8**, 214 (1964).
2. E. Golowich, Phys. Rev. D **4**, 262 (1971).

3. R. L. Jaffe, Phys. Rev. Lett. **38**, 195 (1977) [Erratum-ibid. **38**, 617 (1977)]; Phys. Rev. D **15**, 267 (1977); Phys. Rev. D **15**, 281 (1977).
4. C. Gignoux, B. Silvestre-Brac and J. M. Richard, Phys. Lett. B **193**, 323 (1987).
5. H. J. Lipkin, Phys. Lett. B **195**, 484 (1987).
6. T. Sakai, K. Shimizu and K. Yazaki, Prog. Theor. Phys. Suppl. **137** (2000) 121.
7. D. Ashery, Few Body Syst. Suppl. **10** (1999) 295.
8. L. Y. Glozman and D. O. Riska, Phys. Rept. **268** (1996) 263; L. Y. Glozman, Z. Papp and W. Plessas, Phys. Lett. B **381** (1996) 311.
9. F. Stancu, Few Body Syst. Suppl. **13**, 225 (2001).
10. F. Stancu, S. Pepin and L. Y. Glozman, Phys. Rev. D **57** (1998) 4393
11. S. Pepin and F. Stancu, Phys. Rev. D **57** (1998) 4475.
12. F. Stancu, Phys. Rev. D **58** (1998) 111501
13. A. Aktas *et al.*, [H1 Collaboration], Phys. Lett. **B588** (2008) 17.
14. T. Nakano *et al.* [LEPS Collaboration], Phys. Rev. Lett. **91** (2003) 012002.
15. T. Nakano *et al.* [LEPS Collaboration], Phys. Rev. C **79** (2009) 025210.
16. H. Y. Cheng and W. S. Hou, Phys. Lett. B **566** (2003) 193.
17. T. Barnes, F. E. Close and H. J. Lipkin, Phys. Rev. D **68** (2003) 054006.
18. W. A. Bardeen, E. J. Eichten and C. T. Hill, Phys. Rev. D **68** (2003) 054024.
19. O. Lakhina and E. S. Swanson, Phys. Lett. B **650** (2007) 159.
20. J. L. Rosner, J. Phys. G **34** (2007) S127.
21. S. L. Olsen, arXiv:0901.2371 [hep-ex].
22. S. -K.Choi *et al.* [Belle Collab.], Phys. Rev. Lett. **91** (2003) 262001; D. E. Acosta *et al.* [CDF II Collab.], Phys. Rev. Lett. **93** (2004) 072001; V. M. Abazov *et al.* [D0 Collab.], Phys. Rev. Lett. **93**, (2004) 162002; B. Aubert *et al.* [BABAR Collab.], Phys. Rev. **D71** (2005) 071103.
23. P. Pakhlov *et al.* [Belle Collab.], Phys. Rev. Lett. **100** (2008) 202001.
24. B. Aubert *et al.* [BABAR Collab.], Phys. Rev. Lett. **101** (2008) 082001.
25. S. Uehara *et al.* [Belle Collaboration], Phys. Rev. Lett. **96** (2006) 082003.
26. B. Aubert *et al.* [BABAR Collaboration], Phys. Rev. Lett. **96** (2006) 232001.
27. S. K. Choi *et al.* [BELLE Collaboration], Phys. Rev. Lett. **100** (2008) 142001.
28. R. Mizuk *et al.* [Belle Collaboration], Phys. Rev. D **78** (2008) 072004.
29. X. L. Wang *et al.* [Belle Collaboration], Phys. Rev. Lett. **99** (2007) 142002.
30. T. Aaltonen *et al.* [CDF Collaboration], Phys. Rev. Lett. **102** (2009) 242002.
31. S. -K. Choi *et al.* [Belle Collaboration], Phys. Rev. Lett. **94** (2005) 182002.
32. S. L. Olsen, arXiv:0909.2713 [hep-ex].
33. L. Maiani, F. Piccinini, A. D. Polosa and V. Riquer, Phys. Rev. D **71** (2005) 014028
34. D. Ebert, R. N. Faustov and V. O. Galkin, Phys. Lett. B **634** (2006) 214.
35. H. Hogaasen, J. M. Richard and P. Sorba, Phys. Rev. D **73** (2006) 054013
36. F. Stancu, arXiv:hep-ph/0607077.
37. N. A. Tornqvist, Phys. Lett. B **590** (2004) 209 and references therein.
38. E. Braaten and M. Lu, Phys. Rev. D **76** (2007) 094028.
39. O. Zhang, C. Meng and H. Q. Zheng, arXiv:0901.1553 [hep-ph], Phys. Lett. in press
40. F. Stancu, arXiv:0906.2485 [hep-ph].
41. X. Liu, Y. R. Liu, W. Z. Deng and S. L. Zhu, Phys. Rev. D **77** (2008) 094015
42. X. H. Liu, Q. Zhao and F. E. Close, Phys. Rev. D **77** (2008) 094005.
43. S. Zouzou, B. Silvestre-Brac, C. Gignoux and J. M. Richard, Z. Phys. C **30** (1986) 457.
44. B. Silvestre-Brac and C. Semay, Z. Phys. C **57** (1993) 273; Z. Phys. C **59** (1993) 457.
45. D. M. Brink and F. Stancu, Phys. Rev. D **57** (1998) 6778.
46. D. Janc and M. Rosina, Few Body Syst. **35** (2004) 175.
47. J. Vijande, A. Valcarce and N. Barnea, arXiv:0903.2949 [hep-ph].
48. A. Del Fabbro, D. Janc, M. Rosina and D. Treleani, Phys. Rev. D **71** (2005) 014008.

BLED WORKSHOPS
IN PHYSICS
VOL. 10, NO. 1
p. 62

Proceedings of the Mini-Workshop
Problems in Multi-Quark States
Bled, Slovenia, June 29 - July 6, 2009

Chiral Quark Soliton Model and Nucleon Spin Structure Functions

M. Wakamatsu

Department of Physics, Faculty of Science, Osaka University, Toyonaka, Osaka 560-0043, JAPAN

1 Introduction

What is the CQSM like? To answer this question, it is instructive to ask another simpler question. What is, or what was, the Skyrme model ? In a word, the famous Skyrme model is Bohr's model in baryon physics. The simplest microscpic basis of Bohr's collective model of rotational nuclei is provided by the deformed Hartree-Fock theory supplemented with the subsequent cranking quantization. Very roughly speaking, the relation between the CQSM and the Skyrme model is resembling the relation between these two theories in nuclear physics. Let us start with a brief history of the CQSM.

- The model was first proposed by Diakonov, Petrov and Pobylitsa based on the instanton picture of the QCD vacuum in 1988 [1].
- In 1991 [2], we have established a basis of numerical calculation, which enables us to make nonperturbative estimate of nucleon observables with full inclusion of the deformed Dirac-sea quarks, by extending the method of Kahana, Ripka and Soni [3],[4]. Also derived and discussed in this paper is the nucleon spin sum rule, which reveals the important role of quark orbital angular momentum in the nucleon spin problem.
- In 1993, we noticed the existence of novel $1/N_c$ correction to some isovector observables, which is totally missing within the framework of the Skyrme model, but it certainly exists within the CQSM, so that it resolves the long-standing g_A-problem inherent in the hedgehog soliton model [5] (see also [6]).
- The next important step is an application of the model to the physics of parton distribution functions of the nucleon, initiated by Diakonov et al. [7],[8] and also by Tübingen group [9],[10].

2 Main achivements of the CQSM for low energy observables

Skipping the detailed explanation of the model, I just summarize below several noteworthy achievements of the CQSM for low energy baryon observables.

- First of all, it reproduces unexpectedly small quark spin fraction of the nucleon [2],[11] -[13] in conformity with the famous EMS observation [14] :

$$\Delta\Sigma \simeq 0.35. \tag{1}$$

- Secondly, it reproduces fairly large pion-nucleon sigma-term favored in the recent phenomenological determination [15] (see also [16]) :

$$\Sigma_{\pi N} \simeq 60\,\mathrm{MeV}. \tag{2}$$

- Furthermore, it resolves the famous g_A-problem of the Skyrme model as [5],[6]

$$g_A^{(Skyrme)} = g_A(\Omega^0) + g_A(\Omega^1) \simeq 0.8 + 0.0 = 0.8, \tag{3}$$
$$g_A^{(CQSM)} = g_A(\Omega^0) + g_A(\Omega^1) \simeq 0.8 + 0.4 = 1.2. \tag{4}$$

Unfortunately, most baryon observables are quite insensitive to the differences of low energy models, which results in masking the potential ability of the CQSM as compared with the others. It turns out, however, that that the superiority of the CQSM as a field theoretical model of baryons manifests most drastically in its predictions for the internal partonic structure of the nucleon.

3 On the role and achievements of CQSM in DIS physics

The standard approach to the DIS (deep-inelastic-scattering) physics is based on the so-called *factorization theorem*, which states that the DIS amplitude is factorized into two part, i.e. the *hard part* which can be handled by the perturbative QCD and the *soft part* which contains information on the nonperturbative quark-gluon structure of the nucleon. The soft part is usually treated as a blackbox, which should be determined via experiments. This is a reasonable strategy, since we have no simple device to solve nonperturbative QCD. We however believe that, even if this part is completely fixed by experiments, one still wants to know why those parton distribution functions (PDFs) take the form so determined ! Nonstandard but complementary approach to DIS physics is necessary here to understand hidden chiral dynamics of soft part, based on models or on lattice QCD.

There are several merits of the CQSM over many other effective model of baryons. First, it is a relativistic mean-field theory of quarks, consistent with the large N_c QCD supplemented with the $1/N_c$ expansion. Secondly, the field theoretical nature of the model, i.e. nonperturbative inclusion of polarized Dirac-sea quarks, enables reasonable estimation not only of quark distributions but also of *antiquark* distributions. Finally, only 1 parameter of the model, i.e. the dynamical quark mass M, was already fixed from low energy phenomenology, which means that we can make *parameter-free* predictions for parton distribution functions. As a matter of course, the biggest default of the model is the lack of the explicit gluon degrees of freedom.

In Fig.1, we summarize parameter-free predictions of the CQSM for the three fundamental twist-2 PDFs. They are the unpolarized PDF with isoscalar and isovector combinations, the longitudinally polarized PDF with isoscalar and isovector combinations, and finally the transversities with isoscalar and isovector combinations. Noteworthy here is totally *different behavior* of the Dirac-sea contributions in *different PDFs*.

The crucial importance of the Dirac-sea contribution can most clearly be seen in the isoscalar unpolarized PDF. First, I recall that the distribution function in the negative x region should be identified with the antiquark distribution with the extra minus sign.

$$\bar{q}(x) \;=\; -\,q(-x), \qquad (0 < x < 1). \tag{5}$$

Then, one can see that the positivity of the antiquark distribution $\bar{u}(x) + \bar{d}(x)$ is satisfied only after including the Dirac-sea contribution. It is also seen to generate sea-like soft component in the quark distribution in the small x region, as required in the GRV analysis even at the low energy scale [17].

Turning to the isovector unpolarized PDF, I point out that the $u(x) - d(x)$ is positive with sizable magnitude in the negative x region due to the effect of Dirac-sea contribution. Because of the charge conjugation property of this distribution, it means that $\bar{u}(x) - \bar{d}(x)$ is negative or $\bar{d}(x) - \bar{u}(x)$ is positive in consistency with the famous NMC observation [18]-[20]. One can also confirm that the model prediction for the $\bar{d}(x)/\bar{u}(x)$ ratio is consistent with the Fermi-Lab Drell-Yan data at least qualitatively [13].

Although we do not have enough space to go into the detail, we can also show that the model also reproduces all the characteristic features of the longitudinally polarized structure functions of the proton, neutron and the deuteron without introducing any additional parameters [11],[13].

4 Chiral-odd twist-3 distribution function $e(x)$

The distribution function $e(x)$ is one of the three twist-3 distribution functions of the nucleon. Why is it interesting ? Firstly, its first moment is proportional to the famous πN sigma term. Secondly, within the framework of perturbative QCD, it was noticed that this distribution function may have a delta-function type singularity at $x = 0$ [21]. However, the physical origin of this delta-function type singularity was left unclear within the perturbative consideration.

By utilizing the advantage of the CQSM, in which the effects of Dirac-sea quarks can be treated nonperturbatively, we have tried to clarify the physical origin of this delta-function type singularity [22],[15]. We first verified that, because of the spontaneous chiral symmetry breaking of the QCD vacuum, the scalar quark density of the nucleon does not damp as the distance from the nucleon center becomes large, but it approaches a nonzero negative constant, which is nothing but the vacuum quark condensate. (See. Fig.2.)

It was shown further that this extraordinary nature of the scalar quark density in the nucleon, i.e. the existence of the *infinite range* quark-quark correlation

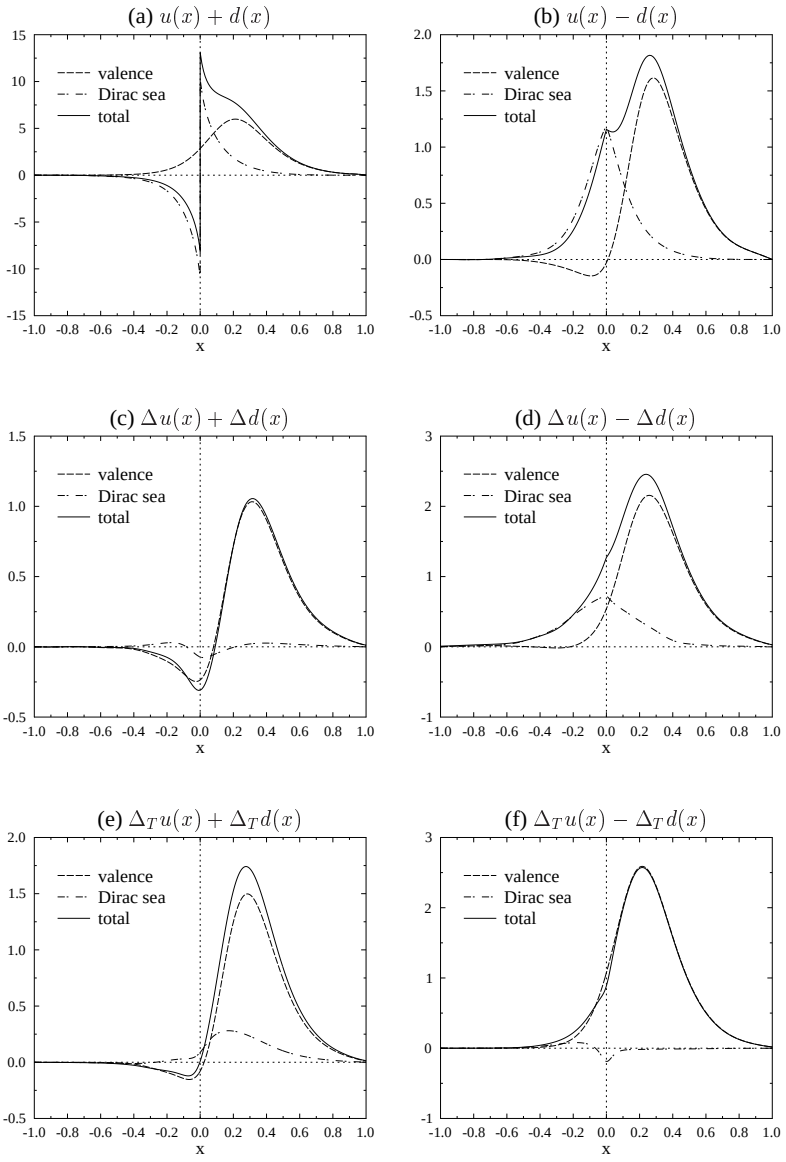

Fig. 1. The CQSM predictions for the fundamental twist-2 PDFs of the nucleon : isoscalar and isovector unpolarized PDFs ((a) and (b)), isoscalar and isovector longitudinally polarized PDFs ((c) and (d)), and isoscalar and isovector transversity distributions ((e) and (f)).

of scalar type, is the physical origin of the delta-function singularity in the chiral-odd twist-3 distribution $e(x)$. This singularity of $e(x)$ will be observed as the violation of πN sigma-term sum rule. To confirm this interesting possibility, we need very precise experimental information for $e(x)$ through the semi-inclusive DIS scatterings.

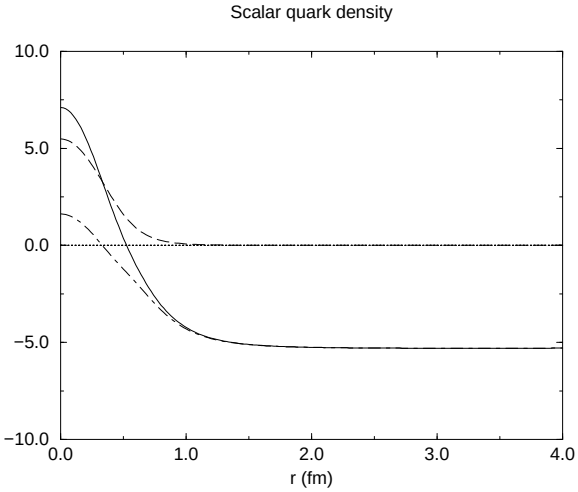

Fig. 2. The scalar quark density predicted by the CQSM.

5 Proton spin problem revisited : current status and resolution

Now, we come back to our biggest concern of study, i.e. the nucleon spin problem. Recent two remarkable progresses may be worthy of mention. First, the quark polarization $\Delta\Sigma$ has been fairly precisely determined, through the high-statistics measurements of deuteron spin structure function by the COMPASS and HERMES groups [23],[24]. Second, a lot of evidences have been accumulated, which indicate that the gluon polarization is likely to be small or at least it cannot be large enough to resolve the puzzle of the missing nucleon spin based on the $U_A(1)$ anomaly scenario. A general consensus now is therefore as follows. About $1/3$ of the nucleon spin is carried by the intrinsic quark spin, while the remaining $2/3$ should be carried by L^Q, Δg, and L^g.

Recently, Thomas advocates a viewpoint that the modern spin discrepancy can well be explained in terms of standard features of the nonperturbative structure of the nucleon, i.e. relativistic motion of valence quarks, the pion cloud required by chiral symmetry, and an exchange current contribution associated with the one-gluon-exchange hyperfine interaction [25]-[27]. His analysis starts from an estimate of the orbital angular momenta of up and down quarks based on the improved (or fine-tuned) cloudy bag model taking account of the above-mentioned effects. Another important factor of his analysis is the observation that the angular momentum is not a renormalization group invariant quantity, so that the above predictions of the model should be associated with a very low energy scale, say, $0.4\,\mathrm{GeV}$. Then, after solving the QCD evolution equations for the up and down quark angular momenta, first derived by Ji, Tang and Hoodbhoy [28], he was led to a remarkable conclusion that the orbital angular momenta of up and down quarks cross over around the scale of $1\,\mathrm{GeV}$. This crossover of L^u and L^d seems absolutely necessary for his scenario to hold. Otherwise, the prediction $L^u - L^d > 0$ of the improved cloudy bag model given at the low energy scale is

incompatible with the current empirical information or lattice QCD simulations at the high energy scale, which gives $L^u < 0, L^d > 0$.

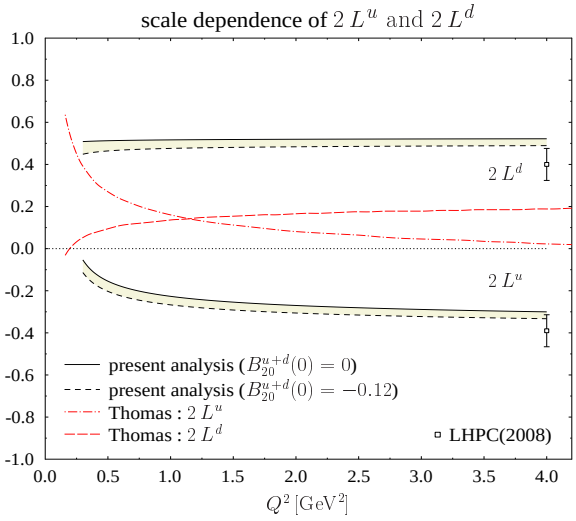

Fig. 3. Our semi-phenomenological predictions of the orbital angular momenta of up and down quarks in the proton are compared with the corresponding results of Thomas' analysis [27]. Also shown for comparison are the predictions of the LHPC lattice simulations for $2\,L^u$, and $2\,L^d$ given at the scale $Q^2 = 4\,\mathrm{GeV}^2$ [34].

On the other hand, we have recently carried out a semi-empirical analysis of the nucleon spin contents based on Ji's angular momentum sum rule, and extracted the orbital angular momentum of up and down quarks as functions of the scale [32]. (See also [33].) Remarkably, we find no crossover of L^u and L^d when Q^2 is varied, in sharp contrast to Thomas' analysis. This difference is remarkable, since if there is no crossover of L^u and L^d, Thomas' scenario for resolving the proton spin puzzle is seriously challenged.

We show in Fig.3 the results of our semi-empirical analysis for L^u and L^d in comparison with the corresponding predictions by Thomas. As already mentioned, Thomas' results show that the orbital angular momenta of up and down quarks cross over around the scale of 1 GeV. In contrast, no crossover of L^u and L^d is observed in our analysis : L^d remains to be larger than L^u down to the scale where the gluon momentum fraction vanishes. Comparing the two, the cause of this difference seems obvious. Thomas claims that his results are qualitatively consistent with the empirical information and the lattice QCD data at high energy scale. (We recall that the sign of L^{u-d} at the high energy scale is constrained by the asymptotic condition $L^{u-d}(Q^2 \to \infty) = -\Delta\Sigma^{u-d}$, which is a necessary consequence of QCD evolution [32],[25].) However, the discrepancy between his results and the recent lattice QCD predictions seems more than qualitative.

In any case, our semi-phenomenological analysis, which is consistent with the empirical information and/or the lattice QCD data for J^u and J^d, indicates that $L^u - L^d$ remains fairly large and negative even at the low energy scale of nonperturbative QCD. If this is confirmed, it is a serious challenge to any low energy models of nucleon, since they must now explain small $\Delta\Sigma^Q$ and large and negative L^{u-d} *simultaneously*. The refined cloudy bag model of Thomas and Myhrer obviously fails to do this job, since it predicts $2L^u \simeq 0.64$ and $2L^d \simeq -0.03$ at the model scale. (See Table.1 of [27]. Shown in this table should be $2L^u$ and $2L^d$ not L^u and L^d.) Is there any low energy model which can pass this examination ? Interestingly, the CQSM can explain both of these peculiar features of the nucleon observables. It has been long known that it can explain very small $\Delta\Sigma^Q$ ($\Delta\Sigma^Q \simeq 0.35$ at the model scale) due to the very nature of the model [2],[35]. Besides, its prediction for L^{u-d} given in [36], i.e. $L^{u-d} \simeq -0.327$ at the model scale, perfectly matches the conclusion obtained in the present semi-empirical analysis.

6 Concluding remarks

To conclude, the CQSM is a unique model of baryons, which has an intimate connection with more popular Skyrme model. Although the former is an effective quark theory, while the latter is an effective meson theory, they share a lot of common features. In spite of many strong similarities, a crucial difference between the two theories was noticed already in the study of ordinary low energy observables of the nucleon. It is a novel $1/N_c$ correction, or more concretely, the 1st order rotational correction, which was found to exist within the framework of the CQSM, while it is totally missing in the Skyrme model. An immediate consequence of this finding is breakdown of the so-called "Cheshire Car principle" or the fermion-boson correspondence. We can show that the origin of this breakdown of fermion-boson equivalence can eventually be traced back to the *noncommutativity* of the two procedures, i.e. the *bosonization* and the *collective quantization* of the rotational motion. Alternatively, we can simply say that an important information buried in the original fermion theory is lost in the process of approximate bosonization. (See [37] for more detail.) After all, the fact is that one is an effective quark (fermion) theory, while the other is an effective pion (meson) theory in $3+1$ dimension.

Superiority or wider applicability of the CQSM over the Skyrme model becomes even more transparent if one extends the object of research from low energy observables to the internal partonic structure of the nucleon (or more generally of any baryons). Since the parton distribution functions measure non-local light-cone correlation between quarks (and gluons) inside the nucleon, there is no way to describe them within the framework of effective meson theories like the Skyrme model. In contrast, this is just the place where the potential power of the CQSM manifest most dramatically. In this talk, we have shown, through several concrete examples, that the CQSM provide us with an excellent tool for theoretically understanding the nonperturbative aspect of the internal partonic structure of the nucleon. In particular, we have given a very plausible solution

to the longstanding "nucleon spin problem". We strongly believe that the proposed solution to this famous puzzle is already close to the truth, and it will be confirmed by experiments to be carried out in the near future.

Acknowledgments I would like to express my sincere thanks to the hospitality of the organizers, Profs. M. Rosina, B. Golli and S. Sirca during the workshop. Warm atmosphere and lively discussion at the workshop are greatly acknowledged. More detailed description of the material presented here can be found in [38].

References

1. D.I. Diakonov, V.Yu. Petrov, and P.V. Pobylista, Nucl. Phys. B **306**, 809 (1988).
2. M. Wakamatsu and H. Yoshiki. Nucl. Phys., A **524**, 561 (1991).
3. S. Kahana and G. Ripka, Nucl. Phys. A **429**, 462 (1984).
4. S. Kahana, G. Ripka, and V. Soni, Nucl. Phys. A **415**, 351 (1984).
5. M. Wakamatsu and T. Watabe, Phys. Lett. B **312**, 184 (1993).
6. Chr.V. Christov, A. Blotz, K. Goeke, P. Pobylitsa, V.Yu. Petrov, M. Wakamatsu, and T. Watabe, Phys. Lett. B **325**, 467 (1994).
7. D.I. Diakonov, V.Yu. Petrov, P.V. Pobylitsa, M.V. Polyakov, and C. Weiss, Nucl.Phys. B **480**, 341 (1996).
8. D.I. Diakonov, V.Yu. Petrov, P.V. Pobylitsa, M.V. Polyakov, and C. Weiss, Phys. Rev. D **56**, 4069 (1997).
9. H. Weigel, H. Gamberg, and H. Reinhardt, Mod. Phys. Lett. A **11**, 3021 (1996).
10. L. Gamberg, H. Reinhardt, and H. Weigel, Phys. Rev. D **58**, 054014 (1998).
11. M. Wakamatsu and T. Kubota, Phys. Rev. D **60**, 034020 (1999).
12. M. Wakamatsu and T. Watabe, Phys. Rev. D **62**, 054009 (2000).
13. M. Wakamatsu, Phys. Rev. D 67, 034005 (2003) ; Phys. Rev. D 67, 034006 (2003).
14. J. Ashman *et al.* (EMC Collaboration), Phys. Lett., B **206**, 364 (1988).
15. Y. Ohnishi and M. Wakamatsu, Phys. Rev. D **69**, 114002 (2004).
16. D.I. Diakonov, V.Yu. Petrov, and M. Praszałowicz, Nucl. Phys. B 323, 53 (1989).
17. M. Glück, E. Reya, and A. Vogt, Z. Phys. C **67**, 433 (1995).
18. M. Wakamatsu, Phys. Rev. D **46**, 3762 (1992).
19. M. Wakamatsu and T. Kubota, Phys. Rev. D **56**, 4069 (1998).
20. P.V. Pobylitsa, M.V. Polyakov, K. Goeke, T. Watabe, and C. Weiss, Phys. Rev. D **59**, 034024 (1999).
21. M. Burkardt and Y. Koike, Nucl. Phys. B **632**, 311 (2002).
22. M. Wakamatsu and Y. Ohnishi, Phys. Rev. D **67**, 114011 (2003).
23. V.Yu. Alexakhin *et al.* (COMPASS Collaboration), Phys. Lett. B **647**, 8 (2007)
24. A. Airapetian *et al.* (HERMES Collaboration), Phys. Rev. D **75**, 012007 (2007).
25. A.W. Thomas, Phys. Rev. Lett. **101**, 102003 (2008).
26. F. Myhrer and A.W. Thomas, Phys. Lett. B **663**, 302 (2008).
27. A.W. Thomas, arXiv:0904.1735 [hep-ph].
28. X. Ji, J. Tang, and P. Hoodbhoy. Phys. Rev. Lett., **76**, 740 (1996).
29. F. Ellinghause *et al.* (HERMES Collaboration), Eur. Phys. J. C **46**, 729 (2006).
30. Z. Ye (HERMES Collaboration), arXiv:hep-ex/0606061.
31. M. Mazouz *et al.* (JLab Hall A Collaboration), Phys. Rev. Lett. **99**, 242501 (2007).
32. M. Wakamatsu and Y. Nakakoji, Phys. Rev. D **77**, 074011 (2008).
33. M. Wakamatsu and Y. Nakakoji, Phys. Rev. D **74**, 054006 (2006).
34. Ph. Hägler *et al.* (LHPC Collaboration), Phys. Rev. D **77**, 094502 (2008).

35. S.J. Brodsky, J. Ellis, and M. Karliner, Phys. Lett. B **206**, 309 (1988)
36. M. Wakamatsu and H. Tsujimoto, Phys. Rev. D **71**, 074001 (2005).
37. M. Wakamatsu, Prog. Theor. Phys. **95**, 143 (1996).
38. M. Wakamatsu, "*Chiral Quark Soliton Model and Nucleon Spin Structure Functions*" in "*Handbook of Solitons : Research, Technology and Applications*", Eds. S.P. Lang and Salim H. Bedore, Nova Science Pub Inc, USA (2009).

Bled Workshops
in Physics
Vol. 10, No. 1
p. 71

Proceedings of the Mini-Workshop
Problems in Multi-Quark States
Bled, Slovenia, June 29 - July 6, 2009

Pion electro-production in the Roper region: K-matrix approach*

B. Golli[a,c], S. Širca[b,c], M. Fiolhais[d]

[a] Faculty of Education, University of Ljubljana, 1000 Ljubljana, Slovenia
[b] Faculty of Mathematics and Physics, University of Ljubljana, 1000 Ljubljana, Slovenia
[c] Jožef Stefan Institute, 1000 Ljubljana, Slovenia
[d] Department of Physics and Centre for Computational Physics, University of Coimbra, 3004-516 Coimbra, Portugal

Abstract. We review a method to calculate the pion electro-production amplitude in a framework of a coupled channel formalism incorporating quasi-bound quark-model states and discuss the results for the M_{1-} and the S_{1-} amplitudes in the P11 partial wave obtained in the Cloudy Bag Model.

1 Introduction

The P11 Roper resonance N(1440) is of particular interest among the low-lying nucleon excitations, not only because of its relatively low mass, but primarily because of the rather peculiar behavior of the scattering and electro-excitation amplitudes. This clearly indicates that the structure of the resonance can not be explained by a simple excitation of the quark core (like most of the other low-lying states). The mesons, in particular the pion and the σ-meson, play an important role, yet the question remains whether it is possible to explain the Roper solely in terms of the quark and meson degrees of freedom or exotic degrees of freedom have to be incorporated like the explicit gluons [1–3].

We have developed a general method to incorporate excited baryons represented as quasi-bound quark-model states into a coupled channel calculation using the K-matrix approach that can be applied to meson scattering as well as to electro and weak-production of mesons [4,5]. The method ensures unitarity through the symmetry of the K-matrix. It can be applied to a class of Hamiltonians with linear meson-baryon coupling, in which case it is possible to construct an exact expression for the T-matrix without explicitly specifying the form of the asymptotic states. The method is particularly suitable to investigate the interplay of different channels involving the low-lying isobars such as the Delta and the chiral mesons which we expect to play the dominant role in the dynamics of the Roper resonance.

* Talk delivered by B. Golli

In the next section we give a short review of the method and in the following section we discuss in more detail the proton and the neutron helicity amplitudes calculated in our model and confront them to the predictions of some phenomenological models.

2 A short overview of the K-matrix approach

We assume that in the energy range of the Roper resonance, the electro-production processes can be described in terms of the γN, πN, $\pi\Delta$ and σN channels. The latter two channels correspond to two-pion decay. The electro-production amplitude $\mathcal{M}_{\pi N}$ is obtained from the Heitler's equation

$$\mathcal{M}_{\pi N} = \mathcal{M}^K_{\pi N} + i\left[T_{\pi N\pi N}\mathcal{M}^K_{\pi N} + T_{\pi N\pi\Delta}\mathcal{M}^K_{\pi\Delta} + T_{\pi N\sigma N}\mathcal{M}^K_{\sigma N}\right], \qquad (1)$$

where $T_{\pi N\,MB}$ are the T-matrices for the $M + B \to \pi + N$ processes (M is ether π or σ; B either N or Δ), while the amplitudes

$$\mathcal{M}^K_{MB} = -\frac{\mathcal{N}_\gamma}{\sqrt{k_0 k_\gamma}}\,\langle\Psi^{MB}(m_J m_I; k_0, l)|\tilde{V}^\gamma_\mu(\mathbf{k}_\gamma)|\Psi_N(m_s m_t)\rangle \qquad (2)$$

are the matrix elements of the EM interaction $\tilde{V}^\gamma_\mu(\mathbf{k}_\gamma)$ between the nucleon ground state Ψ_N and the principal-value state of the MB system. Here k_γ is the photon 3-momentum, k_0 is the momentum and l the angular momentum of the outgoing pion, the m stand for the respective third components of the nucleon spin and isospin and those of the MB system, and $\mathcal{N}_\gamma = \sqrt{k_\gamma\omega_\gamma M_N/W}$. In (1) the T matrices and the M amplitudes involving the $\pi\Delta$ and the σN channels have been already averaged over the invariant masses of the respective hadron.

The principal value states $|\Psi^{MB}\rangle$ assume the form

$$|\Psi^{MB}\rangle = \mathcal{N}_{MB}\left\{[a^\dagger(k_M)|\widetilde{\Psi}_B\rangle]^{\frac{1}{2}\frac{1}{2}} + \sum_{\mathcal{R}} c^{MB}_{\mathcal{R}}|\Phi_{\mathcal{R}}\rangle + \sum_{M'B'}\int \frac{dk\,\chi^{M'B'MB}(k)}{\omega_k + E_{B'}(k) - W}\,[a^\dagger(k)|\widetilde{\Psi}_{B'}\rangle]^{\frac{1}{2}\frac{1}{2}}\right\}. \qquad (3)$$

The first term represents the free meson (π or σ) and the baryon (N or Δ) and defines the channel, the next term is the sum over *bare* tree-quark states $\Phi_{\mathcal{R}}$ involving different excitations of the quark core, the third term introduces meson clouds around different isobars, $E(k)$ is the energy of the recoiled baryon. The sum in the latter term includes also inelastic channels in which case the integration over the mass of the unstable intermediate hadrons (σ or Δ) is implied. The state $\widetilde{\Psi}_{B'}$ represents either the nucleon or the intermediate Δ; in the latter case it is normalized as $\langle\widetilde{\Psi}_\Delta(M'_\Delta)|\widetilde{\Psi}_\Delta(M_\Delta)\rangle = \delta(M_\Delta - M'_\Delta)$. The meson amplitudes $\chi^{M'B'MB}(k)$ are proportional to the (half) off-shell matrix elements of the K-matrix. From the variational principle for the K-matrix it is possible to derive an integral equation for

the meson amplitudes which is equivalent to the Lippmann-Schwinger equation for the K-matrix. The resulting χ amplitude takes the form

$$\chi^{M'B'MB}(k) = -\sum_{\mathcal{R}} \tilde{c}^{MB}_{\mathcal{R}} \widetilde{\mathcal{V}}^{M'}_{B'\mathcal{R}}(k) + \mathcal{D}^{M'B'MB}(k)\,, \tag{4}$$

where $\mathcal{D}^{M'B'MB}(k)$ originates in the non-resonant background processes while the first term represents the contribution of various resonances; in the P11 case these are the nucleon, the N(1440), the N(1710) ... Here

$$\tilde{c}^{MB}_{\mathcal{R}} = \frac{\widetilde{\mathcal{V}}^{M}_{B\mathcal{R}}}{Z_{\mathcal{R}}(W)(W - M_{\mathcal{R}})}\,, \tag{5}$$

where $\widetilde{\mathcal{V}}^{M}_{B\mathcal{R}}$ is the dressed matrix element of the quark-meson interaction between the resonant state and the baryon state in the channel MB, and $Z_{\mathcal{R}}$ is the wave-function normalization. The physical resonant state $\mathcal{R}$ is a superposition of the bare 3-quark states $\Phi_{\mathcal{R}'}$, hence $\widetilde{\mathcal{V}}^{M}_{B\mathcal{R}} = \sum_{\mathcal{R}'} u_{\mathcal{R}\mathcal{R}'} \mathcal{V}^{M}_{B\mathcal{R}'}$, where $\mathcal{V}^{M}_{B\mathcal{R}'}$ are the matrix elements with the bare 3-quark states.

In the vicinity of a resonance, e.g. the Roper N(1440), the term in the sum (4) corresponding to this particular resonance dominates. The amplitudes as well as the channel state (3) can be split into the *resonant* contribution, proportional to the coefficient $\tilde{c}^{MB}_{\mathcal{R}}$ corresponding to the chosen resonance, and the *background* contribution consisting of the non-resonant processes and the contribution from the resonances other than the chosen one. The principal-value state (3) can be cast in the form

$$|\Psi^{MB}\rangle = -K_{\pi N\, MB} \sqrt{\frac{k_0 W}{\pi^2 \omega_0 E_N}} \frac{\sqrt{\mathcal{Z}_{\mathcal{R}}}}{\widetilde{\mathcal{V}}^{\pi}_{N\mathcal{R}}} |\widehat{\Psi}^{res}\rangle + |\Psi^{MB\,(bkg)}\rangle, \tag{6}$$

where

$$|\widehat{\Psi}^{res}_{\mathcal{R}}\rangle = \mathcal{Z}_{\mathcal{R}}^{-\frac{1}{2}} \left[\sum_{\mathcal{R}'} u_{\mathcal{R}\mathcal{R}'}(W) |\Phi_{\mathcal{R}'}\rangle - \int dk\, \frac{\widetilde{\mathcal{V}}^{\pi}_{N\mathcal{R}}(k)[a^{\dagger}(k)|\Psi_N\rangle]^{\frac{1}{2}\frac{1}{2}}}{\omega_k + E_N(k) - W} \right.$$
$$\left. - \sum_{MB} \int dk\, \frac{\widetilde{\mathcal{V}}^{M}_{B\mathcal{R}}(k)[a^{\dagger}(k)|\widehat{\Psi}_B\rangle]^{\frac{1}{2}\frac{1}{2}}}{\omega_k + E_B(k) - W} \right], \tag{7}$$

and $K_{\pi N\, MB}$ is the K-matrix element for the $M + B \to \pi + N$ process. The state (7) has a familiar interpretation of a 3-quark state dressed by a cloud of mesons. The resonant part of the electro-production amplitudes then reads

$$\mathcal{M}^{(res)}_{\pi N} = -\sqrt{\frac{\omega_\gamma E^{\gamma}_N}{\pi^2 \omega_0 E_N}} \frac{\sqrt{Z_{\mathcal{R}}}}{\mathcal{V}_{N\mathcal{R}}} \langle \widehat{\Psi}^{(res)}_{\mathcal{R}}(W) | \tilde{V}^{\gamma} | \Psi_N \rangle\, T_{\pi N\pi N}\,, \tag{8}$$

while the background part satisfies

$$\mathcal{M}^{(bkg)}_{\pi N} = \mathcal{M}^{K\,(bkg)}_{\pi N} + i \left[T_{\pi N\pi N} \mathcal{M}^{K\,(bkg)}_{\pi N} + \overline{T}_{\pi N\pi\Delta} \overline{\mathcal{M}}^{K\,(bkg)}_{\pi\Delta} + \overline{T}_{\pi N\sigma N} \overline{\mathcal{M}}^{K\,(bkg)}_{\sigma N} \right], \tag{9}$$

where $\overline{T}$ and $\overline{\mathcal{M}}$ are the amplitudes averaged over the invariant masses of the intermediate hadron using the averaging procedure introduced in [4].

3 The helicity amplitudes

The electro-production amplitudes at the photon point (i.e. at $Q^2 = 0$) have been extensively discussed in [5]; here we discuss in more detail the helicity amplitudes for the proton and the neutron. In our approach, the transverse and the scalar helicity amplitude are defined as

$$A_{\frac{1}{2}} = -\xi_{\mathcal{R}} \langle \widehat{\Psi}^{\rm res}_{\mathcal{R}} (m'_s = \tfrac{1}{2}) | \tilde{V}^{M1} | \Psi_N (m_s = -\tfrac{1}{2}) \rangle \,, \tag{10}$$

$$S_{\frac{1}{2}} = -\xi_{\mathcal{R}} \langle \widehat{\Psi}^{\rm res}_{\mathcal{R}} (m'_s = \tfrac{1}{2}) | \tilde{V}^{C0} | \Psi_N (m_s = \tfrac{1}{2}) \rangle \,, \tag{11}$$

with $m'_t = m_t = \frac{1}{2}$ for the proton and $m'_t = m_t = -\frac{1}{2}$ for the neutron, and $\xi_{\mathcal{R}} = \mathrm{sign}(g_{\pi N\mathcal{R}}/g_{\pi NN})$. The relation to the electro-production amplitudes at the *pole* of the K-matrix, $W = M_{\mathcal{R}}$, is determined through (8). Using the expression for the elastic width of the resonance $\Gamma_{\pi N} = 2\pi\omega_0 E_N \mathcal{V}^{\pi}_{N\mathcal{R}}(k_0)^2/Z_{\mathcal{R}} k_0 W$ and the relation $\mathrm{Im}T_{\pi N\pi N} = \Gamma_{\pi N}/\Gamma$ (at $W = M_{\mathcal{R}}$) we find

$$\mathrm{Im}\,{}^{p,n}M^{\frac{1}{2}}_{1-} = -\xi_{\mathcal{R}} \sqrt{\frac{k_W M_N \Gamma_{\pi N}}{6\pi k_0 M_{\mathcal{R}} \Gamma^2}}\, A^{p,n}_{\frac{1}{2}} \,, \qquad \mathrm{Im}\,{}^{p,n}S^{\frac{1}{2}}_{1-} = \xi_{\mathcal{R}} \sqrt{\frac{k_W M_N \Gamma_{\pi N}}{3\pi k_0 M_{\mathcal{R}} \Gamma^2}}\, S^{p,n}_{\frac{1}{2}} \,. \tag{12}$$

We have performed the calculation of the electro-production amplitudes in the Cloudy Bag Model (CBM) with the same choice of parameters as in the calculation of the scattering amplitudes [4]. We use the same bag radius for the excited states as for the ground state.

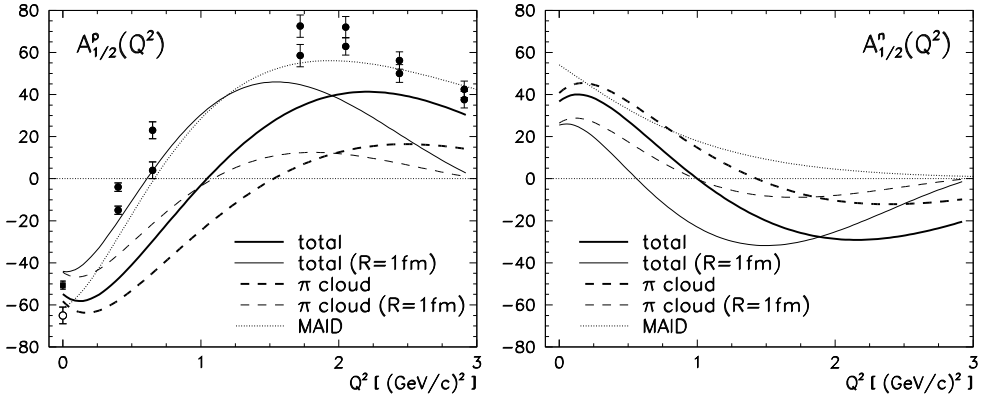

Fig. 1. Transverse helicity amplitudes for the proton (left panel) and the neutron (right panel) at the pole of the K matrix ($W = 1530$ MeV) for two values of the bag radius ($R = 0.83$ fm and $R = 1$ fm). The contribution of the meson cloud includes the $\gamma\pi\pi'$ interaction and the pion corrections to the $\gamma BB'$ vertex. Empty circle: PDG value [6]; full square and circles: analyses of newer JLab experiments. Two values at each $Q^2 \neq 0$ correspond to two different extraction approaches (see [7] for details). The MAID parametrization is given in [8].

The transverse helicity amplitudes for the proton and the neutron are displayed in Fig. 1 at the pole of the K-matrix where the relations (12) are fulfilled,

and in Fig. 2 at the nominal mass of the Roper resonance. The difference between the calculated amplitudes in these two cases arises through the W dependence of the ground state admixture and of the pion amplitudes in (7). We reproduce the value at the photon point for the proton as well as for the neutron. These values are dominated by the pion cloud effects while the contribution from the bare quark core is almost negligible. At higher Q^2 the quark core contribution becomes stronger and positive for the proton (and negative for the neutron) while that of the pion cloud diminishes. As a result the amplitudes exhibit a zero crossing which is observed also in the experiment. At the smaller bag radius, the crossing occurs at somewhat higher Q^2 which may signify a too strong pion field.

Since no experimental data are available for the neutron for $Q^2 \neq 0$, we can compare our prediction only to the phenomenological expression of Ref. [8] where, however, no zero crossing occurs. In our model the zero crossing in the neutron case originates in the same mechanism as in the proton case; precise measurements of pion electro-production on the neutron may therefore provide a serious check for the proposed meson cloud picture.

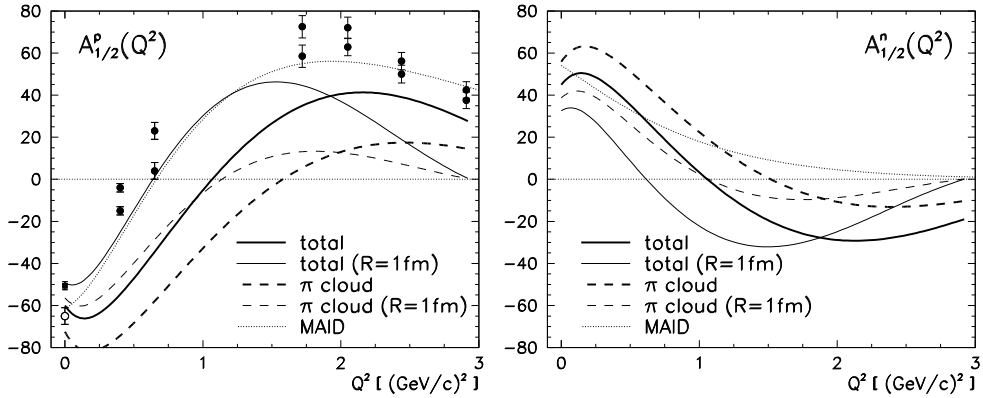

Fig. 2. Transverse helicity amplitudes at the nominal energy of the resonance ($W = 1440$ MeV). Notation as in Fig. 1.

The situation is rather controversial in the case of the scalar helicity amplitudes displayed in Fig. 3. Here we give the calculated values only at the pole of the K-matrix since the dependence on W is weak. The most striking feature is that the amplitudes cross zero while the experimental points – lacking values at low Q^2 – do not indicate this type of behavior. The zero crossing is again a consequence of the same mechanism as in the case of the transverse amplitudes. The MAID phenomenological analysis shows a rather sharp drop at $Q^2 \to 0$ though their amplitude does not cross zero. On the other hand, in this limit the imaginary part of the SAID partial wave analysis [9] does reach a negative value at $W = 1530$ MeV, supporting the possibility of a zero crossing also in this case. From this comparison we can conclude that it is again the pion cloud that governs the behaviour of the amplitudes at low Q^2; this effect is likely to be exaggerated in the present model.

The calculated scalar amplitudes for the neutron displayed in the right panel of Fig. 3 remain close to zero except at low Q^2. This result is less reliable because of a rather strong cancellation of different contributions; yet we do not see a mechanism in our model that could yield a relatively large amplitude of the MAID phenomenological analysis.

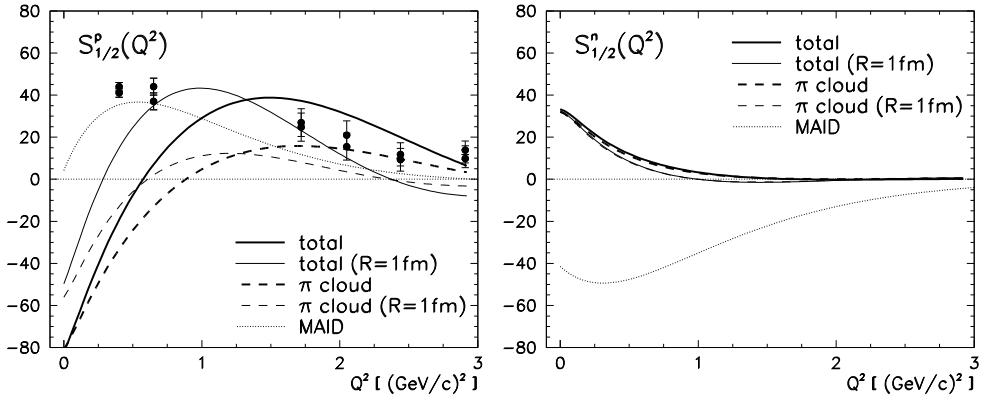

Fig. 3. Scalar helicity amplitudes at the pole of the K matrix ($W = 1530$ MeV). Notation as in Fig. 1.

References

1. Zhenping Li, Volker Burkert, and Zhujun Li, Phys. Rev. D **46** (1992) 70.
2. W. Broniowski, T. D. Cohen and M. K. Banerjee, Phys. Lett. B **187** (1987) 229.
3. P. Alberto, M. Fiolhais, B. Golli, and J. Marques, Phys. Lett. B **523** (2001) 273.
4. B. Golli and S. Širca, Eur. Phys. J. A **38** (2008) 271.
5. B. Golli, S. Širca, and M. Fiolhais, Eur. Phys. J. A **42** (2009) 185.
6. C. Amsler et al. (Particle Data Group), Phys. Lett. B **667** (2008) 1.
7. I. Aznauryan et al. (CLAS Collaboration), Phys. Rev. C **78** (2008) 045209.
8. L. Tiator, D. Drechsel, S. S. Kamalov, M. Vanderhaeghen, in: Proceedings of NSTAR2009, Beijing, to be published in Chinese Physics C (HEP & NP) **33** (2009), `arXiv:0909.2335v1 [nucl-th]`, D. Drechsel, S. S. Kamalov, L. Tiator, Eur. Phys. J. A **34** (2007) 69.
9. R. Arndt et al., Phys. Rev. C **52** (1995) 2120; R. Arndt et al., Phys. Rev. C **69** (2004) 035213.

Bled Workshops
in Physics
Vol. 10, No. 1
p. 77

Proceedings of the Mini-Workshop
Problems in Multi-Quark States
Bled, Slovenia, June 29 - July 6, 2009

What have we learned from the Nambu–Jona-Lasinio model

Mitja Rosina[a,b]

[a]Faculty of Mathematics and Physics, University of Ljubljana, Jadranska 19, P.O. Box 2964, 1001 Ljubljana, Slovenia
[b]J. Stefan Institute, 1000 Ljubljana, Slovenia

Abstract. The Nambu–Jona-Lasinio model has played an important conceptual and pedagogical role in hadronic physics to visualize the spontaneous chiral symmetry breaking, the formation of the massive constituent quark and the behaviour of pion and sigma meson as a chiral rotation and vibration. I shall give a brief review of three new developments, (i) some observables for pion, (ii)more consistent results in three-flavour systems after introducing three-body and four-body interactions, and (iii) additional perspectives offered by algebraic models, in particular the two-level quasispin model,

1 Introduction

The Nambu–Jona-Lasinio model (NJL) is still inspiring hadronic physicists to gain a deeper qualitative or even semiquantitative understanding of the spontaneous chiral symmetry breaking, the formation of the massive constituent quark and the properties of light mesons. Further encouragement is coming from the progress how to derive NJL from QCD in a reasonable approximation, for example the Bogolyubov compensation method which is presented by Boris Arbuzov in these Proceedings.

On one hand, one is interested in further simplifications of NJL in order to see the role of 1/N expansions, sum rules and the effective pion-pion interaction (Sect. 4), as well as the bosonization in momentum space (Sect. 2). On the other hand, the applicability of the model is largely extended by further "complications" such as the three-body and four-body forces (Sect. 3).

I apologize that the review of our work is much longer than that of our friends, but you can find their presentation in these Proceedings.

2 Electromagnetic polarizabilities of pion

The Coimbra group [1] presented the calculation of pion electromagnetic dipole and quadrupole polarizabilities. They obtain the sign and magnitude in agreement with the respective experimental analysis based on the dispersion sum rules. The result are consistent also with the chiral perturbation theory.

For the neutral pion, the difference of the electric and magnetic dipole polarizabilities shows that the box contribution is largely canceled by the scalar exchange. For the charged pion, however, the pion exchange diagram builds together with the box a gauge invariant amplitude which is an order of magnitude smaller than the sigma-exchange diagram, and the pion loops are absent.

In the quadrupole polarizability difference of the neutral pion, the pion loop is about twice the sigma-exchange and dominates. For the charged pion, the pion-loop diagram has the same magnitude as the sigma-exchange term.

3 The effect of three-body and four-body interactions

The NJL model has been consistently extended to three-flavour systems, and recently, electromagnetic and weak decays of scalar and vector mesons have been calculated in leading orders of Feynman graphs [2,3]. For a good description of vector mesons, a vector-vector and axial vector-axial vector interaction is needed in addition to the usual scalar-scalar and pseudoscaar-pseudoscalar interaction.

Long ago, a three-body interaction (also called the "six-quark" t'Hooft interaction) was introduced in order to split the singlet and octet mesons – the U(1) symmetry problem. However it destabilizes the vacuum. The introduction of the four-body force (also called the "eight-quark interaction") not only stabilizes the vacuum, but also influences the phase transition in hot dense systems and in strong magnetic fields [4]. This is a promising research topic for NJL.

4 The two-level quasispin model

In the Mini-Workshop Bled 2006, 2007 and 2008 [5–8] Borut Oblak and I presented a soluble two-level quasispin model of spontaneous chiral symmetry breaking, inspired by the Nambu–Jona-Lasinio model. It is the hadronic analogue of the Lipkin model in nuclear physics.

The model is characterized by a finite number N of quarks occupying a finite number $N = N_c N_f \mathcal{V}\Lambda^3/3\pi^2$ of states in the Dirac sea as well as in the valence space due to a sharp momentum cutoff Λ, and a periodic boundary condition in a box $\mathcal{V}$. We further simplify the one-flavour Nambu – Jona-Lasinio Hamiltonian ($N_f = 1, N_c = 3$) by taking all quark kinetic energies equal to $\frac{3}{4}\Lambda$ and by neglecting the interaction terms which change the individual quark momenta:

$$H = \sum_{k=1}^{N} \left(\gamma_5(k) h(k) \tfrac{3}{4}\Lambda + m_0 \beta(k) \right) - \frac{2G}{\mathcal{V}} \left(\sum_{k=1}^{N} \beta(k) \sum_{l=1}^{N} \beta(l) + \sum_{k=1}^{N} i\beta(k)\gamma_5(k) \sum_{l=1}^{N} i\beta(l)\gamma_5(l) \right).$$

Here $h = \boldsymbol{\sigma}\cdot\mathbf{p}/p$ is helicity and γ_5 and β are Dirac matrices. In terms of quasispin operators which obey spin commutation relations ($\alpha = x, y, z$)

$$R_\alpha = \sum_{k=1}^{N} \frac{1+h(k)}{2} j_\alpha(k)\,, \quad L_\alpha = \sum_{k=1}^{N} \frac{1-h(k)}{2} j_\alpha(k)\,, \quad J_\alpha = R_\alpha + L_\alpha = \sum_{k=1}^{N} j_\alpha(k)\,,$$

the model Hamiltonian can be written as

$$H = 2P(R_z - L_z) + 2m_0 J_x - 2g(J_x^2 + J_y^2)\,.$$

It commutes with R^2 and L^2 but not with R_z and L_z. Nevertheless, it is convenient to work in the basis $|\, R, L, R_z, L_z \,\rangle$ and diagonalize the Hamiltonian for fixed R and L.

From the quasispin model of the Nambu–Jona-Lasinio type one can learn several lessons:

(i) We show that the popular model parameters [9,10], $\Lambda = 648$ MeV, $G = 40.6$ MeV fm^3, $m_0 = 4.58$ MeV, yield the phenomenological values of quark constituent mass, quark condensate and pion mass **both** in the full Nambu – Jona-Lasinio model as well as in our quasispin model (using in both cases the Hartree-Fock + RPA approximations).

(ii) In the large N limit the exact results of our quasispin model approach the HF+RPA values, thus giving credit to using HF+RPA in usual calculations.

(iii) In the quasispin model it is very instructive that the number of colours N_c and the number of spatial states $\mathcal{V}\Lambda^3/6\pi^2$ appear on equal footing in the product $N = 2N_c\mathcal{V}\Lambda^3/6\pi^2$. The colour and the momentum quantum number together are just the house number of the particle since the interaction does not depend on them. Therefore it is the same limit $N \to \infty$ whether we take the large N_c limit or a large block $\mathcal{V}$. This explains why even with 3 colours the quasispin model behaves similarly as the theorems regarding large N_c limit suggest (good HF approximation, suppression of off-diagonal terms and their effects, etc.).

(iv) Most low-lying states in the excitation spectrum can be interpreted as multi-pion states and one can deduce the effective pion-pion interaction and scattering length. Also, some intruder states can be recognized as sigma-meson excitations or their admixtures to multi-pion states.
Since we are working in a finite volume $\mathcal{V}$ with periodic boundary conditions we cannot impose scattering boundary conditions. It is instructive that one can nevertheless extract information on scattering from a discrete spectrum. Energy levels of n-pion states can be interpreted to contain the average effective pion-pion potential $\bar{V}$: $E_{n\pi} = n\, m_\pi + \frac{1}{2}n(n-1)\bar{V}$.
We calculate the s-state scattering length in the first-order Born approximation (also derived by M.Lüscher [11] in a much more "sophisticated" way)

$$a = \frac{m_\pi/2}{2\pi}\int V(\mathbf{r})\,d^3r = \frac{m_\pi}{4\pi}\bar{V}\mathcal{V}\,.$$

In our example for $N = 192$ we have $\bar{V} = -7.1$ MeV and $\mathcal{V} = \pi^2 N/\Lambda^3 = 53\,\mathrm{fm}^3$ This gives $a\, m_\pi = (m_\pi^2/4\pi)\bar{V}\mathcal{V} = -0.0836$ not far from phenomenological value (see [5,8]).

References

1. B. Hiller, W. Broniowski, A. A. Osipov, A. H. Blin, these Proceedings (2009); also available at arXiv:0909.4867.
2. V. Bernard, A. H. Blin, B. Hiller, U-G. Meissner, and M. C. Ruivo, Phys. Lett. **B305**, 163 (1993); also hep-ph/9302245
3. Yu. L. Kalinovski and M. K. Volkov, hep-ph/08091795
4. A. A. Osipov, B. Hiller, A. H. Blin, J. Moreira, these Proceedings (2009); also available at arXiv:0910.0371.
5. M. Rosina and B. T. Oblak, Bled Workshops in Physics **7**, No.1, 92 (2006); also available at http://www-f1.ijs.si/BledPub.
6. M. Rosina and B. T. Oblak, Bled Workshops in Physics **8**, No.1, 66 (2007); also available at http://www-f1.ijs.si/BledPub.
7. M. Rosina and B. T. Oblak, Bled Workshops in Physics **9**, No.1, 98 (2008); also available at http://www-f1.ijs.si/BledPub.
8. M. Rosina, Few Body Systems (2009), in print
9. M. Fiolhais, J. da Providência, M. Rosina and C. A. de Sousa, Phys. Rev. C **56**, 3311 (1997).
10. M. Buballa, Phys. Reports **407**, 205 (2005).
11. M. Lüscher, Commun. Math. Phys. **104**, 177 (1986); **105**, 153 (1986); Nucl. Phys. **B354**, 531 (1991).

BLED WORKSHOPS
IN PHYSICS
VOL. 10, NO. 1
p. 81

Proceedings of the Mini-Workshop
Problems in Multi-Quark States
Bled, Slovenia, June 29 - July 6, 2009

Pion electro-production in the Roper region: planned experiment at the MAMI/A1 setup

S. Širca

Faculty of Mathematics and Physics, University of Ljubljana, 1000 Ljubljana, Slovenia
Jožef Stefan Institute, 1000 Ljubljana, Slovenia

Abstract. This paper describes technical details of the experiment proposal submitted to the MAMI/ELSA Program Advisory Committe 2009 to study the structure of the Roper resonance by a measurement of recoil proton polarization components in the $p(\vec{e},e'\vec{p})\pi^0$ reaction. These components exhibit strong sensitivities to the resonant Roper multipoles M_{1-} and S_{1-}. The measurements will offer a unique insight for extracting information on the $N \to R$ transition through comparison with the state-of-the-art models, and will also provide severe constraints on these models in the second resonance region.

1 Introduction

The $P_{11}(1440)$ (Roper) resonance [1] is the lowest positive-parity $N^\star$ state. It is visible in partial-wave decompositions of $\pi N \to \pi N$ and $\pi N \to \pi\pi N$ scattering [2,3] as a shoulder around 1440 MeV with a width of about 350 MeV [4]. Its large width causes it to merge with the adjacent $D_{13}(1520)$ and $S_{11}(1535)$ resonances, and therefore it can not be resolved from the W-dependence of the cross-section alone. A more selective and sensitive experiment has been designed in which the structure of the Roper will be probed by measuring the recoil proton polarization components P'_x, P_y, and P'_z in the $p(\vec{e},e'\vec{p})\pi^0$ reaction at a specific value of Q^2, W and centre-of-mass angle θ. It is for the first time that the Roper resonance is being approached by means of the recoil-polarization technique, although this strategy benefits substantially from the experience gained in the well-studied $N \to \Delta$ transition.

2 Relation to other experiments

The region of the Roper resonance has been explored to various extents in the past both at Jefferson Lab and MAMI. In most of the experiments, only cross-sections (angular distributions) were measured. Only a handful of single- and double-polarization measurements have been performed so far.

2.1 Jefferson Lab: Hall B (CLAS)

Kinematically most extensive data sets on single-pion electro-production in the nucleon resonance regions come from Hall B at JLab. Angular distributions and W-dependence of the electron beam asymmetry $\sigma_{LT'}$ have been measured for both charged and neutral channels in the $P_{33}(1232)$ region at $Q^2 = 0.4$ and $0.65\,(\mathrm{GeV/c})^2$ [5,6]. Dispersion-relation (DR) techniques and unitary isobar models (UIM) have been applied to analyze the CLAS $\sigma_{LT'}$ data in this range of Q^2 and spanning also the second resonance region, in order to extract the contributions of the $P_{33}(1232)$, $P_{11}(1440)$, $D_{13}(1520)$, and $S_{11}(1535)$ resonances to single-pion production [7].

A complete angular coverage was achieved, and several relevant amplitudes could be separated in a partial-wave analysis restricted to $l \leq 2$. The Legendre moments D_0, D_1, and D_2 of the expansions

$$\sigma_\alpha = D_0 + D_1\,P_1(\cos\theta^\star_\pi) + D_2\,P_2(\cos\theta^\star_\pi) + \cdots$$

for different partial cross-sections σ_α (or corresponding structure functions) were determined, e.g. for $\sigma_\alpha \equiv \sigma_T + \varepsilon\sigma_L$. To achieve a good fit of θ^*_π- and W-dependence of $\sigma_{LT'}$, a simultaneous adjustment of the M_{1-} and S_{1-} amplitudes was needed. Since both the $p\pi^0$ and the $n\pi^+$ channel were measured, the transverse helicity amplitude $A^p_{1/2} \propto_p M^{1/2}_{1-}$ as well as the scalar $S^p_{1/2} \propto_p S^{1/2}_{1-}$ could be extracted. The results show a rapid fall-off of $A^p_{1/2}$ and indicate its zero-crossing at approximately $Q^2 = 0.5\,(\mathrm{GeV/c})^2$.

In Hall B, there is also an approved experiment E03-105 [8] to measure single-pion photo-production in both $p(\gamma,\pi^+)n$ and $p(\gamma,p)\pi^0$ channels, with polarized beam and longitudinally and transversely polarized target using CLAS. It will measure two single- (T and P) and three double-polarization observables (G, F, and H); in addition, the experiment E01-104 will measure the double-polarization observable E. The measurements will span the range $1300 \leq W \leq 2150\,\mathrm{MeV}$ and achieve an angular coverage of $-0.9 \leq \cos\theta^\star \leq 0.9$.

It is believed that this data will greatly constrain partial-wave analyses in photo-production and reduce model-dependent uncertainties in the extraction of nucleon resonance properties. A similar goal, but in electro-production, and utilizing the recoil-polarimetry technique, has been put forward by the Hall A Collaboration at JLab [9]. To some extent this experiment would be complementary to the effort with CLAS. However, due to Laboratory beam-time constraints, it has been deferred.

2.2 Jefferson Lab: Hall A

Polarized electron beam and recoil-polarimetry capability of Hall A also allow access to double-polarization observables in single-pion electro-production. Recoil-polarization observables are composed of different combinations of multipole amplitudes than observables accessible in the case of a polarized target.

The acceptance of CLAS is large enough to achieve a complete angular coverage of the outgoing hadrons. This is not possible in the case of relatively small

angular openings of the Hall A HRS spectrometers *except* at high Q^2 where the Lorentz boost from the center-of-mass to lab frame focuses the reaction products into a cone narrow enough to provide a virtually complete out-of-plane acceptance. The E91-011 experiment in Hall A in the $p(\vec{e},e'\vec{p})\pi^0$ channel [10] was performed at sufficiently high $Q^2 = (1.0 \pm 0.2)\,(\mathrm{GeV/c})^2$ and $W = (1.23 \pm 0.02)\,\mathrm{GeV}$ to allow for a measurement of all accessible response functions, even those that vanish for coplanar kinematics. Two Rosenbluth combinations and 14 structure functions could be separated, allowing for a restricted partial-wave analysis giving access to all $l \leq 1$ multipole amplitudes relevant to the $N \rightarrow \Delta$ transition. Both multipoles indicate a rising trend approaching the $W \sim 1440\,\mathrm{MeV}$ region, again pointing towards the Roper.

Unfortunately, the cross-sections at $W \sim 1440\,\mathrm{MeV}$ (for any Q^2) are about an order of magnitude smaller than in the Δ-peak. For high $Q^2 \sim 1\,(\mathrm{GeV/c})^2$, where a large out-of-plane coverage would allow for a decent partial-wave analysis in Hall A, the cross-sections are even smaller. Furthermore, due to the zero-crossing uncertainty of the M_{1-} multipole, it is not clear what value of Q^2 to choose in order to have a prominent M1 signal. Furthermore, models indicate that the crucial features of the Roper multipoles (or helicity amplitudes) are visible at relatively small Q^2 of a few $0.1\,(\mathrm{GeV/c})^2$, nullifying the boost-advantage of the HRS spectrometers.

We note in addition that higher partial waves ($l \geq 2$) in all JLab partial-wave analyses so far needed to be constrained by models (just as in the CLAS experiments). Thus, even with (almost) complete angular coverages, existing data sets of finite statistical certainty do not allow for a "full" partial-wave analysis to sufficiently large l.

2.3 MAMI/A2

In photo-production, the double-polarization asymmetry G for linearly polarized photons (P_γ) and target nucleons polarized longitudinally (P_z) along the photon momentum, exhibits a very strong sensitivity to the Roper resonance. It is defined as

$$G = \frac{d\sigma(\Phi = 45^\circ, z) - d\sigma(\Phi = -45^\circ, z)}{d\sigma(\Phi = 45^\circ, z) + d\sigma(\Phi = -45^\circ, z)}\,,$$

where Φ is the angle between the photon polarization plane and the reaction plane. The cross-section has the form

$$d\sigma(\theta_\pi, \Phi) = d\sigma(\theta_\pi)\Big(1 - P_\gamma\,\Sigma(\theta_\pi)\,\cos 2\Phi + P_\gamma P_z\,G(\theta_\pi)\,\sin 2\Phi\Big)\,.$$

In the $\vec{\gamma}\vec{p} \rightarrow p\pi^0$ reaction, G depends on the interference of the much better-known M_{1+} multipole governed by the $\Delta(1232)$, and the M_{1-} driven by the Roper,

$$G(\theta_\pi) \simeq \sin^2\theta_\pi\;\mathrm{Im}M_{1+}\,\mathrm{Re}M_{1-}\,.$$

The asymmetry G will be measured by virtue of its $\sin 2\Phi$-dependence at the A2 Collaboration at MAMI with the Φ-symmetric detector DAPHNE. The expected sensitivity is shown in Fig. 1. In addition to the $p\pi^0$, the $n\pi^+$ channel will be measured, allowing for the isospin decomposition of the partial waves.

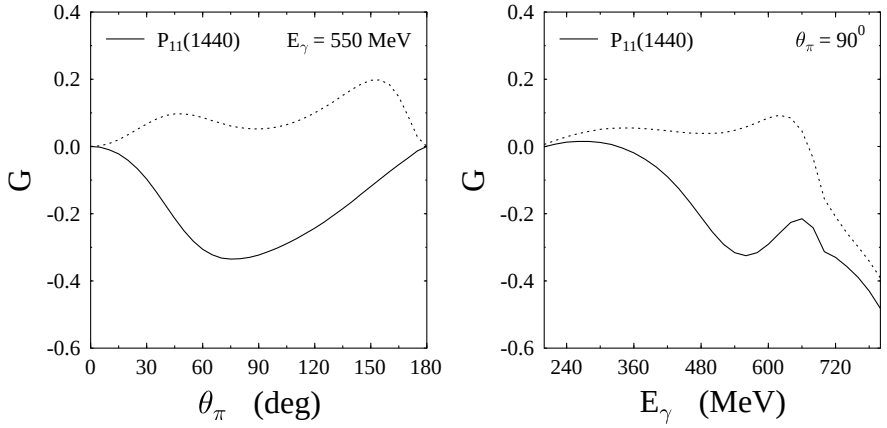

Fig. 1. MAID prediction for G in $\vec{\gamma}\vec{p} \to p\pi^0$: angular distribution at $W = 1440\,\mathrm{MeV}$ and energy dependence at $\theta_\pi = 90^\circ$. The dotted curves correspond to the Roper switched off.

2.4 MAMI: A1

All three recoil polarization components (P'_x/P_e, P_y, and P'_z/P_e) in the $p(\vec{e}, e'\vec{p})\pi^0$ reaction at the Δ resonance, at $Q^2 = 0.121\,(\mathrm{GeV/c})^2$ have been measured by the A1 Collaboration at MAMI [11]. These components, in particular the P'_x, were shown to be highly sensitive to the Coulomb quadrupole to magnetic dipole ratio

$$\mathrm{CMR} = \mathrm{Im}S_{1+}^{(3/2)}/\mathrm{Im}M_{1+}^{(3/2)}$$

in the $N \to \Delta$ transition. (For the results of a similar, far more ambitious experiment at higher Q^2 at JLab, see [12].)

3 Proposed measurement at MAMI/A1

A straight-forward extension of the $N \to \Delta$ program in the $\vec{p}\pi^0$ channel into the Roper region appears to be unfeasible at Mainz/A1 due to instrumental constraints. Wishing to cover a reasonably broad kinematic range in the Roper region, one typically encounters angular and momentum settings and focal-plane polarimetry conditions which are unfavourable for the A1 spectrometer setup (assuming the existence of a fully equipped and operational KAOS spectrometer).

However, a good compromise can be found by going to non-parallel (or non-anti-parallel) kinematics for the proton. By doing this, we sacrifice some of the high sensitivities to the inclusion/exclusion of the Roper seen in the predicted polarization components, but we tune the kinematics such that we balance well between the physics sensitivities and maintaining good figures-of-merit for the FPP, as well as satisfying all geometry and momentum requirements. We have proposed the following baseline kinematics:

$$E_e = 1500\,\mathrm{MeV}\,, \qquad Q^2 = 0.1\,\mathrm{GeV}^2\,, \qquad E'_e = 811\,\mathrm{MeV/c}\,, \qquad \theta_e = 16.5^\circ$$

for the electron (to be detected in Spectrometer B) and corresponding to an invariant mass of $W = 1440\,\mathrm{MeV}$. The hadron kinematics was chosen to be at $\theta_{cms} = 90°$, which translates into

$$p_p = 668\,\mathrm{MeV/c}\,, \qquad T_p = 214\,\mathrm{MeV}\,, \qquad \theta_p = 54.2°$$

to be covered by Spectrometer A. The proton kinetic energy in the center of the carbon secondary scatterer in the FPP is then about $T_{cc} \approx 200\,\mathrm{MeV}$, which translates into a favourable figure-of-merit (FOM) of about $f_{FPP} \approx 0.006$. The FOM drops to ≈ 0.003 for $\theta \approx 75°$.

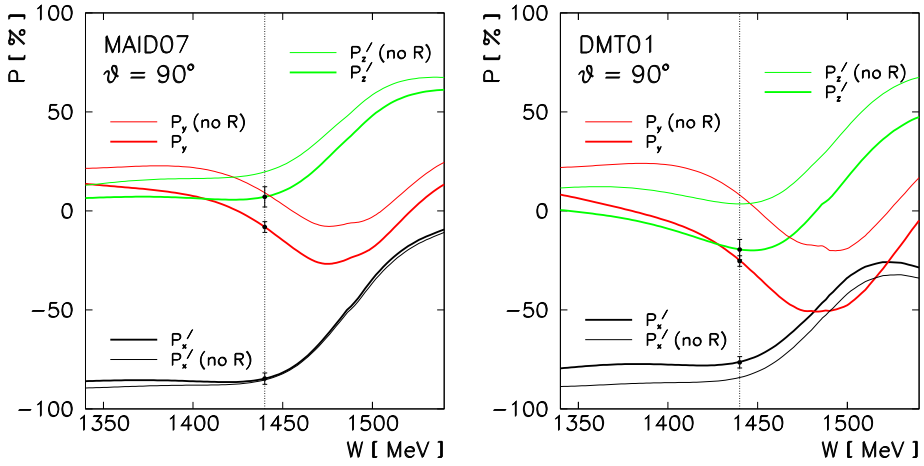

Fig. 2. Expected uncertainties on P'_x, P_y and P'_z for 100 h beamtime; W-dependence.

The following estimates have been done with the dipole approximation for the precession matrix ($\chi \approx 215°$), assuming 100 h of 10 μA beam with $P_e = 75\,\%$ polarization on a 5 cm LH_2 target, and reasonably conservative cuts in the simulation. One obtains ≈ 7000 counts/hour (before the FPP cuts) and the error estimates (for $\theta = 90°$)

$$\Delta P'_x = \frac{1}{P_e}\sqrt{\frac{2}{N_0\,f}} \approx 0.029$$

$$\Delta P_y = \frac{1}{\cos\chi}\sqrt{\frac{2}{N_0\,f}} \approx 0.027$$

$$\Delta P'_z = \frac{1}{P_e}\frac{1}{\sin\chi}\sqrt{\frac{2}{N_0\,f}} \approx 0.051$$

Figure 2 shows the level of accuracy that can be achieved under these assumptions for the polarization components P'_x, P_y and P'_z, shown here as a function of W. One can see that we are sensitive mostly to transverse helicity amplitudes and that P'_x in some sense is useless except for calibration purposes.

3.1 Relation of polarization components to mutipoles

The cross-section for the $p(\vec{e},e'\vec{p})\pi^0$, allowing for both a polarized electron beam and detection of the recoil proton polarization, is given by

$$\frac{d\sigma}{dE'_e\,d\Omega_e\,d\Omega^\star_p} = \frac{\sigma_0}{2}\left\{1 + \mathbf{P}\cdot\hat{\mathbf{s}}_r + h\left[A_e + \mathbf{P}'\cdot\hat{\mathbf{s}}_r\right]\right\},$$

where $\sigma_0 \equiv d\sigma(\hat{\mathbf{s}}_r)+d\sigma(-\hat{\mathbf{s}}_r)$ is the unpolarized cross-section, $\hat{\mathbf{s}}_r$ is the proton spin vector in its rest frame, h is the helicity of the incident electrons, $\mathbf{P}$ is the induced proton polarization, A_e is the beam analyzing power, and $\mathbf{P}'$ is the vector of spin-transfer coefficients. The polarization of the recoiled proton consists of a helicity-independent (induced) and a helicity-dependent (transferred) part, $\mathbf{\Pi} \equiv \mathbf{P} + h\mathbf{P}'$. (Alternative notations for the polarization components is $P'_x \leftrightarrow -P_t$, $P_n \leftrightarrow P_y$, and $P'_z \leftrightarrow -P_l$.)

The structure functions contain the following combinations of the multipoles relevant for the Roper (the corresponding polarization component is given in the bracket before the structure function):

$$(P_n)R^n_T = -\mathrm{Im}\,E^*_{0+}\,(3E_{1+} + M_{1+} + 2M_{1-})$$

contains the leading M_{1-} amplitude in the imaginary part of the interference with the E_{0+} non-resonant amplitude; this is matched with the

$$(P_l)R^l_{TT'} \propto \mathrm{Re}\,E^*_{0+}\,(3E_{1+} + M_{1+} + 2M_{1-})$$

response which contains the real part of the same interference. The terms

$$\begin{aligned}(P_n)R^n_{TL} &\text{ contains } \mathrm{Im}\,L^*_{1-}M_{1-}\,,\\ (P_l)R^l_{TL'} &\text{ contains } \mathrm{Re}\,L^*_{1-}M_{1-}\end{aligned}$$

contain (real and imaginary) interferences of both resonant multipoles but these probably have less relevance because both are very small. In addition, there are the

$$\begin{aligned}(P_n)R^n_L &\propto -2\,\mathrm{Im}\,L^*_{0+}\,(2L_{1+} - L_{1-})\,,\\ (P_t)R^t_{TL'} &\propto \mathrm{Re}\left\{L^*_{0+}\,(2M_{1+} + M_{1-}) + \left(2L^*_{1+} - L^*_{1-}\right)E_{0+} + \cdots\right\}\end{aligned}$$

terms, as well as the $(P_n)R^n_{TT}$ that contains $\sin\theta\cos\theta\,M^*_{1+}M_{1-}$. The latter term is not accessible at $\theta = 90^\circ$.

Even with only two angular points ($\theta = 90^\circ$ and $\theta = 75^\circ$), a strong physics case can be made. The experiment will possess enough power to distinguish between Roper on/off calculations in both MAID2007 and DMT2001 models at these kinematics. The differences in the models originate in different treatments of resonances in isobar models (like MAID) versus those of dynamical models (like DMT), that is, of having "dressed" vs. "bare" resonant vertices.

References

1. L. D. Roper, Phys. Rev. Lett. **12** (1964) 340.
2. D. M. Manley, E. M. Saleski, Phys. Rev. D **45** (1992) 4002.
3. R. E. Cutkosky, C. P. Forsyth, R. E. Hendrick, R. L. Kelly, Phys. Rev. D **20** (1979) 2839.
4. S. Eidelman et al. (Particle Data Group), Phys. Lett. B **592** (2004) 1.
5. K. Joo et al. (CLAS Collaboration), Phys. Rev. C **68** (2003) 032201(R).
6. K. Joo et al. (CLAS Collaboration), Phys. Rev. C **70** (2004) 042201(R).
7. I. Aznauryan, V. D. Burkert, H. Egiyan, K. Joo, R. Minehart, L. C. Smith, Phys. Rev. C **71** (2005) 015201.
8. N. Benmouna, G. O'Rielly, I. Strakovski, S. Strauch, JLab Experiment E03-105.
9. O. Gayou, S. Gilad, S. Širca, A. Sarty (co-spokespersons), JLab Proposal PR05-010.
10. J. J. Kelly, A. Sarty, S. Frullani (co-spokespersons), JLab Experiment E91-011.
11. Th. Pospischil et al. (A1 Collaboration), Phys. Rev. Lett. **86** (2001) 2959.
12. J. J. Kelly et al. (Hall A Collaboration), Phys. Rev. Lett. **95** (2005) 102001; see also J. J. Kelly et al. (Hall A Collaboration), Phys. Rev. C **75** (2007) 025201.

BLED WORKSHOPS
IN PHYSICS
VOL. 10, NO. 1
p. 88

Proceedings of the Mini-Workshop
Problems in Multi-Quark States
Bled, Slovenia, June 29 - July 6, 2009

Hadronic spectroscopy at Belle*

M. Bračko[a,b] and T. Živko[b], representing the Belle Collaboration

[a] University of Maribor, Smetanova ulica 17, SI-2000 Maribor, Slovenia
[b] Jožef Stefan Institute, Jamova cesta 39, SI-1000 Ljubljana, Slovenia

Abstract. The Belle experiment continues with study of D_{sJ} particles, as well as charmonium and charmonium-like states. Recent results on these topics are briefly mentioned.

Belle is an experiment at the e^+e^- collider KEKB [1]. The main goal of the experiment is a precision measurement of CP violation in the system of B mesons. The asymmetric KEKB collider operates around the center-of-mass energy of the $\Upsilon(4S)$ resonance; the total collected integrated luminosity is about 945 fb^{-1} in July 2009. The large amount of data and excellent detector performances enable successful study of other topics besides properties of B mesons. In what follows, news from Belle about charmed strange mesons, charmonium and charmonium-like states will be briefly mentioned. Details of the reported analyses can be found in quoted references.

New charmed strange meson, $D_{sJ}(2700)^+$, was observed in the decay channel D^0K^+ [2]. Angular analysis favours spin-parity assignment 1^-. It is possible that this particle is $X(2690)$, which was previously observed by *BABAR* [3].

Partial wave analysis of another charmed strange meson, $D_{s1}(2536)^+$, in decay channel $D^{*+}K^0_S$ revealed domination of the S wave [4], at variance with HQET prediction.

Properties of charmonium-like state, $X(3872)$, were further studied. Positive charge parity is established [5], while favoured J^P is 1^+ or 2^-. Belle updated the analysis of the $X(3872)$ in the $D^0\bar{D}^{*0}$ decay channel [6]. The measured mass value is compatible with the new *BABAR* measurement [7]. According to all measurements, the favoured interpretation is that the $X(3872)$ is a mixture of the $D^0\bar{D}^{*0}$ molecule and a $c\bar{c}$ state.

A new state, named $Z^+(4430)$ and decaying to $\psi(2S)\pi^+$, is observed in the B meson decays to $K\pi^\pm\psi(2S)$ final state [8]. An updated measurement, based on a full Dalitz plot analysis of the $K\pi^\pm\psi(2S)$ final state, was performed recently [9]. Results of this analysis confirm the original discovery of the $Z^+(4430)$.

Two new states, $Z^+(4050)$ and $Z^+(4250)$, decaying to $\chi_{c1}\pi^+$, were observed in $K^-\chi_{c1}\pi^+$ decays of $\overline{B}^0$ [10]. All three observed charged charmonium-like states – $Z^+(4430)$, $Z^+(4050)$ and $Z^+(4250)$ – are serious tetraquark candidates.

* Talk delivered by T. Živko

New particles, $X(3940)$ and $X(4160)$, decaying to $D^*\bar{D}$ and $D^*\bar{D}^*$ were observed in events with double $c\bar{c}$ production [11]. The established experimental technique was used to measure the cross section for $e^+e^- \to J/\psi c\bar{c}$ in a model independent way [12].

Several new Y states and peaks in mass plots were observed in initial state radiation events [13]. These states are regarded as serious charmonium - gluon hybrid candidates [14].

As new experimental data are still accumulated and many studies are ongoing, more interesting results on these and similar topics are to be expected from Belle in the near future.

References

1. A. Abashian *et al.* (Belle Coll.), Nucl. Instr. and Meth. A **479**, 117 (2002).
2. J. Brodzicka *et al.* (Belle Coll.), Phys. Rev. Lett. **100**, 092001 (2008).
3. B. Aubert *et al.* (*BABAR* Coll.), Phys. Rev. Lett. **97**, 222001 (2006).
4. V. Balagura, *et al.* (Belle Coll.), Phys. Rev. D **77**, 032001 (2008).
5. B. Aubert *et al.* (*BABAR* Coll.), Phys. Rev. Lett. **102**, 132001 (2009).
6. I. Adachi *et al.* (Belle Coll.), arXiv:0810.0358v2 [hep-ex], to be submitted to Phys. Rev. Lett.
7. B. Aubert *et al.* (*BABAR* Coll.), Phys. Rev. D **77**, 011102 (2008).
8. S.-K. Choi, *et al.* (Belle Coll.), Phys. Rev. Lett. **100**, 142001 (2008).
9. R. Mizuk, *et al.* (Belle Coll.), Phys. Rev. D **80**, 031104 (2009).
10. R. Mizuk, *et al.* (Belle Coll.), Phys. Rev. D **78**, 072004 (2008).
11. P. Pakhlov *et al.* (Belle Coll.), Phys. Rev. Lett. **100**, 202001 (2008).
12. P. Pakhlov, *et al.* (Belle Coll.), Phys. Rev. D **79**, 071101 (2009).
13. G. Pakhlova, *et al.* (Belle Coll.), Phys. Rev. Lett. **101**, 172001 (2009).
14. E. Swanson, proceedings of the Rencontres de Moriond 2009 Conference (*QCD and High Energy Interactions*).

BLEJSKE DELAVNICE IZ FIZIKE, LETNIK 10, ŠT. 1, ISSN 1580-4992

BLED WORKSHOPS IN PHYSICS, VOL. 10, NO. 1

Zbornik delavnice 'Problems in Multi-Quark States',
Bled, 29 junij – 6. julij 2009

Proceedings of the Mini-Workshop 'Problems in Multi-Quark States',
Bled, June 29 – July 6, 2009

Uredili in oblikovali Bojan Golli, Mitja Rosina, Simon Širca

Publikacijo sofinancira Javna agencija za knjigo Republike Slovenije

Tehnični urednik Vladimir Bensa

Založilo: DMFA – založništvo, Jadranska 19, 1000 Ljubljana, Slovenija

Natisnila ALFAGRAF TRADE v nakladi 110 izvodov

Publikacija DMFA številka 1761

Brezplačni izvod za udeležence delavnice